

TU Delft
Acoustics by
Additive Manufacturing

2012

Technische Universiteit Delft

ACOUSTICS BY ADDITIVE MANUFACTURING

1st mentor:

**Micehla
Turrin**

2nd mentor:

**Arjan
van Timmeren**

3rd mentor:

**Martin
Tenpierik**

student:

**Foteini
Setaki**

SN 4120701

**TU
Delft**

Faculty of
Architecture

Department of
Building Technology

2012

Acknowledgements

I wish to thank Arch. Michela Turrin, Dr.ir. Arjan van Timmeren and Dr.ir. Martin Tenpierik for their valuable contribution, their active involvement and inspiration.

I would also like to thank for their great support: Dr.ir. Evert de Rooter, Peutz bv, Toon Roels, Maarten Valckenaers, Materialise, the Chair of Design Informatics, the Chair Climate Design Building Physics and the department of Department Architectural Engineering + Technology.

4	Introduction		
5	Framework		
6	Methodology		
8	Additive Manufacturing		
	Digital Fabrication		
	AM: Definition - Procedure		
	Machines - Techniques		
14	Acoustics		
	Basics		
	Absorbers		
	Diffusers		
	Geometry + Sound		
19	AM and Acoustics		
	Scenarios on AM + acoustics		
	2 scenarios on diffusers		
	Fractal Diffuser		
	Optimised curved surface		
	2 scenarios on absorbers		
	Passive destructive interference		
	Grading density of material structure		
	Summary - Decision - Conclusions		
23	Passive Destructive Interference		
28	Phase 1: Preliminary Measurements		
	Measurement Details		
	Fabrication		
	Design of the samples		
	Tested Parameters		
	ΔL		
	Diameter of tubes		
	Geometry		
	Results	76	Phase 3: Design
	Statistics		Applications
	Summary - Conclusion		Design Concepts
			Modifications
42	Phase 2: Measurements		
	Measurement Details	102	Summary - Conclusions -Reflections
	High Frequencies		
	Small Samples	104	Bibliography
	Calibration		
	Coherence with theory		
	Material Properties	106	Appendix
	Diameter		
	Length		
	Summary		
	Low Frequencies		
	Big Samples		
	Coherence with theory		
	Diameter		
	Length		
			Material Thickness
			Exposed Geometry
			Multiple Channels
			Grading Cross-Section
			Measurements' accuracy
			Summary
			Statistics



The emergence of new tools -in terms of new software and new fabrication techniques- raise the potentials in engaging design with performance and allows visioning new forms and new types of building products.

This study focuses on exploring the merging field of **additive manufacturing** and **acoustics** and introduces a new type of sound absorber which is regulating **performance** by its geometrical characteristics. In this manner, a direct relation between geometry, fabrication and acoustic performance is suggested.

This project seeks to connect design with acoustic performance by taking advantage of new parametric and computational design techniques, and by utilizing additive manufacturing to produce complex structures.

For this reason, it becomes essential to measure and understand the acoustic consequences of different geometrical configurations and material characteristics. The rules governing these acoustic alterations can be encoded into a design system through parametric modelling and allow the architectural design with performance driven criteria.

Essentially this research aims to liberate the design and manufacturing of acoustic devices and through the use of additive manufacturing to suggest new types of acoustic treatment in architecture. The introduction of additive manufacturing processes to the production of acoustic devices could allow the integration of highly complex shapes without traditional manufacturing constraints. Furthermore, exploitation of these capabilities could lead to new acoustic structures with improved performance or function over existing solutions.

Framework

The emergence of new tools – in terms of new software and new fabrication techniques – raises new potential in the design process that is engaged with performance, and allows envisioning new types of building components. Current research and development in the fields of architecture and computation, suggest a triangular relation between computation, fabrication and performance. The emerging tools suggest a continuum from design to manufacturing and enrich the design process with new methods and techniques. On the same time, performance-driven architecture becomes a key factor for the design¹. The aim of this study is to explore the relation between digital modelling, digital manufacturing and performance, through the paradigm of a sound absorber.

It is well known that acoustic performance is material dependent. Furthermore, acoustic engineering principles establish relationships between room volume, room shape, surface geometry and the acoustic performance of space². Therefore the modulation of geometry by the criteria of material, acoustic performance and fabrication in the digital model will become the main concern of this study.

The implementation of physical and material properties, in combination with the recent developments in fabrication, shifts the role of the digital model further away from representation towards a manufacturing process³. The emerging tools enable the direct rela-

tion of the design process with material properties, performance and fabrication technique. Additive manufacturing techniques can change the abilities of designers to engage with the material structures and performance.

Digital fabrication and more specifically additive manufacturing offer the opportunity to produce custom elements, which have the potential to create rooms with a specific acoustical characteristic. Besides the possibility to produce individual non-repeating building elements digital fabrication opens the opportunity to gain control over acoustic performance on different scales simultaneously, for example: on global geometry or on material scale, etc.

This framework suggests not only a continuum between design and manufacturing, but also a functional relation between geometry, manufacturing technique, material properties and performance. This study will take advantage of the emerging tools and will attempt to develop a digitally controlled system of an acoustic panel with local variations that alter material organization and acoustic performance.

Experimental prototypes and applications have been developed by various authors concerning the implementation of performance in the design process; examples include the work of Neri Oxman, Norbert Palz, Achim Menges, as well as numerous others, who undoubtedly have influenced directly or indirectly the present research project.

Problem statement

This project seeks to connect design with acoustic performance by taking advantage of new parametric and computational design techniques, and by utilizing additive manufacturing to produce complex structures.

Current limitations in the established methods of the design process do not enable sound, material and fabrication technique to act as design drivers. This project will explore the field through the case study of a sound absorber and will suggest a set of geometrical rules to regulate acoustic performance.

Short description

As mentioned before, the emerging tools suggest the incorporation of performance-driven criteria in the design process and allow to envision new types of forms and new types of products. The new possibilities are further explored through the case study of a sound absorber.

This research will try to combine the additive manufacturing process with the functional requirements of room acoustics. The challenge will be to suggest a new type of acoustic device that regulates its performance through its geometrical characteristics. In order to formulate the design-guidelines for such a sound absorber, physical tests will take place. The ultimate aim of this study will be to establish a new product where form, material and performance are inherently related and constitute integral aspects of the manufacturing process.

¹ B. Kolarevic, *Architecture in the Digital Age: Design and Manufacturing*, Taylor & Francis, 2005, pp. 11-28

² H. Kuttruff, *Room Acoustics*, fifth edition, Spon Press, 2009, pp. 294-330

³ M. Hensel, A. Menges, M. Weinstock, *Emergent technologies and design, Towards a biological paradigm for architecture*, Routledge, 2010, pp.102-115

1_Literature review - problem definition

The starting point of this project is the systematic research on the available technology in additive manufacturing techniques and the corresponding materials used. It first focuses on recent developments in the rapid prototyping and manufacturing industry and specifically in the field of architecture and construction. This process enables an overview on the field of additive manufacturing techniques and contributes in further developing the ideas on the graduation project. In parallel, the field of acoustics is being explored. Furthermore, literature on research projects with relevant topics conducted in other universities or institutes is collected.

The systematic literature review not only contributes in further defining and clarifying the research topic, but also in selecting the appropriate technology and the corresponding material used. Additionally, the study in acoustics provides with the mathematical models that inform the physical tests and the design process.

2_ 4 acoustic device concepts

In order to further investigate the merging field of additive manufacturing and acoustics it is necessary to reflect on new types of acoustic devices that regulate their performance through geometry. Based on the literature review, 4 acoustic device concepts are suggested and analysed: two sound diffusers and two sound absorbers.

3_Passive destructive interference

The chosen acoustic device is based on the principles of passive destructive interference. For this reason, relevant literature is gathered and studied to understand better the phenomenon.

4_Phase 1 : Physical tests

The outcome of the literature review revealed that there are only a few publications on passive destructive interference. Hence, it becomes crucial to execute physical tests, in order to fill in the gaps of the available theory.

The first set of measurements is based on a boolean logic. It is mostly conceived to give answers of the type False/ True. The following parameters are examined for the frequencies between 800 to 5000Hz:

- geometry in terms of diameter, length, orientation and level of complexity,
- coherence with theory.

5_Phase 2 : Physical tests

The analysis and evaluation of the first set of measurements give some encouraging results; several assumptions are confirmed and new questions arise. By scaling up the samples, it is now possible to measure the acoustic performance in frequencies between 100 and 1600Hz. Additionally, further information is extracted about:

- geometry in terms of diameter, length, orientation and level of complexity,
- material in relation to acoustic performance,
- coherence with theory,
- measurement accuracy, etc.

6_Design guidelines

The physical tests of Phase 1 and 2 enrich the knowledge on passive destructive interference and make possible to formulate the design guidelines of the sound absorber. The design-rules are generic and may apply in various designs. Furthermore, several issues are highlighted for future investigation on the same topic.

7_Design concepts-Case study

Based on the knowledge gained via the physical tests, several design concepts are developed and evaluated. At this stage, acoustic specifications are translated into geometry. The chosen design, is further examined by applying it in a specific space with certain acoustic demands and architectural restrictions. The evaluation of the experiments of phase 1 and 2, not only informs the design process but also allows a rough estimation of the absorber's performance. Originally, it was planned to scale up the samples and execute physical tests of a bigger absorbing structure. This part is not accomplished because of practical concerns.

7_Evaluation - Reflections

Evaluation is a necessary step before and after each chapter. This report constitutes the documentation of every investigated aspect of the research project; it endeavours to become valuable for future research projects which can take advantage of or get inspired by this effort.



1: Vila Olimpica
2: Guggenheim Museum
3: Lord's Cricket Ground Media Stand
4: Zollhoff Towers

Computational and manufacturing techniques can create a direct link between design and fabrication. Besides the visual representation of structures, the emerging digital tools enable architects to incorporate physical properties and performance into the design process.

Digital Fabrication

Branko Kolarevic in his book *Architecture in the Digital Age*, suggests that the digital age has radically reconfigured the relationship between conception and production, creating a direct link between computation and construction. Building projects today are not only born out digitally, but they are also realised digitally through "file-to-factory" processes of computer numerically controlled (CNC) fabrication technologies⁴.

The manufacturing technologies involve one, or a combination of, three basic approaches additive, formative and subtractive⁵:

- _ Additive: describes the process of adding material to build up the product.
- _ Formative: describes the process of forming the product through the use of moulds for example.
- _ Subtractive: describes the process of forming the product by removing material through cutting, milling or grinding.

Despite the recent advances in manufacturing technologies offering a number of current and potential applications the construction sector still uses existing technologies⁶. The construction industry of today

⁴ B. Kolarevic, op.cit., pp. 29-55

⁵ R. Buswel, R. Soar, A. Gibb, A. Thorpe, *Freeform Construction: Mega-scale Rapid Manufacturing for construction*, *Automation in Construction* 16, 2007, pp. 224-231

⁶ C. Pasquire, R. Soar, A. Gibb, *Beyond pre-fabrication - The potential of next generation technologies to make a step change in construction manufacturing*, *Proceedings IGLC-14*, July 2006, Santiago, Chile, pp. 243-254

has not significantly changed in essence since a half a century ago. It remains labour intensive, site based and constrained by the prevailing weather. In terms of technological development, it can be argued that construction is behind other industries such as aerospace, automotive and ship building⁷.

Digital Fabrication in Construction

The technology that revolutionised the aerospace and automotive sectors is "today" been transferred to the construction industry. In general, the construction industry is becoming more familiar with Digital Fabrication. Solid modelling tools become more popular among architects and Rapid Prototyping is finding its place in the design procedure. The use of solid modelling simplifies the process design information transfer, while digital information is being used increasingly to communicate design parameters to manufacturers.

Some early examples, where digital fabrication is applied in a large scale for the creation of building structural components and facades constitute:

_The Vila Olimpica [Frank Gehry, Barcelona, Spain, 1989 – 1992]

This project was designed in a solid modelling tool mostly used by the aerospace industry [CATIA]. The digital model data was also used in the fabrication of the structure.

_Guggenheim Museum [Frank Gehry, Bilbao, Spain, 1997]

_Lord's Cricket Ground Media Stand [Future Systems, London, United Kingdom, 1998 – 1999]: CNC cutting

_ Zollhoff Towers [Frank Gehry, Dusseldorf, Germany]

⁷ R. Buswel, R. Soar, A. Gibb, op.cit., pp. 224-231



For this building, CNC Plasma-arc cutting of sheet steel was used to form the masonry supports. The load bearing, curved, external wall panels were produced using blocks of lightweight polystyrene and CNC machined to produce hundreds of different curved moulds that became the forms for casting the reinforced concrete. The computer has also made an impact on design⁸.



_BMW pavilion [Bernhard Franken, Frankfurt / Main, Germany, 1999]

The form of the structure was defined by a computer simulation of two water droplets merging. Data from the simulation was used to define the space frame which was cut from aluminium using CNC processes. The frame supported a clear skin comprising of many double curved, acrylic panels. These were formed by heating the precut acrylic panels and allowing them to deform over polystyrene moulds that had been created using multi-axis milling⁹.



_ Great Court British Museum [Foster&Partners, London, United Kingdom, 1994-2000]: CNC cutting/milling

_Restaurant Georges [Jacob+MacFarlane, Paris, France, 1999 – 2000]: CNC cutting

_Walt Disney Concert Hall [Frank Gehry, Los Angeles, USA, 1999–2003]: CNC



This short reference to materialised buildings that have taken advantage of digital fabrication techniques indicates that the two most common applications of digital fabrication in construction are mostly:
1_CNC cutting processes used to form structural steel members, and
2_CNC milling processes employed to create large moulds for casting or shaping.

From Rapid Prototyping to Additive Manufacturing

As mentioned before, a revolution in manufacturing has led to a new generation of technology increasing the automation of processes and underpinned by digital fabrication¹⁰. One stream within these technologies is known as Additive Manufacturing.

The discussed additive processes were originally intended for Rapid Prototyping and are currently being used for Manufacture. The evolution in material science and machine technology, among others, has eventually moved this process into the manufacture and end use parts are made directly by these technique. In the field of Rapid Prototyping, Tooling and Manufacture, a number of processes, such as stereolithography and selective laser sintering, may be considered as established rather than emerging. However, with respect to the field of Manufacture these processes are quite new.

There are currently a wide range of engineering fields where rapid manufacturing technology has been used: Aerospace, Automotive, Dentistry, Motor sports¹¹. Additionally, a growing number of consumer goods companies have also started to use additive manufacturing to produce goods, such as Game avatars, Toys, Furniture, Home accessories, Art pieces, collectables and Fashion products, etc. Additive manufacturing is used to build physical models, prototypes, patterns, tooling components, and production parts in plastic, metal, ceramic, and composite materials. In architecture, the particular technology is mostly used today to produce physical scale models.

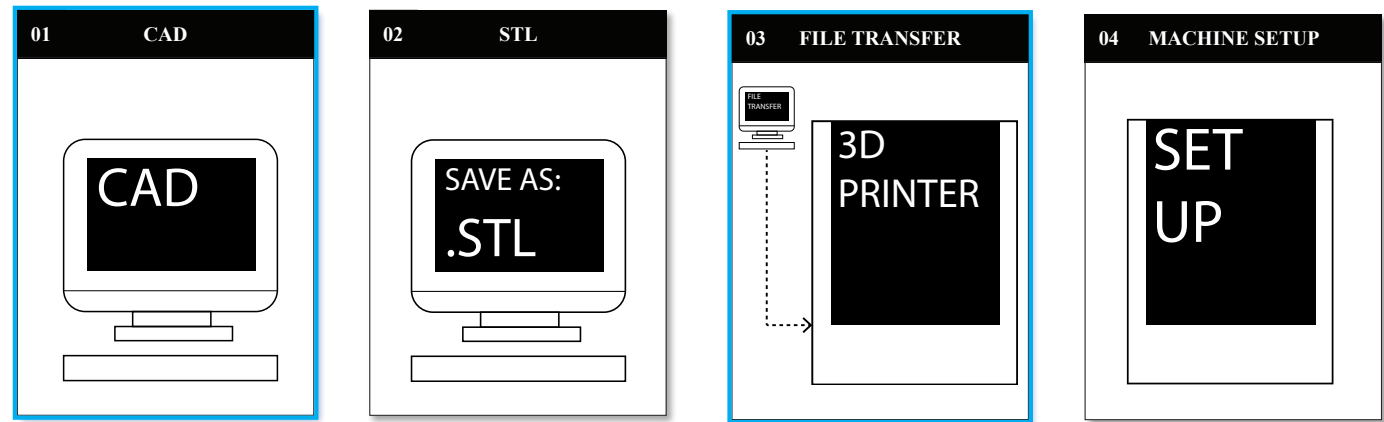
- 1: BMW pavilion
- 2: Great Court British Museum
- 3: Restaurant Georges
- 4: Walt Disney Concert Hall

⁸ C. Pasquire, R. Soar, A. Gibb, op.cit., pp. 243-254

⁹ C. Pasquire, R. Soar, A. Gibb, op.cit., pp. 243-254

¹⁰ C. Pasquire, R. Soar, A. Gibb, op.cit., pp. 243-254

¹¹ Wohlers, Additive Manufacturing State of the Industry, NZ Rapid Product Development Conference 2011



NOTE: To differentiate, the process is called Additive Manufacturing if the product is put to direct end use, Rapid prototyping if the product is used for conceptualisation, testing, analysis but not as an end product¹².

Additive Manufacturing : Term Definition

The term Additive Manufacturing is used in a variety of industries to describe a process where parts of an object are made by adding material in layers (as opposed to subtractive manufacturing methodologies). Each layer constitutes a thin cross-section of the part derived from the original CAD data. Referred to it in short as AM, the basic principle of this technology is that a model, initially generated using a three-dimensional Computer Aided Design (3D CAD) system, can be fabricated directly without the need

for process planning¹³.

This definition relates to the way the processes fabricate parts by adding material in layers and contrast to machining technology that removes, or subtracts material from a block of raw material. Currently, every commercial process works in a layer-wise fashion to build up three-dimensional objects. However, it might be that in the future, systems may add material in other ways. Furthermore, the term Manufacturing makes a better connotation to the fact that the final output corresponds to the end use product¹⁴.

Other terms that are in use and refer to the same process, are:

Automated Fabrication, Freeform Fabrication, Solid Freeform Fabrication, Layer-based Manufacturing, Stereolithography, 3D Printing, Rapid Prototyping

¹³ I.Gibson, D.W.Rosen, B.Stucker, Additive Manufacturing Technologies, Rapid Prototyping to Direct Digital Manufacturing, Springer, 2010, pp. 1-15

¹⁴ I.Gibson, D.W.Rosen, B.Stucker, *ibid.*, pp. 1-15

The common procedure

AM involves a number of steps that bring the digital drawing to materialization. The procedure alters in relation to the machine used, but in general most AM processes follow, to some degree at least, the following eight steps¹⁵:

1_ CAD

All AM parts need to first be defined digitally. This can involve the use of almost any professional CAD solid modelling software, but the output must be a 3D solid or surface representation.

2_ STL convert

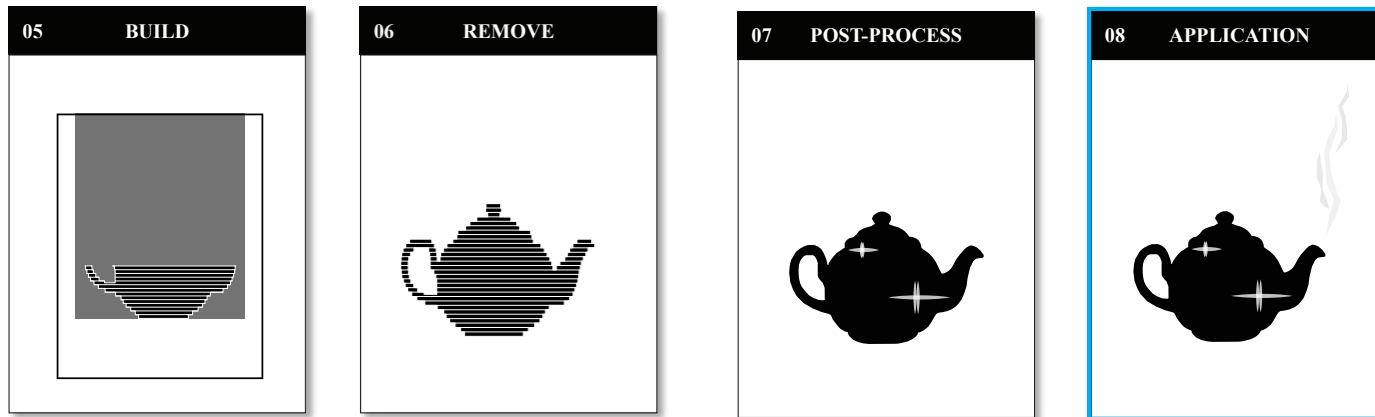
Nearly every AM machine accepts the STL file format, and nearly every CAD system can output such a file format. This file describes the external closed surfaces of the original CAD model and serves the basis for calculation of the slices.

3_ File transfer to machine

At this stage it might be necessary to do certain manipulation of the file so that it has the correct scale,

¹⁵ I.Gibson, D.W.Rosen, B.Stucker, *ibid.*, pp. 1-15

¹² C. Pasquire, R. Soar, A. Gibb, *op.cit.*, pp. 243-254



the common procedure of AM

position, and orientation for building.

4_ Machine setup

The AM machine must be properly set up before use. Settings, such as material constraints, energy source, layer thickness, timings, etc might be needed to define.

5_ Build

This stage is almost totally automated. The machine can largely carry on without supervision. Only superficial monitoring of the machine needs to take place at this time to ensure that no errors occur [running out of material, power or software glitches, etc].

6_ Remove

Once the AM machine has completed the build, the parts must be removed.

7_ Post-process

Parts may require an amount of additional cleaning up before they are ready for use.

8_ Application

Parts may now be ready to be used. However, they may also require additional treatment before they are acceptable for use. For example, they may require priming and painting to give an acceptable surface texture and finish.

Advantages

AM enables fast, flexible and reconfigurable manufacturing to occur that offers benefits to manufacturers and consumers. According to relevant literature, the use of AM can realise significant benefits in the design, manufacture and distribution of a part or components, including:

- _ Economic low-volume production
- _ Increased flexibility and productivity
- _ Design freedom
- _ Less data conversion
- _ Reduction in process steps
- _ Reduction in required resources
- _ Better control over material
- _ Simple interface detailing
- _ New opportunities for customization
- _ Piece part reductions to greatly simplify product assembly
- _ Improvements in product performance
- _ Multi-functionality
- _ Potentially green (savings are mentioned in CO₂, water and virgin material)

Restrictions

Additive Manufacturing is relatively new digital fabrication technique.

The most important constraint rely on:

- material,
- size,
- economic constraints,
- part accuracy,
- material variety and
- mechanical performance.

Current Applications

- direct part production 15.0%
- tooling components 3.7%
- patterns for metal castings 9.3%
- patterns for prototype tooling 13.2%
- fit and assembly 13.1%
- functional models 18.9%
- visual aids 15.2%
- others 2.3%

Machines - Basic Principles

There are many techniques which exist and are emerging in AM. These are commonly classified into six basic techniques, making the part or prototype¹⁶, these are:

1_ Stereolithography (SL or SLA)

The stereolithography process works using an ultraviolet (UV) laser to initiate a curing reaction in a photocurable resin. Using a computer aided design (CAD) file to drive the laser; a selected portion of the surface of a vat of resin is cured and solidified on to a platform. The platform is then lowered, and a fresh layer of liquid resin is deposited over the previous layer. The laser then scans a new layer that bonds to the previous layer. After building, parts are removed from the machine and platform, supports removed and post-processing in a UV and/or thermal oven are used to cure any uncured resin¹⁷.

2_ Laser Sintering/Fusion (LS or SLS)

The process is in many ways similar to stereolithography, but the powdered raw material is sintered or melted by a laser that selectively scans the surface of a powder bed to create a two dimensional solid shape. A fresh layer of powder is then added to the top of the bed so that a subsequent two-dimensional profile can be traced by the laser bonding it to the layer below. The process continues to create a full three-dimensional object and the un-fused powder acts as a supporting material which obviates the need for support removal during post-processing.

3_ Fused Deposition Modelling (FDM)

The fused deposition modelling (FDM) process cre-

ates parts by extruding material (normally a thermoplastic polymer) through a nozzle that traverses in X and Y to create each two-dimensional layer. In each layer separate nozzles extrude and deposit material that forms the parts and material that form supports where required. The use of a nozzle limits resolution and accuracy. Also the need for the nozzles to physically traverse the build area limits build speed, but the process is very easy to set up and can operate in an office or factory environment.

4_ Laminate Manufacture (LM or LOM)

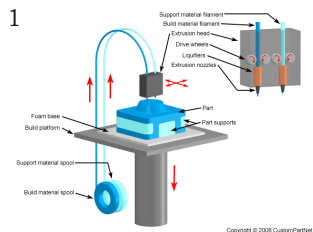
A number of technologies have been developed to create three-dimensional parts by cutting and stacking two-dimensional sheets of various materials. Different approaches have been used to cut sheets, bond them together and remove waste material from each sheet.

5_ Jetting (MJM)

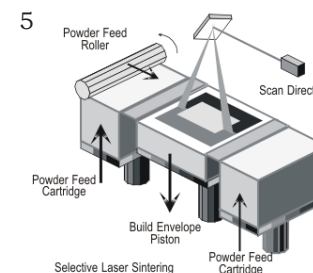
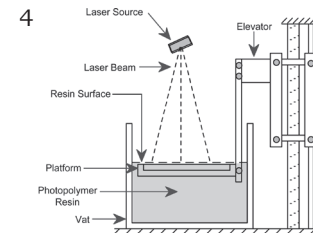
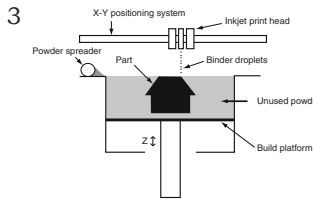
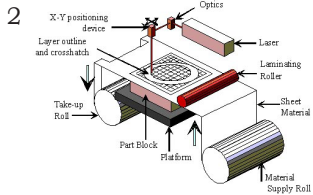
The process uses an array of printing heads to simultaneously selectively deposit an acrylate-based photopolymer. Each layer is then cured by a trailing UV lamp that passes over the deposited material.

6_ 3D Printing (3DP)

'1D' jetting technology the process has a relatively high throughput in terms of creating green parts similar to those by metal selective laser sintering described above. Post-processing is similar to that for selective laser sintered parts, but surface finish usually requires some form of machining to create a surface suitable for tooling. In terms of RM, there have been no published examples but the process may be suited to more rigorous applications where polymers will not suffice.



Copyright © 2008 CustomPartNet

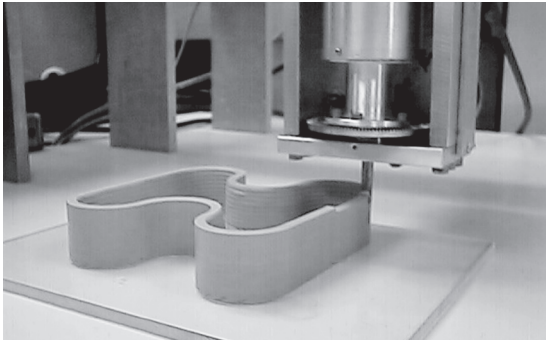


- 1: Fused Deposition Modelling
- 2: Laminate Manufacture
- 3: 3D Printing
- 4: Stereolithography
- 5: Selective Laser Sintering

¹⁶ R. Noorani, Rapid Prototyping – Principles and Applications, John Wiley and Sons, 2006

¹⁷ N. Hopkinson, R.J.M. Hague and P.M. Dickens (editors), Rapid Manufacturing, An Industrial Revolution for the Digital Age, John Wiley & Sons, 2006, pp. 56-80

1



2



3



- 1: Contour Crafting
- 2: D-Shape
- 3: Free-form Construction

Large Scale AM

Since the mid-1990s there is a growing interest in applying AM in construction¹⁸. Currently, there are three processes that manufacture in an architectural scale:

_Contour Crafting

An interesting development based on FDM is contour crafting (CC), a process invented at the University of Southern California by Behrokh Khoshnevis. CC has been demonstrated to produce large structures. The process extrudes the internal and external 'skin' of the wall to form a permanent shutter that is then backfilled with a bulk compound similar to concrete. Thixotropic materials with rapid curing properties and low shrinkage characteristics, consecutive layers of the wall can be rapidly built up. The wall material deposition process is a two stage operation. In order to improve the finish of the visible surfaces, the shutter material is shaped by a secondary manipulator, or trowel, as it is extruded. The combination of processes results in a system that can deposit (relatively) large quantities of material while maintaining a high quality surface finish.

_D-Shape (Developed by Enrico Dini)

A large-scale fabrication technology that is similar to the 3D printing Technology. It deposits a thin layer of sand over the full bed size of the printer (4x4 meters). This sand has been pre-mixed with a catalyst that chemically hardens when it comes into contact with inorganic binder. This binder is jetted onto the sand through a series of jets.

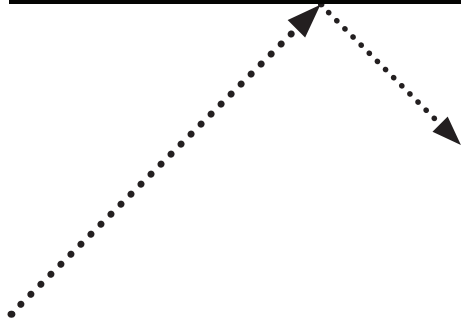
_Free-form Construction

The process deposits concrete through a computer controlled nozzle. The process can be easily compared to an FDM technology, with the difference that here concrete is extruded instead of plastic. The concrete is deposited without the use of any formwork. Therefore the process allows for a limited freedom in geometrical complexity. The machine is capable of producing large parts out of concrete (2x2x2 metres).

¹⁸ J. Gardiner, Sustainability and Construction-Scale Rapid Manufacturing: Opportunities for Architecture and the Construction Industry, Proceedings of RAPID 2009 Conference, 2009

Sound striking a surface

ABSORPTION

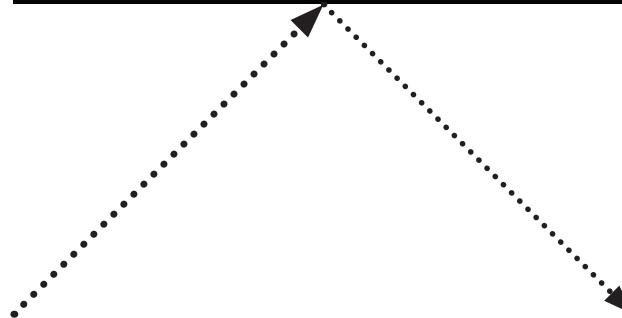


Acoustics constitute essential performance criteria for architecture. Even though sound is not perceivable through vision and many people tend to recognize it only unconsciously; sound plays an important role in the way people experience and sense space. Space can be said to perform well or poorly in terms of its acoustic qualities. The “invisible” soundscape is interpreted by principles which are amenable to scientific treatment. It is a challenge for designers to understand the rules governing the acoustic field and be able to incorporate acoustic performance criteria in the design process.

Basics

The sound that is heard in most environments is a combination of the direct sound straight from the source or sources and the indirect reflections from surfaces and other objects. Consequently, the sound of the past exists simultaneously with the sounds of the present. Hence, one of the central topics in acoustics is how to manipulate these reflections that affect the way the sound propagates, and is ultimately

REFLECTION



perceived.

When sound strikes on a surface, sound is transmitted, absorbed or reflected; the surface’s acoustic properties determine the amount of energy going into transmission, absorption or reflection. The reflected sound can either be redirected by large flat surfaces (specularly reflected) or scattered by a diffusing surface. Architectural acoustic design relates to the room volume, the room shape and the surface treatments. Wallace Sabine, was the first to discover the relationship between sound, space, and material.

Acoustic spaces can be loosely organised into three categories:

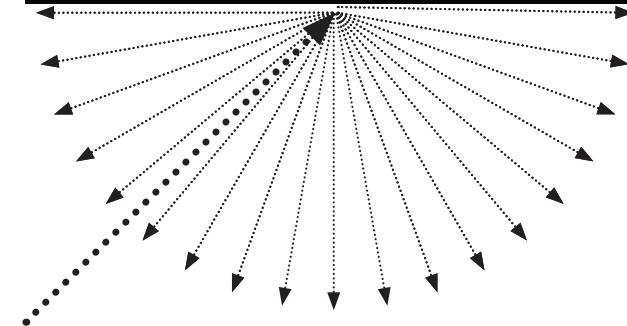
1_sound production space [concert halls for classical music, theatre for speech, etc]

In large sound production rooms, reflection and diffuse reflection are the primary acoustic tools.

2_sound reproduction space [recording studios, home theatres, etc]

In a sound reproduction room acoustics should be

DIFFUSION



neutral. Absorption and diffuse reflection play a key role. Specular reflection is a minor contributor.

3_noise control environments space [gymnasiums, swimming pools, factories, etc]

The objective in this case, is simply to reduce the reverberance and sound level. Uniform distribution of absorption is the primary acoustic tool, and specular reflection and diffuse reflection have more minor roles.

It becomes obvious that the specific demands of the function of architectural space associate with different acoustic manipulations.

This research considers two primary types of acoustic surfaces: absorbers and diffusers. There are also hybrid surfaces that combine these two performance characteristics in different degrees. The information collected in this section attempts to focus mostly on the basic principles and on the established relationship of geometry and material to the physical properties of sound.

Absorbers

Absorbers are usually denoted as porous, panel resonators or Helmholtz resonators, depending upon the primary absorption mechanism. Helmholtz resonators are defined by their geometry; panel resonators are defined by their geometry and structural vibration properties of panel; porous absorbers are defined by their geometry and the acoustic properties of the porous material. In general, the best place for absorption is the ceiling or on the higher parts of walls¹⁹.

_ Porous absorbers²⁰

Typical porous absorbers are carpets, acoustic tiles, acoustic (open cell) foams, curtains, cushions, cotton and mineral wools such as fibreglass. They constitute materials where sound propagation occurs in a network of interconnected pores in such a way that viscous and thermal effects cause acoustic energy to be dissipated²¹. Porous absorbers are widely used to treat acoustic problems, in cavity walls and noisy environments to reduce noise and in rooms to reduce reverberance.

The thickness of the porous material is related to the frequency of sound absorbed. A rough figure sometimes quoted is that the material needs to be at least a tenth of a wavelength thick to cause significant

absorption, and a quarter of a wavelength to absorb all the incident sound. For the porous absorber to create significant absorption, it needs to be placed somewhere where the particle velocity is high. Additionally, the performance of the porous absorber varies with the angle of incidence and the material density.

Material types frequently used to manufacture porous absorbing panels are: mineral wool, foam, sustainable materials, curtains, carpets, acoustic plaster, coustone, aerogel, activated carbon.

_ Resonators²²

There are two common forms of the device: the first is the Helmholtz absorber and the second is a membrane or panel absorber. These treatments are commonly employed to treat low frequency room modes and as parts of silencers within ventilation systems. Wide band absorption is difficult to achieve in one resonator device, and so one of the frequent challenges in the design of those structures is to extend the bandwidth.

Resonant absorbers involve a mass vibrating against a spring. In the case of a Helmholtz absorber, the mass is a plug of air in the opening of the perforated sheet. For a membrane (or panel) absorber, the mass is a sheet of material such as rubber, mass loaded vinyl or plywood which vibrates. The spring in both cases is provided by air enclosed in the cavity.

Diffusers

One of the most significant occurrences in diffuser design, if not the most important event, was the invention of the phase grating diffuser by Schroeder. The Schroeder diffuser offers the possibility of producing 'optimum' diffusion, and also requires only a small number of simple design equations²³.

Schroeder diffusers consist of a series of wells of the same width and different depths. The wells are separated by thin fins. The depths of the wells are determined by a mathematical number sequence. Single plane diffusers cause scattering in one plane, in the other direction, the extruded nature of the surface makes it behave like a plane surface.

The bandwidth of a Schroeder diffuser is limited at high frequencies by the well width and at low frequencies by the maximum depth. To provide full spectrum sound diffusion in a single integrated diffuser, the self-similarity property of fractals can be combined with the uniform scattering property of Schroeder diffusers to produce a fractal diffuser. The surface consists of nested self-similar scaled diffusers, each of which covers a specific frequency range and offers wide area coverage. Most diffuser design is about breaking up wavelengths by surface roughness or impedance changes.

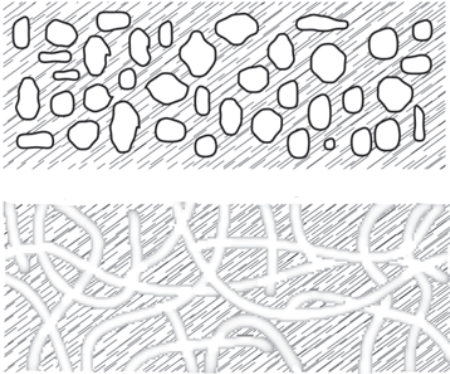
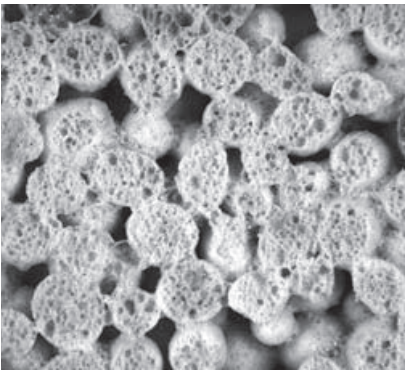
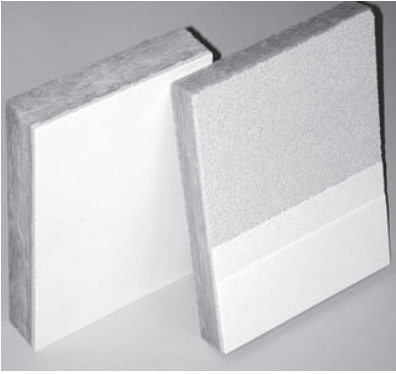
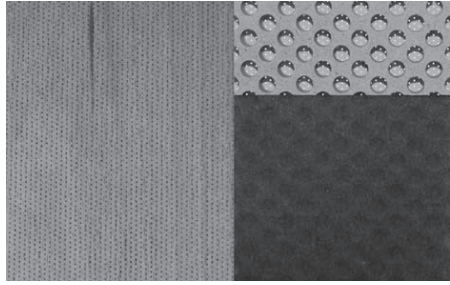
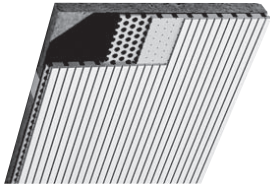
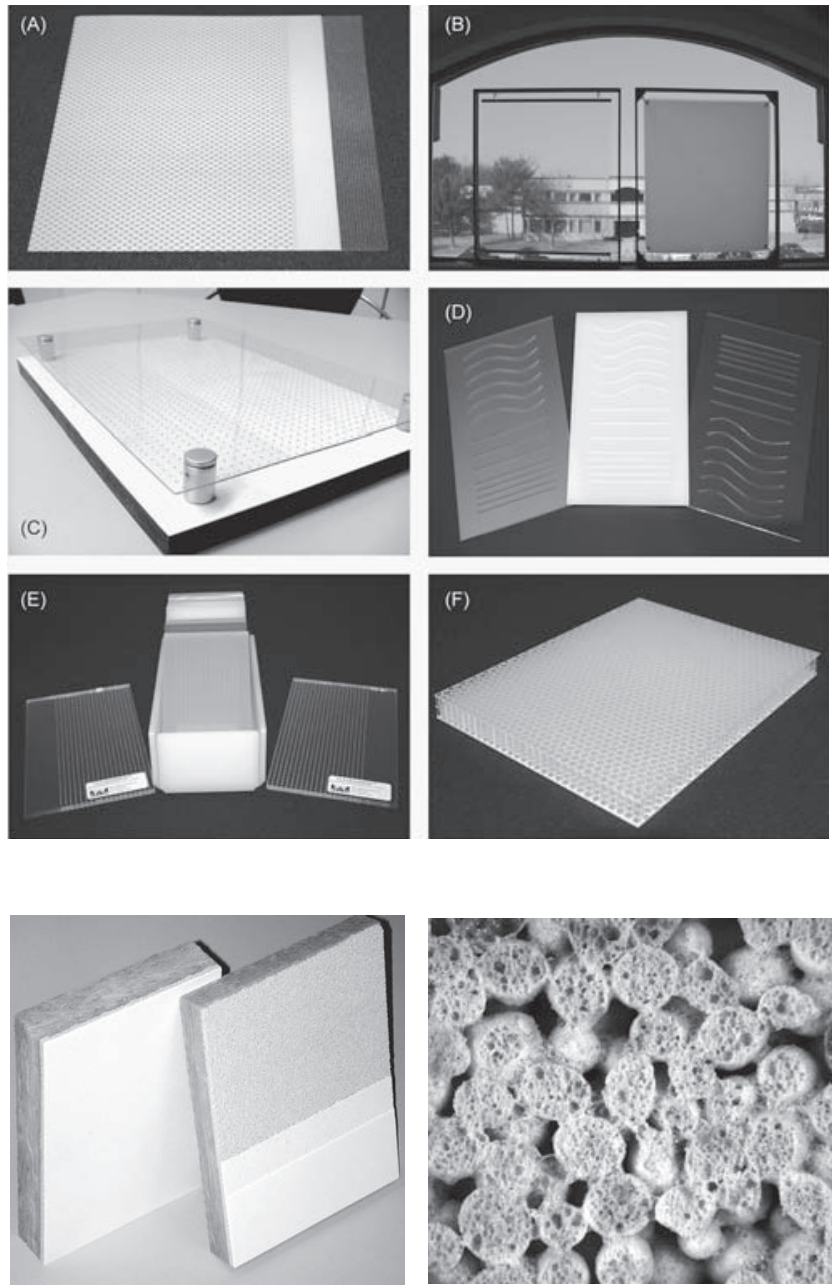
¹⁹ T.J. Cox, P. D'Antonio, *Acoustic Absorbers and Diffusers, Theory, design and application*, Second edition, Taylor & Francis, 2009, pp. 7-30

²⁰ T.J. Cox, P. D'Antonio, *ibid.*, pp. 157-195

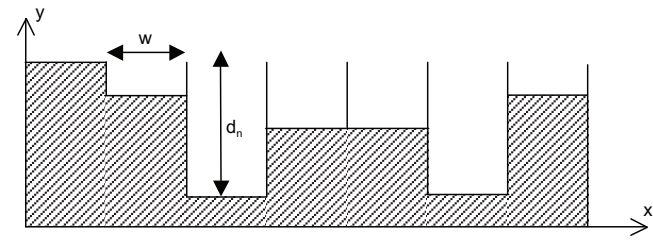
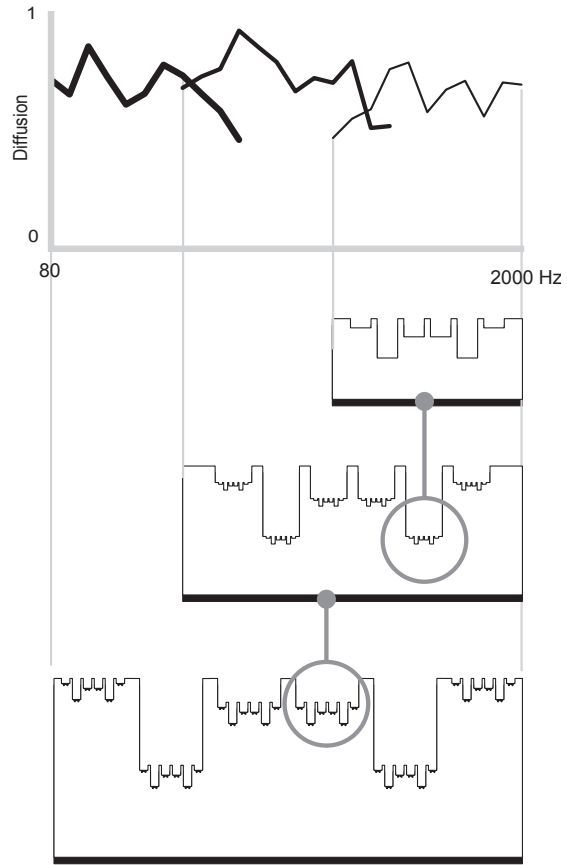
²¹ T.J. Cox, P. D'Antonio, *ibid.*, pp. 157-195

²² T.J. Cox, P. D'Antonio, *ibid.*, pp. 196-229

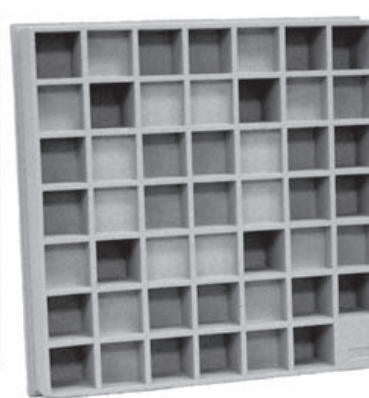
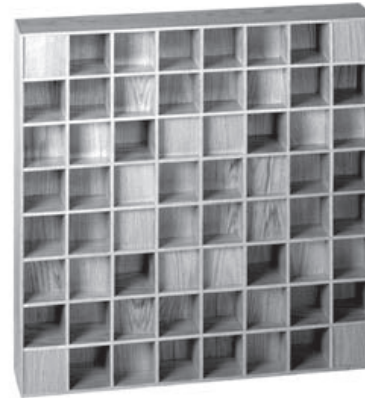
²³ T.J. Cox, P. D'Antonio, *ibid.*, pp. 289-330



Different types of absorbers, applied in the market



A DiffRACTAL®, which imbeds high frequency diffusers within a low frequency diffuser to deal with periodicity, absorption and bandwidth problems (top figure after D'Antonio and Konnert).



Schroeder diffuser

Geometry and sound

It should be remembered that even a plane surface can cause significant diffraction from its edges, provided the surface has a similar size to the acoustic wavelength²⁴. Triangles or pyramids can produce dispersion, redirection and specular reflection depending on the geometry used. Applied correctly, triangles and pyramids can form notch diffusers, where the energy in certain directions is much reduced. Curved surfaces are more obviously diffusers and more universally used; indeed a simple sphere or cylinder is very effective at spatially spreading reflections, but this is not the only ingredient needed for a good diffuser. Furthermore, a solitary sphere or cylinder is not very useful and so many spheres or cylinders next to each other are needed. Then the scattering is as much about how the objects are arranged, periodically or randomly, as about the scattering characteristic of the individual sphere or cylinder. A well-designed curved surface has the advantage of blending with modern architectural designs.

²⁴ T.J. Cox, P. D'Antonio, *ibid.*, pp. 331-372

Acoustic Design Procedure

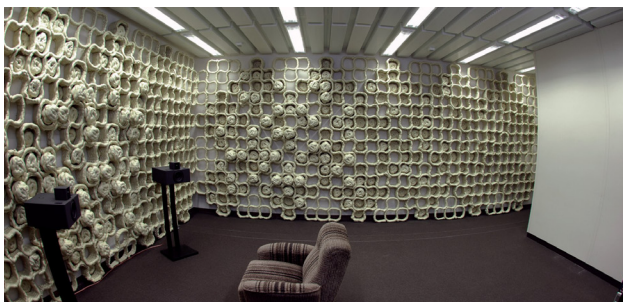
While being on the procedure of designing the acoustics of a space, it becomes crucial to first clarify the space's future purpose use²⁵. Additionally, it is necessary to gain some idea of the objective structure of the sound field to be expected, for instance the values of the parameters characterising the acoustical behaviour of the room etc. There are also a few objective sound field properties which determine the acoustic performance of space and need to be taken into consideration during the design process; they depend on constructional data and become crucial in acoustic performance. These are the shape of room, the volume of the room, the space layout and materials.

Currently there is a lack of generally accepted procedure which leads with absolute certainty to a good result. Nevertheless, a few standard methods of acoustical design have evolved which have proven useful.

²⁵ H. Kuttruff, *op.cit.*, pp. 294-330



1

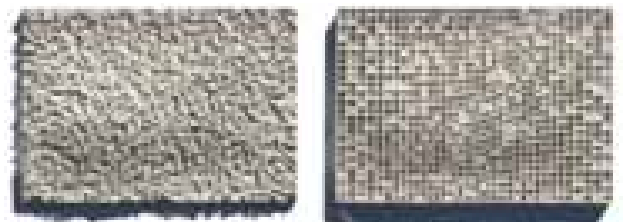


2

1: wall panel structure made by SLS (Loughborough University)

2: acoustical active wall panels (ETH Zurich)

3: Parametric Acoustic Surfaces (CITA)



3

The in-parallel investigation of the fields of AM and acoustics outlines a fascinating opportunity of using AM for the manufacturing of acoustic panels. Acoustic panels among other building elements seem to be suitable for applying AM. While, specific demands and constraints of acoustic panels such as material resolution, scale, etc seem to be satisfied by the production technique.

Furthermore, AM in combination with specialised design tools can form and materialize new acoustically performative geometries.

Relevant research projects

It seems that there is a stream of thought that moves towards the same direction. Relevant research projects have been conducted in various universities and institutes, including ETH Zurich, CITA and Loughborough University.

In 2007, the research team of Loughborough University investigated the implications of solid fabrication on acoustic absorbers²⁶. Selective laser sintering has been used in the investigation of the performance and manufacturing possibilities and limitations of a novel destructive interference absorber. The nature of the geometry of the novel absorber has demonstrated that the design flexibility afforded by solid freeform fabrication processes holds potential for

²⁶ O.B. Godbold, R.C. Soar, R.A. Buswell, Implications of solid freeform fabrication on acoustic absorbers, *Rapid Prototyping Journal*, Issue 13, Volume 5, 2007, pp. 298–303

applications incorporating new types of acoustic absorber.

One year later, a team from ETH Zurich explored the design and application of digitally fabricated wall panels for room-acoustical architectural interventions. In particular, they investigated the room-acoustical criteria applying to everyday used spaces. They proposed a digital design and fabrication process developed to create non-standardised panels and examined two case studies where the process was applied on the acoustical improvement of a specific room situation²⁷.

Brady Peters from CITA, has published in 2009 and 2010 the results of his research in developing digital parametric tools that enable sound to be a design parameter in architecture²⁸.

The different approaches to the same topic might differentiate in their focus or at their starting point. They share the beliefs that sound modulation during the design process can improve the performance of physical space and that the new techniques allow designers to think of new types of sound devices.

²⁷ T. Bonwetsch, R. Baertschi, S. Oesterle (2008), Adding Performance Criteria to Digital Fabrication Room-Acoustical Information of Diffuse Resonant Panels, *Silicon+Skin, Biological Processes and Computation*, Proceedings of the 28th Annual Conference of the Association for Computer Aided Design in Architecture, Minneapolis, pp. 364-369

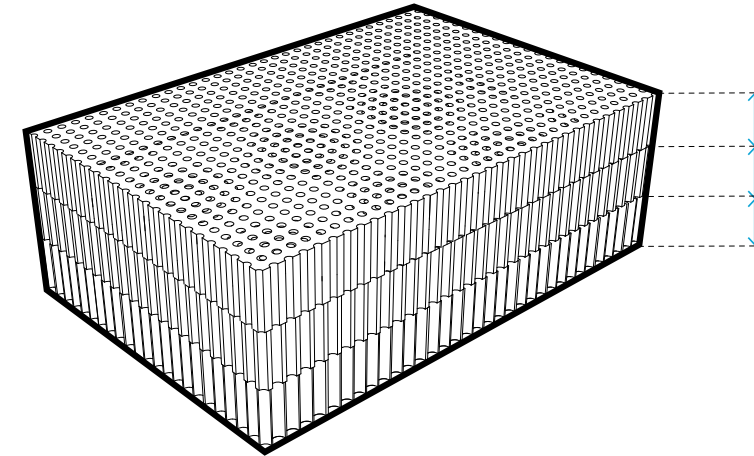
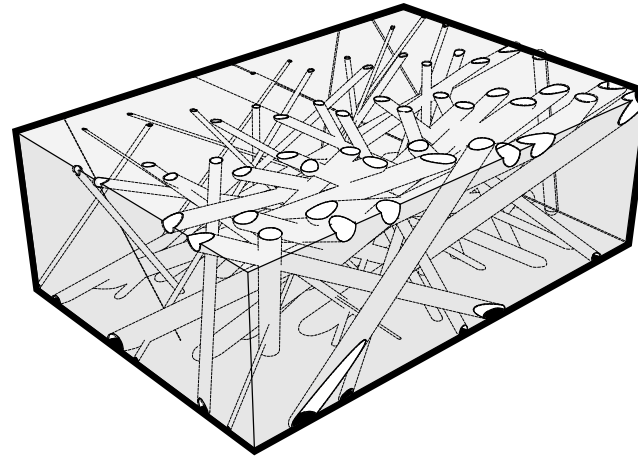
²⁸ B. Peters, Parametric Acoustic Surfaces, *ACADIA 09: reForm()*: Proceedings of the 29th Annual Conference of the Association for Computer Aided Design in Architecture (ACADIA) pp. 174-181

Scenario 1:
Passive destructive interference

Scenario 2:
Grading surface on material surface

$$f = c / 2(l_2 - l_1)$$

[c] speed of sound in air
[l₁] length of the short
air path
[l₂] length of the longer
air path



Two scenarios on absorbers:

1_Passive destructive interference

The concept suggests the absorption of sound by passive destructive interference. Active absorption systems use this principle by applying an out of phase sound field to incoming sound waves. The two waves interfere destructively cancelling the sound energy from both sources creating a reduction in overall sound level.

The challenge for this work will be to investigate the possibility of designing a passive-destructive absorber. The principle advantage of this approach is the increased freedom in the design which has the potential for conformal shaping.

2_Grading density of material structure

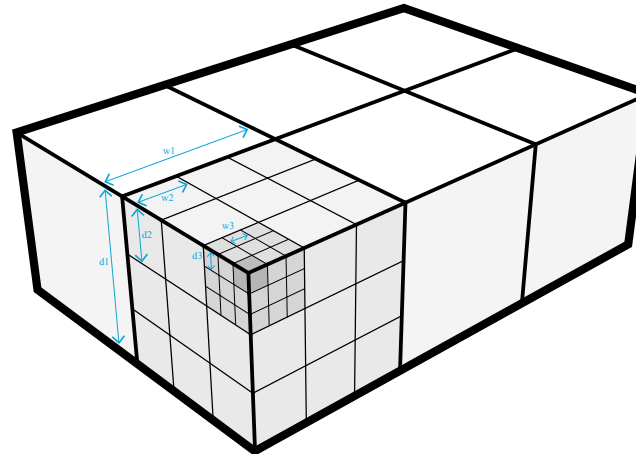
This scenario is loosely based on the multi-layer absorbers principle. In general, to ensure the acoustic absorption of the multi-layer absorbers, selecting appropriate absorbing materials is the primary concern. Several recent literatures depicted that the surface geometry of absorbing materials also control the performance of the acoustic absorption. However, there are still limited investigations on the influence of the inner structures employed in the multi-layer absorbers. One of the main objectives of this concept would be to study the effect of the inner structures on the acoustic absorption of the multi-layer absorbers.

The extended research on AM and acoustics, leads to the proposal of four different design concepts. The proposals refer to absorbing or diffusing devices which intent to take full advantage of the fabrication technique.

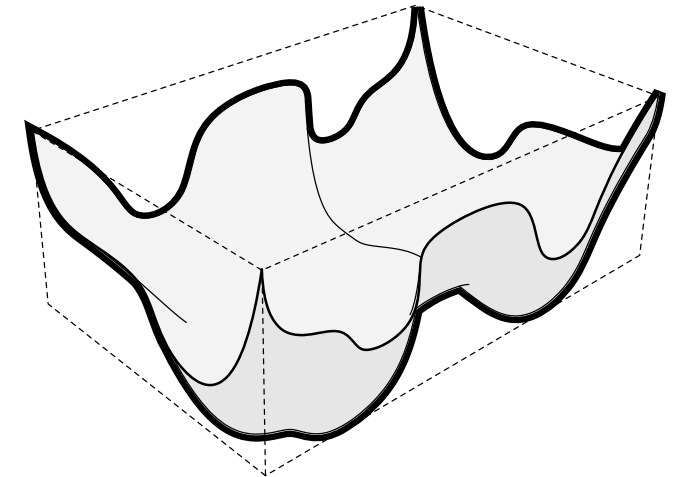
Scenario 3:
Fractal Diffuser

$w = \lambda / 2$
[w] width of cube
[λ] wavelength

$d = \lambda_0 / 2$
[d] depth of cube
[λ_0] design wavelength



Scenario 4:
Optimization of curved surface



Two scenarios on diffusers:

3_Fractal Diffuser

This concept suggests the design of a sound diffusing device that covers the full sound spectrum based on the Schroeder diffuser principle. The bandwidth of a conventional Schroeder diffuser is limited at high frequencies by the well width and at low frequencies by the maximum depth. To provide full spectrum sound diffusion in a single integrated diffuser, the self-similarity property of fractals can be combined with the uniform scattering property of Schroeder diffusers to produce a fractal diffuser. The proposed diffusing surface will consist of nested self-similar scaled diffusers, each of which will cover a specific frequency range and will offer wide area coverage. Each diffuser will provide uniform scattering over a specific range of frequencies so that the

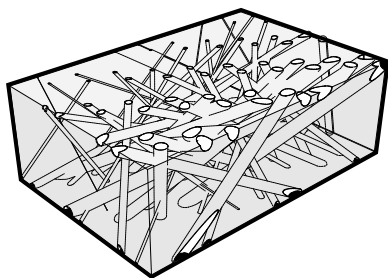
effective bandwidth is extended. Fractals are surfaces with a different visual aesthetic compared to common sound diffusers and so offer the possibility of expanding the pallet of surfaces available to designers.

4_Optimised curved surface

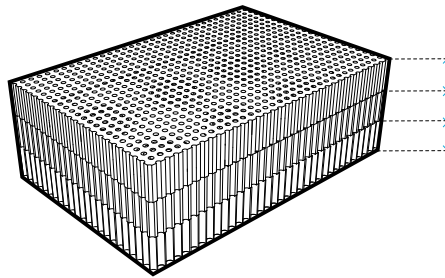
The hypothesis in this case, is that each architectural space is unique and therefore the diffusing surface needs to adjust to its specific acoustic demands. AM supports both to the suggested complex (curved) geometry and the customised solutions. Optimization processes are common techniques and have been exploited in a wide range of engineering applications.

To achieve an optimization of diffusers, several key ingredients need to be in place: a validated prediction model, a figure of merit or error parameter, an optimization algorithm to change the well depth sequences, etc. One advantage of curved diffusers over more complex surfaces is their simpler construction leading to potentially lower costs and lower absorption. An increase in the number of harmonics in the series increases the complexity of the diffuser shape which may cause excess absorption and increased cost.

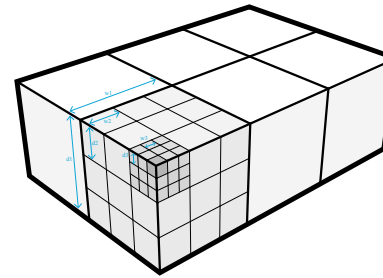
- +
- -



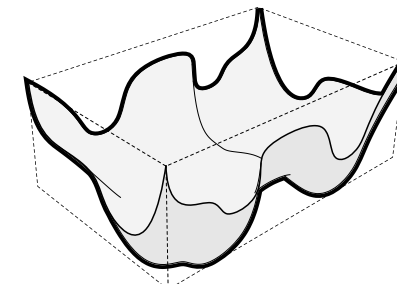
Scenario 1:
Passive destructive interference



Scenario 2:
Grading density of material structure



Scenario 1:
Fractal Diffuser



Scenario 2:
Optimization of curved surface

Geometry:	● ● ○ ○ ○ ○
Fabrication:	● ● ● ● ○
Measurement:	● ● ● ● ●
Market:	● ● ● ● ○

Geometry:	● ○ ○ ○ ○
Fabrication:	● ● ○ ○ ○
Measurement:	● ● ● ● ●
Market:	● ● ● ● ○

Geometry:	● ● ● ○ ○
Fabrication:	● ● ● ● ○
Measurement:	● ○ ○ ○ ○
Market:	● ● ● ○ ○

Geometry:	● ● ● ● ○
Fabrication:	● ● ● ● ○
Measurement:	● ○ ○ ○ ○
Market:	● ● ● ○ ○

Decision making

The four concepts are evaluated according to the following criteria:

1_ relevance of acoustic principle to **geometry**:

In general, the performance of diffusers is more obviously related to geometry, in a reasonable and manufacturable scale. In contrary, sound absorption (especially at mid and high frequencies) is usually based on material properties and not to on geometrical configurations.

2_ **fabrication**

All the proposed scenarios on absorbers and diffusers are possibly fabricated with AM. There is an indication that the prototypes of the scenario 2 (grading

density of material structure) might be difficult to be post-processed due to the small scale of their gaps.

3_ **measuring technique**

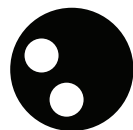
It is well known, that there are standardised methods that give directions on how to measure both absorbers and diffusers. The criteria in this case relates mostly to our accessibility to the needed measuring equipment and the corresponding size of the sample [see also: Appendix]. The measurement of the absorbers seem to be more advantageous for both parameters.

4_ Available **market**

Sound absorbing devices are more widely utilised

within buildings to modulate the room acoustics. In this sense, the idea to further develop an absorber concept might be more interesting since there are more application possibilities.

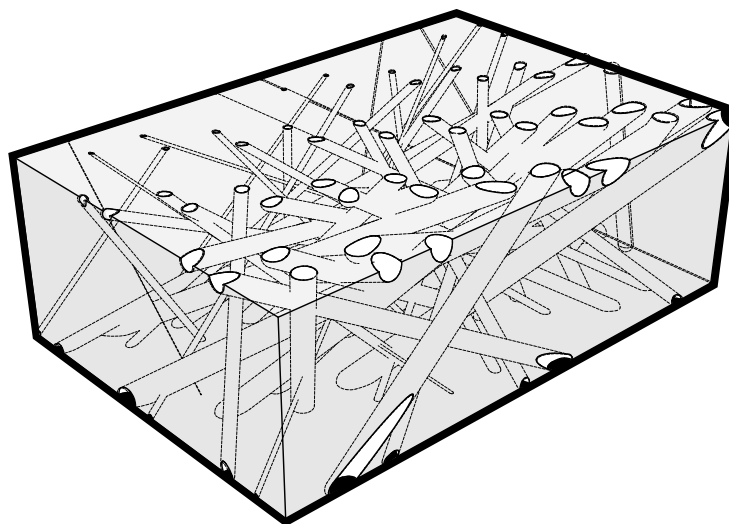
The assessment of the 4 concepts according to the proposed criteria indicates that the scenario of the passive destructive interference absorber is appropriate at most to continue further.



Concept: Passive Destructive Interference

$$f = c / 2(l_2 - l_1)$$

[c] speed of sound in air
[l₁] length of the short
air path
[l₂] length of the longer
air path



In physics, **interference** is a phenomenon in which two waves superimpose to form a resultant wave of greater or lower amplitude. Interference usually refers to the interaction of waves that are correlated or coherent with each other, either because they come from the same source or because they have the same or nearly the same frequency. Interference effects can be observed with all types of waves, for example, light, radio, acoustic, and surface water waves¹.

When the crests overlap, the superposition wave reaches a maximum height. This height is the sum of their amplitudes. This sort of interference is called **constructive interference**, because it increases the overall amplitude.

Alternately, when the crest of a wave overlaps with the trough of another wave, the waves cancel each other out to some degree. If the waves are symmetrical (i.e. the same wave function, but shifted by a phase or half-wavelength), they will cancel each other completely. This sort of interference is called destructive interference. The two interfering waves do not need to have equal amplitudes in opposite directions for **destructive interference** to occur.

Destructive interference can be applied in sound absorbers. Active absorption systems already use this principle by applying an out of phase sound field to incoming sound waves.

The challenge for this work was to investigate the possibility of designing a passive-destructive absorber. There is little or no work published in the literature on this subject.

The speed of sound in air can be considered constant, within fixed atmospheric conditions. If an incident sound wave is sent along two paths of different length, the two waves will be out of phase at a given point. The amount of phase shift between the two waves is dependant on the relative path lengths and the wavelength of the sound. When the difference between path lengths is equal to half the incident wavelength, the waves will be 180° out of phase and the combined sound waves will destructively interfere. The frequency of absorption f (Hz) can be expressed as:

$$f = (2n-1)*c / 2*\Delta L$$

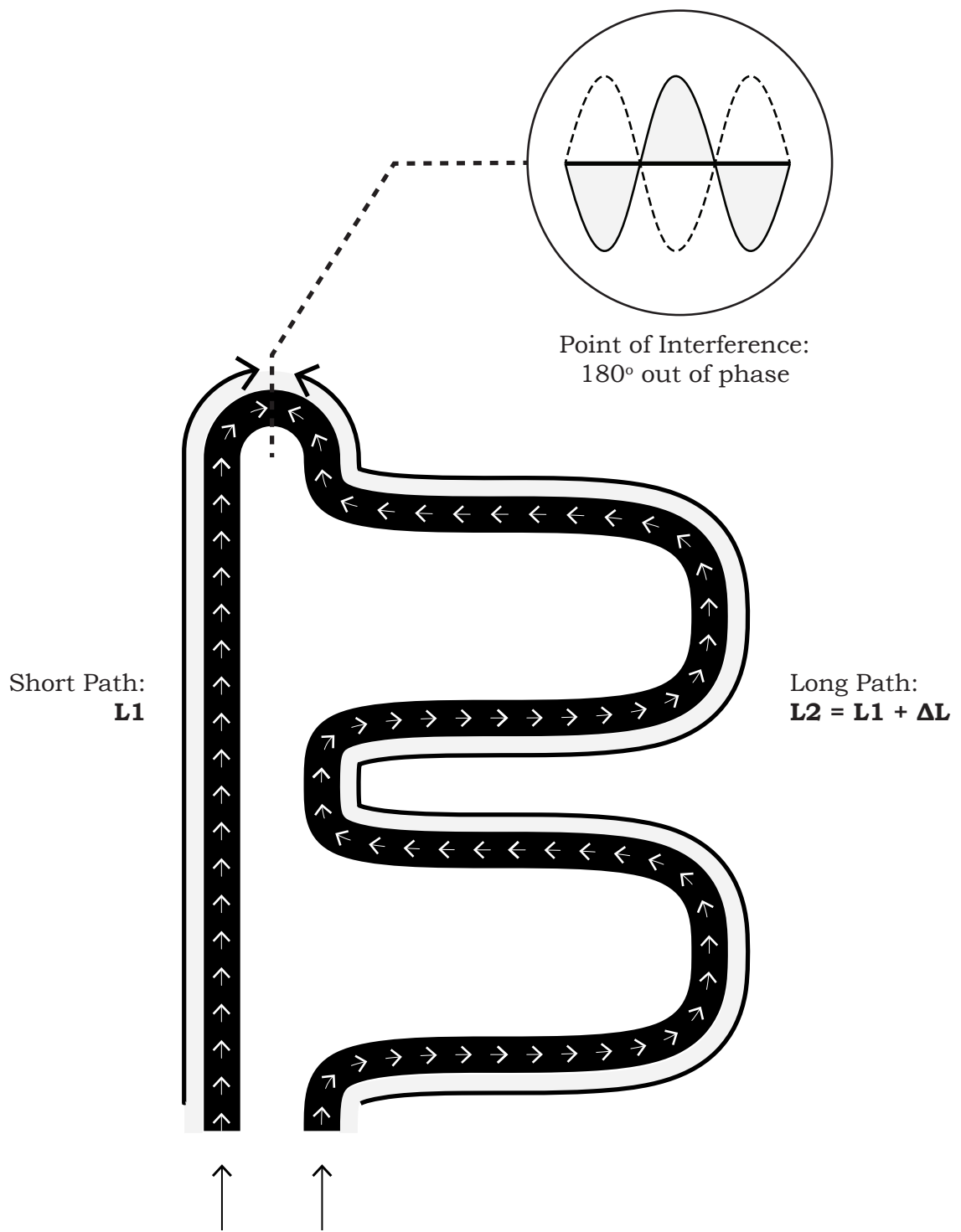
where ΔL (m) is the length of the long air path minus the length of the shorter air path.

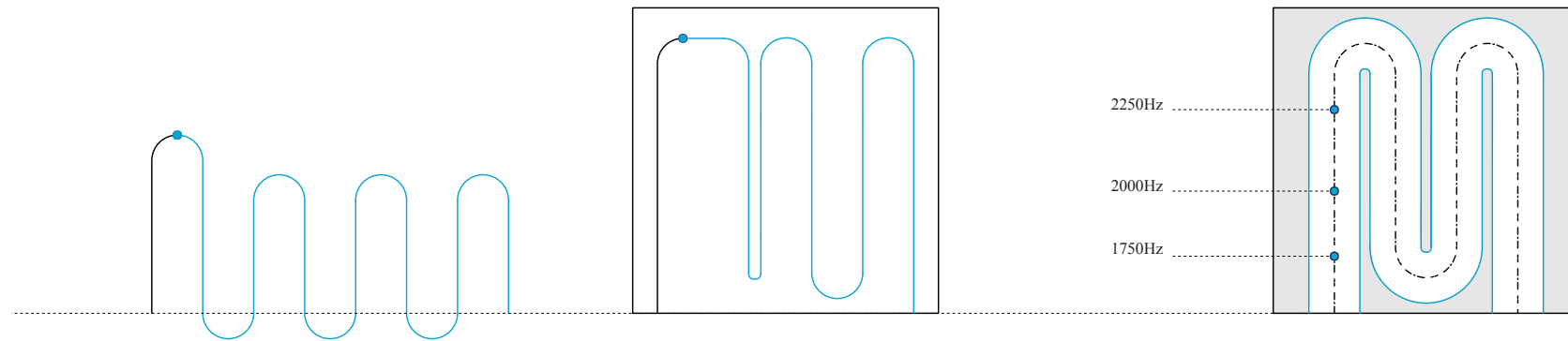
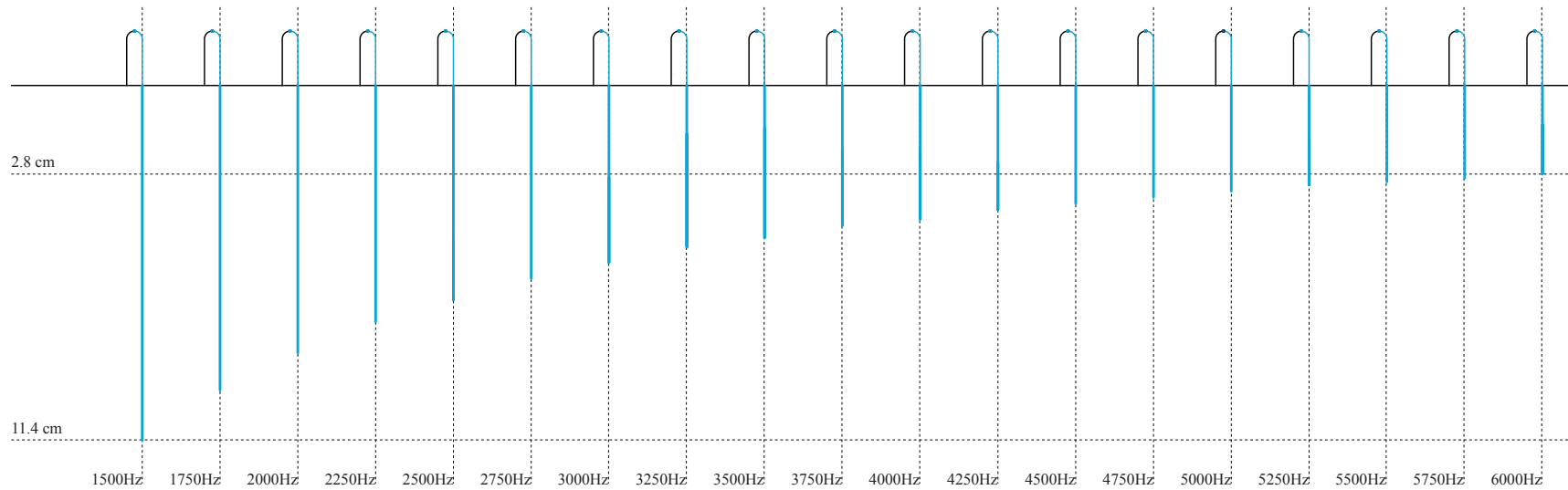
¹⁰ [http://en.wikipedia.org/wiki/Interference_\(wave_propagation\)](http://en.wikipedia.org/wiki/Interference_(wave_propagation)) (last visit: 01/05/2012)

the principles of operation of the passive, destructive interference device

$$f = (2n-1) c / 2 (L2 - L1)$$

- [f] frequency
- [c] speed of sound in air
- [n] random integer
- [L1] length of the short air path
- [L2] length of the long air path





Unfortunately, the literature review did not reveal much more on the theory of passive destructive interference. For this reason, it was critical to proceed in some physical tests, to better understand the phenomenon.

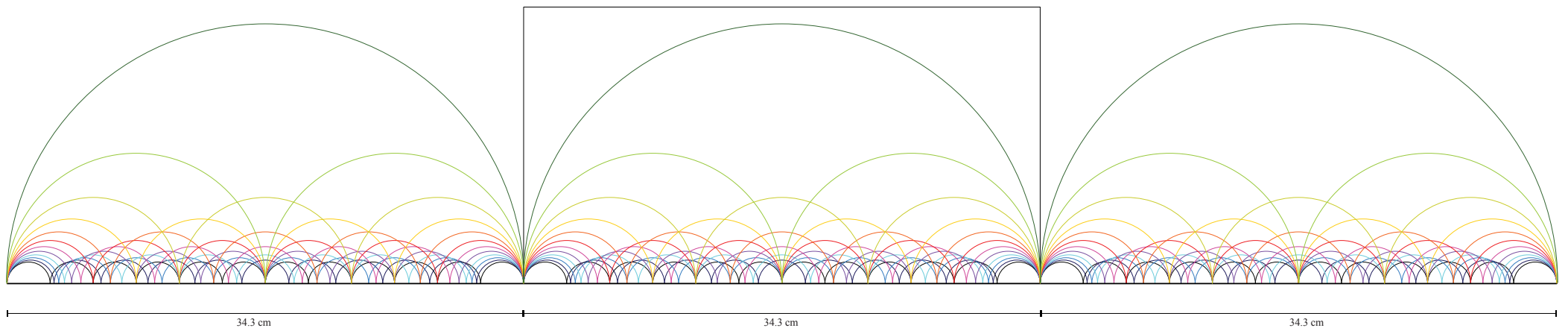
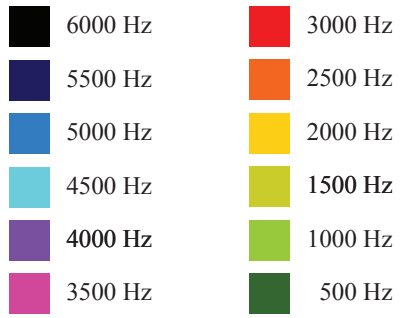
A first reaction was to comprehend the given equation and doing some first assumptions. By visualising the different ΔL with their corresponding frequencies, it was speculated that there was no need to design air-paths which are assigned to one specific

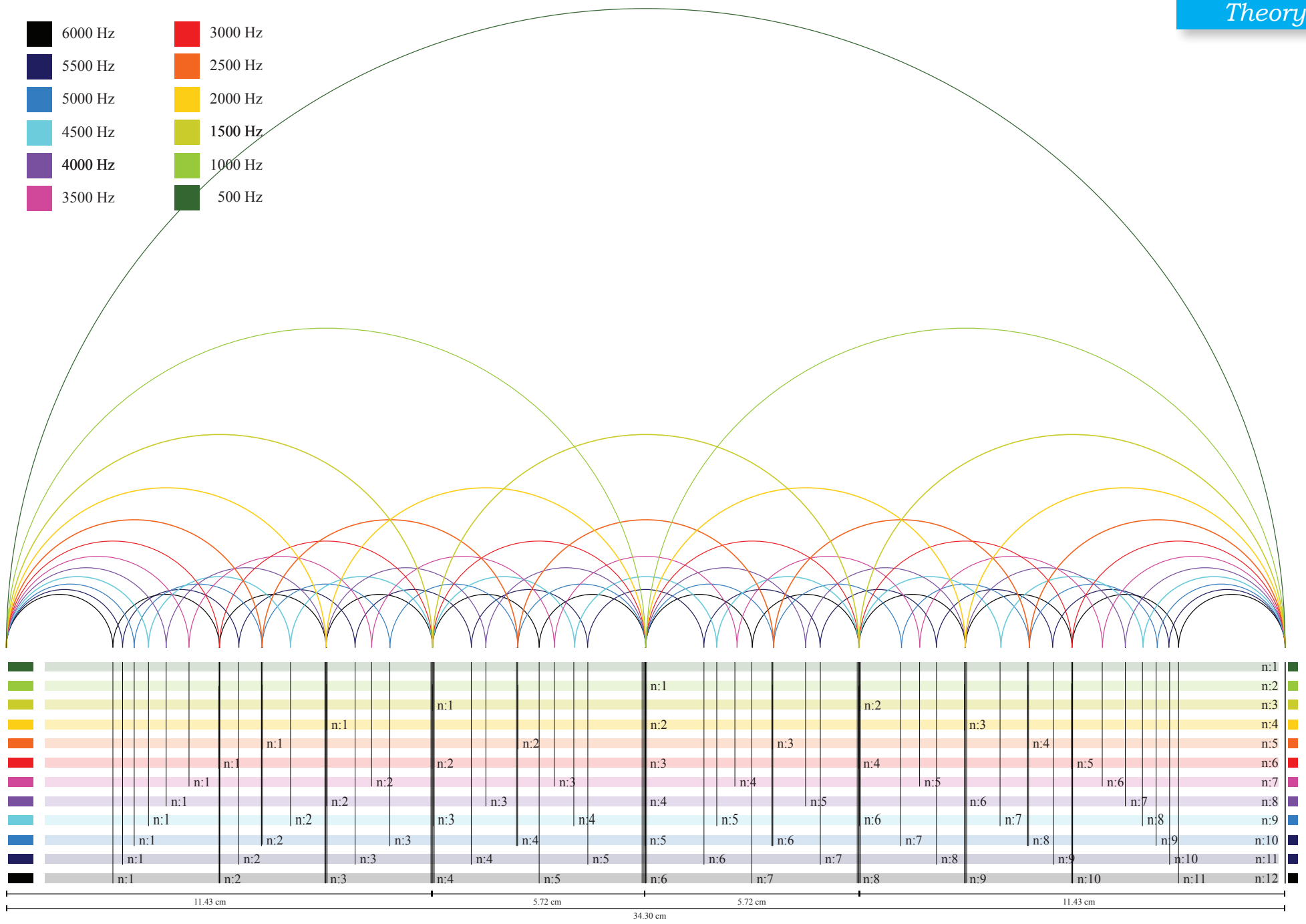
frequencies. The theory is not neglecting the possibility that along one air-path, more wavelengths would cancel each other at a different point. In other words, if this assumption turns to be true, one air-path would absorb more frequencies.

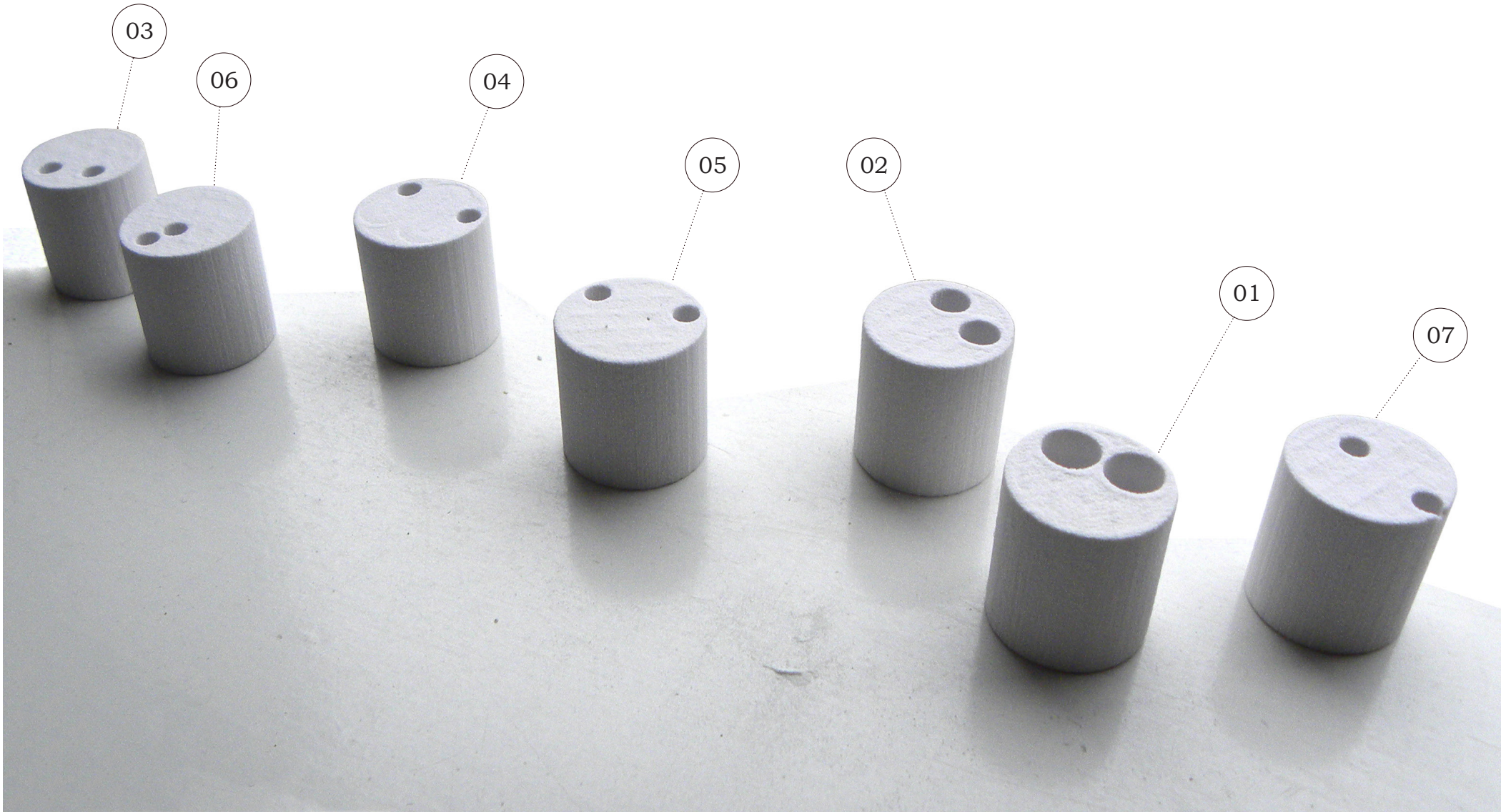
A different approach in visualising theory was by designing circles with radius equal to length given at a specific frequency. Doing so for frequencies between 500 and 6000Hz, it becomes obvious that a repetition pattern emerges every 34.3cm, where all

frequencies "synchronise". A close up to one period reveals also additional "interesting" lengths at : 17.15cm [where half of the examined frequencies meet], 11.43cm [where one third of the examined frequencies meet], etc.

But, still there are a lot of gaps in theory that need to be filled in. It is not clear yet if and how geometry in terms of **length**, **diameter** and **shape** can manipulate acoustic performance.







In order to fill in the gaps of the theory, to understand better how the principal works and to confirm the first assumption, it was decided to proceed in making physical tests. As a starting point, it was preferred to work with small samples and measure the acoustic performance of the specimens. The impedance tube was the most suitable tool for this reason.

The main aim of this chapter is to define the relation between the performance of the absorber and its geometrical specifications: air-tube diameter, air-tube length and air-tube geometry.

Design of the samples

The shape and configuration of the samples were designed to fit within the test apparatus. The overall volume of the test pieces that house the absorbers is restricted by the apparatus to be cylindrical and have a volume of 21.2 cm³ [diameter of 3cm and 3cm height]. The small size of the samples limited the design options. However, this does not mean that the final sound absorber will be restricted to the sample's geometry. The main idea was to test one parameter per sample and by comparison, cover more questions.

For this set of measurements, seven samples have been designed and fabricated. The measurements of the samples were expected to confirm the assumptions and better define the parameters that affect the acoustic performance of the sound absorber. The first results are mostly intended to indicate if a parameter is effective or not. Due to the small amount of the specimens, it will be hard to make general conclusions. In order to limit the percentages of failure to the conclusions, the samples are designed

in a very simple way so that only one parameter is tested each time. So, when testing the diameter, length and geometry are identical [sample 1, 2, 3]. When testing the length, diameter and geometry are identical [sample 4, 7 and 5, 6]. When testing geometry, length and diameter are the same [sample 4, 5 and 6, 7].

Fabrication

The samples of the preliminary measurements were fabricated with the machines facilitated by the faculty of Architecture TU Delft. The faculty owns two different types of rapid manufacturing machines:

- the Z310 from Zcorp, which prints in starch powder [zp131].
- the Dimension Elite, which prints in ABS+ plastic.

The Z310 was chosen for several reasons: more economical, faster and most important: it is powder based technique. This allows the easy removal of the powder within the complex geometry of the air-tubes of the sample.

The samples with long and geometrically complex air tubes were more demanding in post-processing. It was difficult to remove the powder and to verify that the samples were completely cleaned. The removal of unsintered powder from the enclosed areas was accomplished with the use of compressed air. The remaining powder can affect the absorption results, providing resistance which may increase absorption.

Measurements

The first measurements took place in a company specialised in the fields of acoustic, called Peutz bv [Mook/ Molenhoek/ <http://www.peutz.nl/>] on the 14th of March 2012.

For the preliminary measurements, it was used the impedance tube with a testing diameter of 3cm [Bruel & Kjaer].

With this tool, the direct absorption coefficient has been measured at the following frequencies: 800/ 1000/ 1250/ 1600/ 2000/ 2500/ 3150/ 4000/ 5000 Hz.

The term sound absorption coefficient [α], describes the ratio of the sound power entering the surface of the test object (without return) to the incident sound power for a plane wave at normal incidence¹.

The **normal sound absorption coefficient** follows the measured amplitudes |P_{max}| and |P_{min}| at a given frequency. If the sound pressure in the impedance tube is measured in a logarithmic scale (in decibels), and the difference in level between the pressure maximum and the pressure minimum is ΔL dB, then:

$$S = 10^{\frac{\Delta L}{20}}$$

The sound absorption coefficient then follows from:

$$\alpha = \frac{4 \cdot 10^{\frac{\Delta L}{20}}}{\left(10^{\frac{\Delta L}{20}} + 1\right)^2}$$

It is notable that the normal sound absorption coefficient constitutes a reliable indication of the absorber's performance. Despite this fact, it is not necessarily relating to the absorber's performance at random sound incidence.

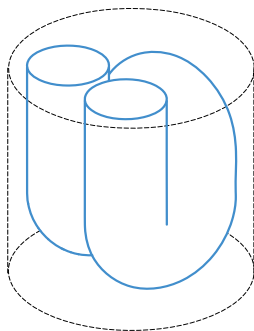
The measurements followed the international stand-

¹ ISO 10534-1:1996

Diameter

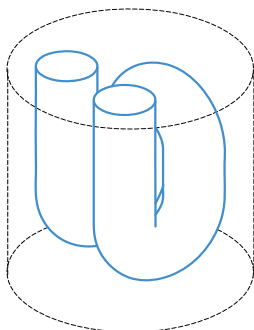
n 0.1

$L_{tot} = 10.28\text{cm}$
 $D = 1.00\text{ cm}$



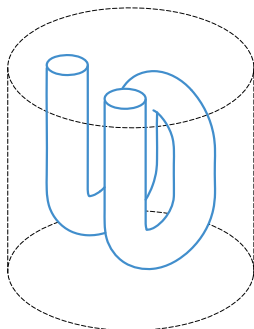
n 0.2

$L_{tot} = 10.28\text{cm}$
 $D = 0.75\text{ cm}$



n 0.3

$L_{tot} = 10.28\text{cm}$
 $D = 0.5\text{ cm}$

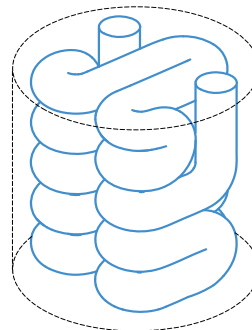


Geometry

Length

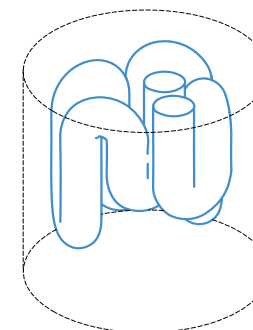
n 0.4

$L_{tot} = 36.7\text{cm}$
 $D = 0.5\text{ cm}$



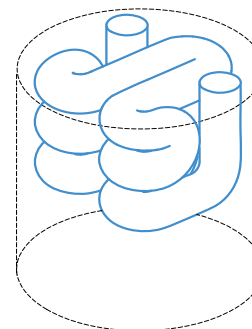
n 0.6

$L_{tot} = 19.55\text{cm}$
 $D = 0.5\text{ cm}$



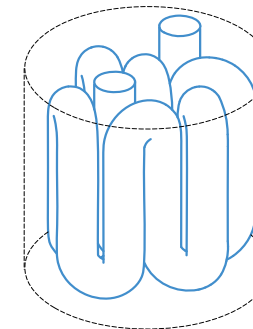
n 0.5

$L_{tot} = 19.55\text{cm}$
 $D = 0.5\text{ cm}$



n 0.7

$L_{tot} = 36.7\text{cm}$
 $D = 0.5\text{ cm}$



The analysis of the results begins with the recognition of the acoustic phenomena that occur during the measurements.

In some cases, destructive interference is not taking place. For this reason further calculations are executed with the intention to comprehend if the specimens are performing according to other known resonant absorption principles. Each sample's performance is evaluated according to its compatibility and accordance to the following acoustic phenomena:

1. Passive destructive interference

[see also: p. 21-25]

The speed of sound in air can be considered constant, within fixed atmospheric conditions. As mentioned before, if an incident sound wave is sent along two paths of different length, the two waves will be out of phase at a given point. The amount of phase shift between the two waves is dependant on the relative path lengths and the wavelength of the sound. When the difference between path lengths is equal to half the incident wavelength, the waves will be 180° out of phase and the combined sound waves will destructively interfere.

$$f = \frac{(2n - 1)c}{2\Delta L}$$

- [f] interference frequency [Hz]
- [c] speed of sound in air [m/s]
- [n] random integer 1, 2, 3, ...
- [ΔL] difference in length [m]

The difference in length [ΔL] relates to the location of the interference point, which is not defined by theory. In this study, it is proposed that interference occurs between the 1/4 [one-quarter] of the total

length of the air path and the upper surface of the absorbers. This suggestion can be expressed as a set of boundaries that describes ΔL as follows:

$$L_{tot}/2 < \Delta L < L_{tot}$$

From this interpretation of ΔL, derives also a set of boundaries that predicts the frequencies where destructive interference occurs:

$$\frac{(2n - 1)c}{2 L_{tot}} < f < \frac{(2n - 1)c}{L_{tot}}$$

The development of the two bands of values for ΔL and f, will play a key role in the analysis of the measured performance of the samples in the following chapters.

2. Quarter wavelength tube

Quarter wave tubes have normally one open and one closed end and are uniform in their cross-sectional extents along their lengths. Their length is the one-fourth of the wave length of the frequency which they are to attenuate. A sound wave entering the tube will travel to the closed end and will be reflected back to the entrance where it arrives opposite in phase to the oncoming wave. This interference between the two waves results in attenuation¹.

In the case of the tested samples, the open end lies on the upper surface and the close end in the middle of the air-path. In this sense, each sample contains 2 quarter wavelength tubes. The following equation describes the principle:

$$\frac{L_{tot}}{2} = (2n - 1) \cdot \frac{\lambda}{4}, \text{ this results the equation bellow:}$$

¹ <http://www.google.nl/patents?hl=nl&lr=&vid=USPAT3396812&id=UHXWAAAAEBAJ&oi=fnd&dq=quarter+wave+tubes&printsec=a&stract#v=onepage&q=quarter%20wave%20tubes&f=false> [last visit: 11/06/2012]

$$f = \frac{(2n - 1)c}{2 L_{tot}}$$

- [f] interference frequency
- [c] speed of sound in air
- [n] random integer 1, 2, 3, ...
- [L_{tot}] total length of the air path. Here: L_{tot} = 0.5*L_{tot}

It is notable that the formula that defines the quarter wavelength tube coincides with the minimum value for the destructive interference frequency band, as proposed in the previous paragraph.

3. Helmholtz resonator

Air in a cavity, whose dimensions are small compared with the wavelength, acts as a spring. When the cavity has a small opening to the outside air, the air in the neck moves as a single mass, the mechanical analogue of which is a mass supported by a spring, thus forming a simple resonator. This is called Helmholtz resonator². The resonance frequency, is given by³:

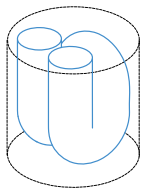
$$f = \frac{c}{2\pi} \sqrt{\frac{S}{V2\Delta L}}$$

- [f] resonance frequency
- [c] speed of sound in air
- [S] area of the opening
- [V] cavity volume
- [ΔL] end correction. In this case: ΔL = $\frac{4d}{3\pi}$

² Z. Maekawa, J.H. Rindel, P. Lord, Environmental and architectural acoustics, Spon Press, 1997, p. 120

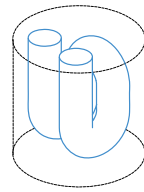
³ The proposed equation is a simplified version of the original equation $f = \frac{c}{2\pi} \sqrt{\frac{S}{V(I + 2\Delta L)}}$

[I+ΔL] corresponds to the effective neck length. Here: L = 0.



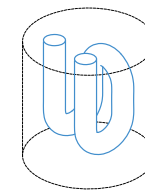
n 0.1

Ltot = 10.28 cm
D = 1 cm



n 0.2

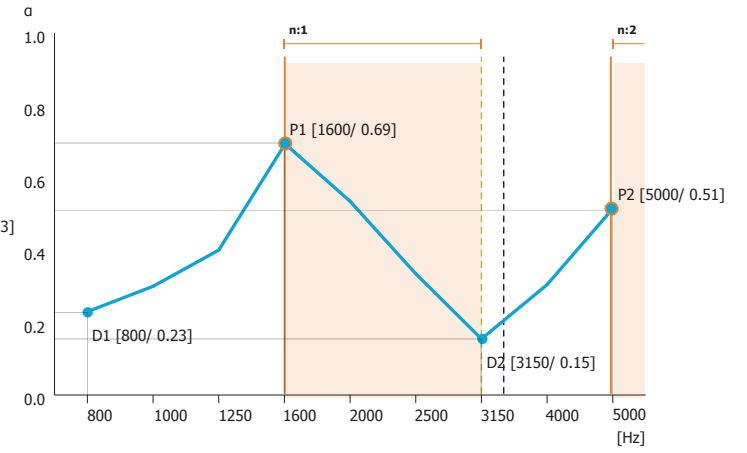
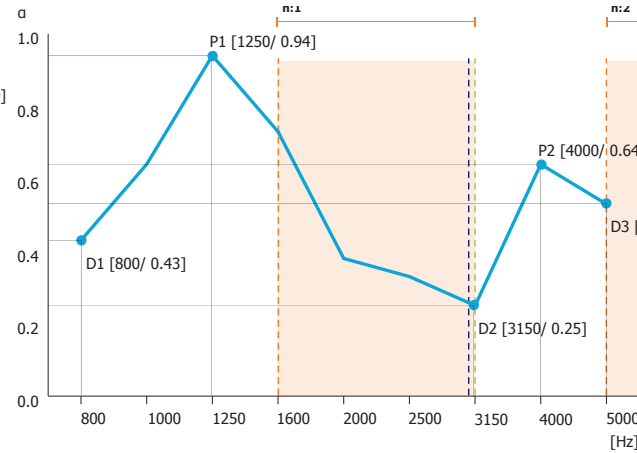
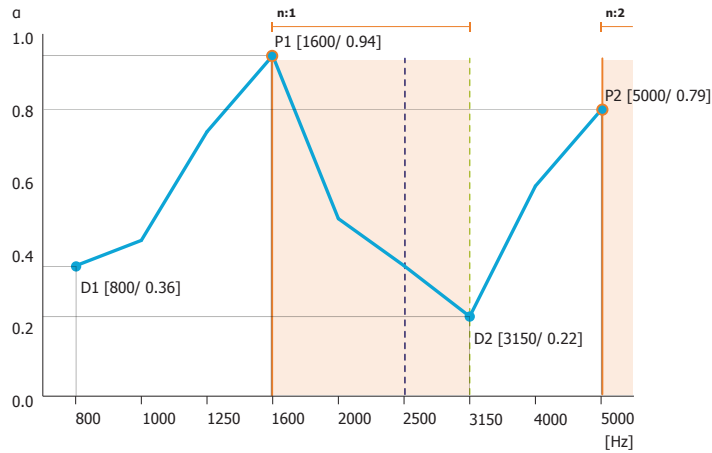
Ltot = 10.28 cm
D = 0.75 cm



n 0.3

Ltot = 10.28 cm
D = 0.5 cm

- Destructive Interference
- Quarter Wavelength tube
- Helmholtz Resonator



Sample 0.1

Sample 0.1 has a global diameter of 2.8 cm and height 3cm. It contains one air-path with a total length of 10.28 cm and with a diameter of 1 cm. According to the theory, peaks are expected to occur in two frequency bands: 1668-3336 Hz (n=1) and 5004-10009 Hz (n=2).

During the measurements, 2 peak frequencies have been identified, namely at 1600 Hz ($\alpha=0.94$) and 5000 Hz ($\alpha=0.79$). Both peaks are located within the suggested frequency bands. Therefore, the measured results are considered as fully aligned with theory of **destructive interference**. Further investigation shows that the sample is not behaving as a Helmholtz resonator ($f=2613\text{Hz}$), nor as a quarter wavelength tube ($f=3336\text{Hz}$).

Sample 0.2

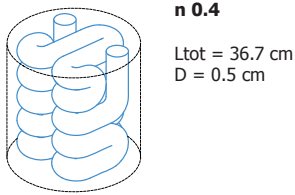
Sample 0.2 has a global diameter of 2.8 cm and height 3cm. It contains one air-path with a total length of 10.28 cm and with a diameter of 0.75 cm. According to the theory, peaks are expected to occur in two frequency bands: 1668-3336 Hz (n=1) and 5004-10009 Hz (n=2).

During the measurements, 2 peak frequencies have been identified, namely at 1250 Hz ($\alpha=0.94$) and 4000 Hz ($\alpha=0.64$). Non of the peaks is located within the suggested frequency bands. Further calculations show that the sample is not behaving as a Helmholtz resonator ($f=2613\text{Hz}$), nor as a quarter wavelength tube ($f=3336\text{Hz}$).

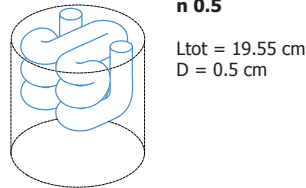
Sample 0.3

Sample 0.3 has a global diameter of 2.8 cm and height 3cm. It contains one air-path with a total length of 10.28 cm and with a diameter of 0.5 cm. According to the theory, peaks are expected to occur in two frequency bands: 1668-3336 Hz (n=1) and 5004-10009 Hz (n=2).

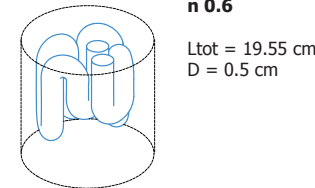
During the measurements, 2 peak frequencies have been performed, namely at 1600 Hz ($\alpha=0.69$) and 5000 Hz ($\alpha=0.51$). Both peaks are located within the suggested frequency bands. Therefore, the measured results are considered as fully aligned with theory of **destructive interference**. Further investigation shows that the sample is not behaving as a Helmholtz resonator ($f=2613\text{Hz}$), nor as a quarter wavelength tube ($f=3336\text{Hz}$).



n 0.4
Ltot = 36.7 cm
D = 0.5 cm

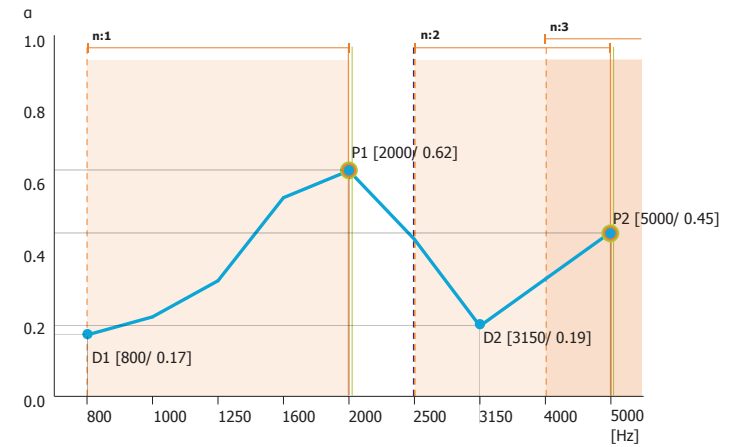
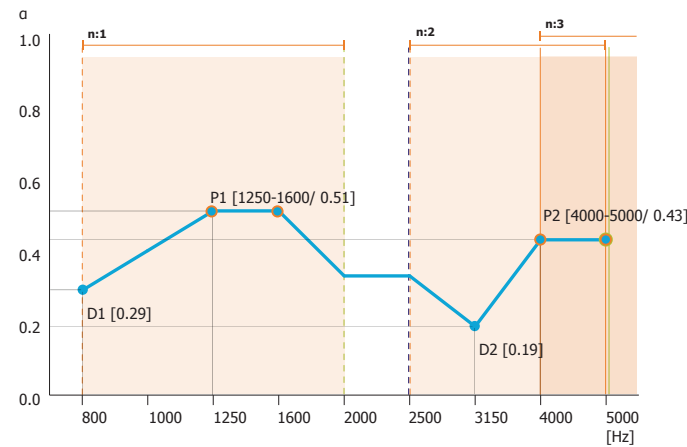
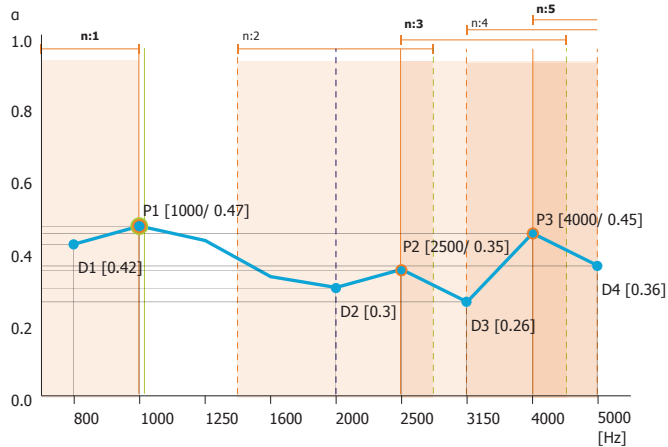


n 0.5
Ltot = 19.55 cm
D = 0.5 cm



n 0.6
Ltot = 19.55 cm
D = 0.5 cm

- Destructive Interference
- Quarter Wavelength tube
- Helmholtz Resonator



Sample 0.4

Sample 0.4 has a global diameter of 2.8 cm and height 3cm. It contains one air-path with a total length of 36.7 cm and with a diameter of 0.5 cm. The analysis suggest 5 frequency bands where peaks might occur: 467-934Hz (n=1), 1401-2803Hz (n=2), 2336-4673Hz (n=3), 3271- 6542 (n=4) and 4205-8411Hz (n=5).

During the measurements, 3 peak frequencies have been identified, at: 1000 Hz ($\alpha=0.47$), 2500 Hz ($\alpha=0.35$) and 4000 Hz ($\alpha=0.45$). The peaks are located within the suggested frequency bands. Therefore, the measured results are considered as aligned with theory of **destructive interference**. The first peak might be caused also by quarter wavelength tube principles. Further calculations show that the sample is not performing as a Helmholtz resonator.

Sample 0.5

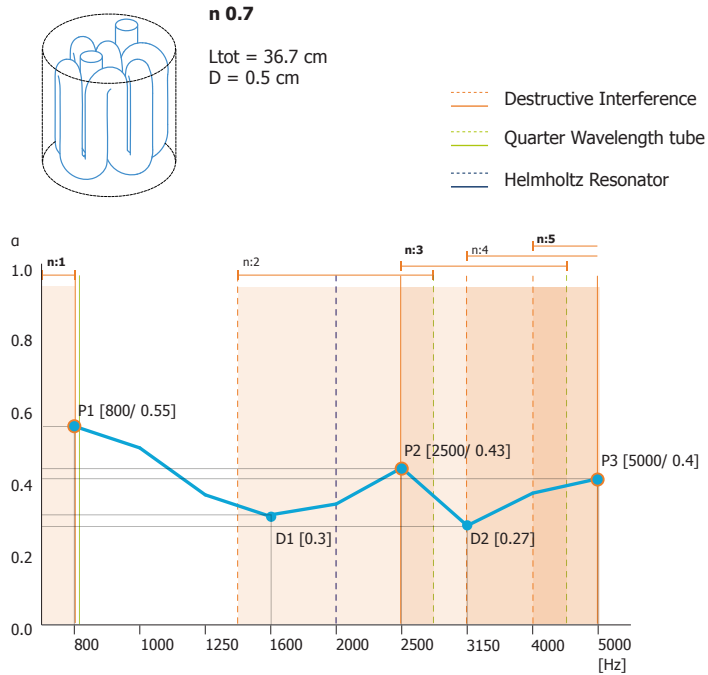
Sample 0.5 has a global diameter of 2.8 cm and height 3cm. It contains one air-path with a total length of 19.55 cm and with a diameter of 0.5 cm. The analysis suggest 3 frequency bands where peaks might occur: 877-1754Hz (n=1), 2631-5263Hz (n=2) and 4386-8772Hz (n=3).

During the measurements, 2 peak frequencies have been identified, namely between 1250 and 1600 Hz ($\alpha=0.51$) and between 4000 and 5000 Hz ($\alpha=0.43$). The peaks are located within the suggested frequency bands. Therefore, the measured results are considered as aligned with theory of **destructive interference**. The peak at 5000 Hz might be caused also by quarter wavelength tube principles. Further calculations show that the sample is not performing as a Helmholtz resonator.

Sample 0.6

Sample 0.6 has a global diameter of 2.8 cm and height 3cm. It contains one air-path with a total length of 19.55 cm and with a diameter of 0.5 cm. The analysis suggest 3 frequency bands where peaks are expected to occur: 877-1754Hz (n=1), 2631-5263Hz (n=2) and 4386-8772Hz (n=3).

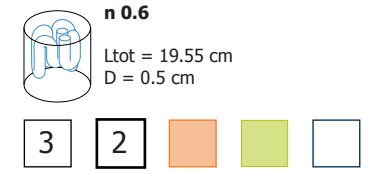
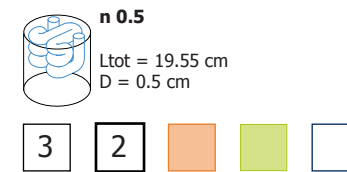
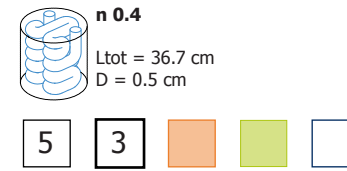
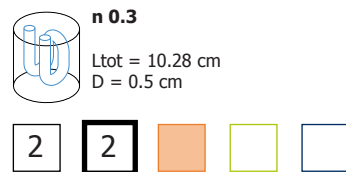
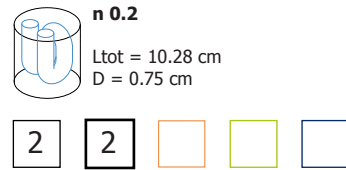
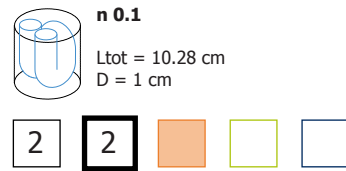
During the measurements, 2 peak frequencies have been identified, namely at 2000 Hz ($\alpha=0.62$) and 5000 Hz ($\alpha=0.45$). The peaks are located within the suggested frequency bands. Therefore, the measured results are considered as aligned with theory of **destructive interference**. Both peaks might be caused also by quarter wavelength tube principles. Further calculations show that the sample is not performing as a Helmholtz resonator.



Sample 0.7

Sample 0.7 has a global diameter of 2.8 cm and height 3cm. It contains one air-path with a total length of 36.7 cm and with a diameter of 0.5 cm. The analysis suggest 5 frequency bands where peaks are expected to occur: 467-934Hz (n=1), 1401-2803Hz (n=2), 2336-4673Hz (n=3), 3271- 6542 (n=4) and 4205-8411Hz (n=5).

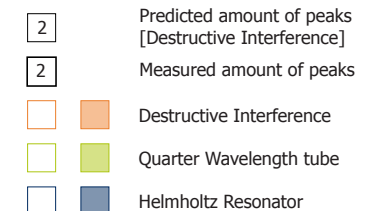
During the measurements, 3 peak frequencies have been identified, at: 800 Hz ($\alpha=0.55$), 2500 Hz ($\alpha=0.43$) and 5000 Hz ($\alpha=0.40$). The peaks are located within the suggested frequency bands. Therefore, the measured results are considered as fully aligned with theory of **destructive interference**. The first peak might be caused also by quarter wavelength tube principles. The sample is not performing as a Helmholtz resonator.

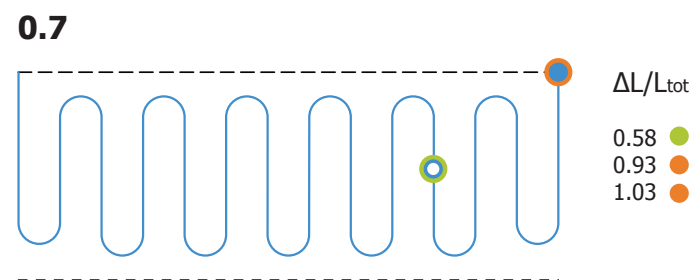
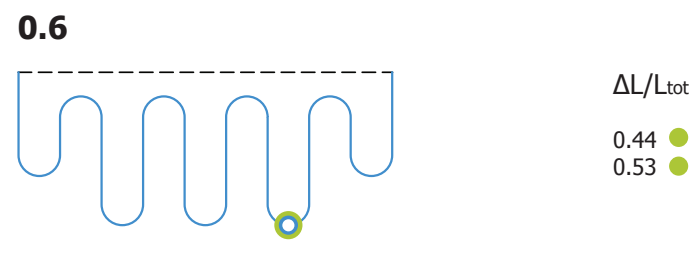
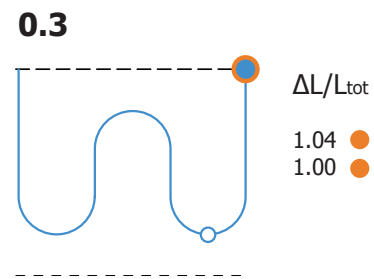
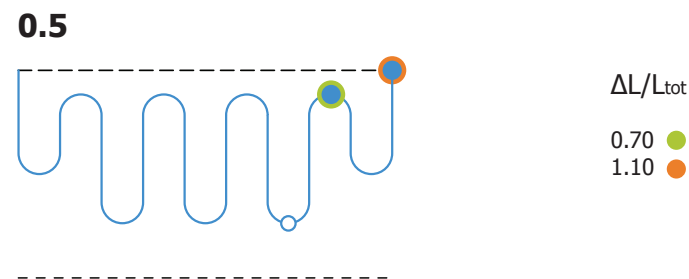
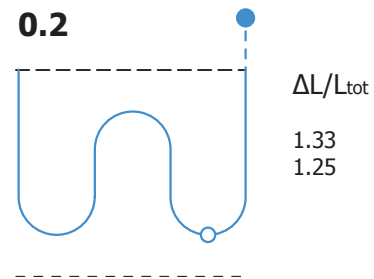
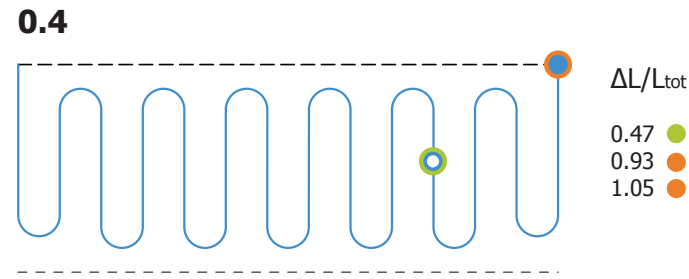
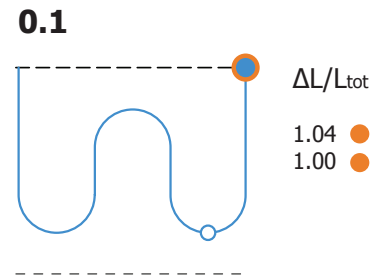


Summary

In this section, the focus was on analysing and further comprehending the measured performance of the 7 samples by linking it to related theories on resonant and interference absorption.

The peak frequencies of six samples [0.1/ 0.3/ 0.4/ 0.5/ 0.6/ 0.7] are aligned with destructive interference theory. There is an indication that four samples [0.4/ 0.5/ 0.6/ 0.7] might behave also similar to quarter wavelength tube. The performance of sample 0.2 was not possible to be linked with a known acoustic behaviour. None of the tested absorbers performs as a Helmholtz resonator. It seems that samples with simpler geometry, perform better. Furthermore, there was an attempt to relate performance to geometrical characteristics, but it was not possible to define clear and safe points.





- Surface
- Quarter length
- **Interference point** due to destructive interference on the surface
- **Interference point** due to destructive interference second boundary or quarter wavelength tube

The objective of this part of the analysis, is to define the position of the interference point along the tested air-paths. As mentioned earlier in this report, the equation of passive destructive interference is:

$$f = \frac{(2n - 1)c}{2\Delta L}$$

- [f] interference frequency
- [c] speed of sound in air
- [n] random integer 1, 2, 3, ...
- [ΔL] length difference

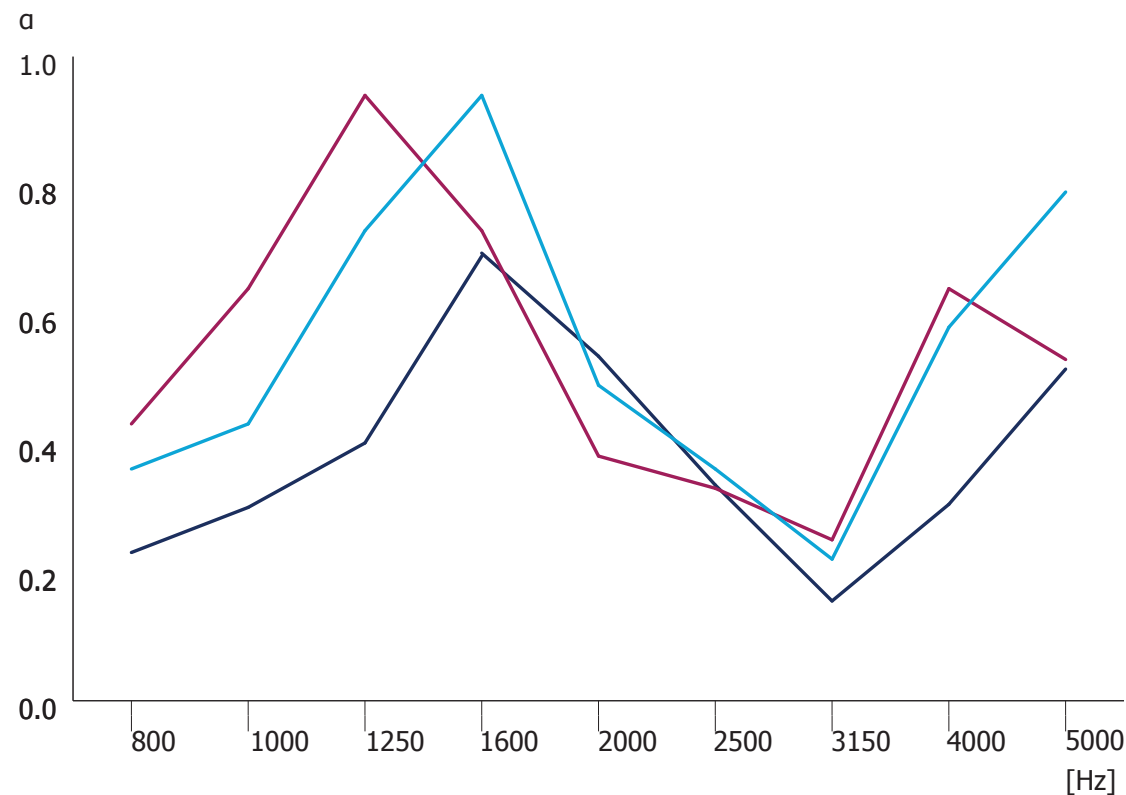
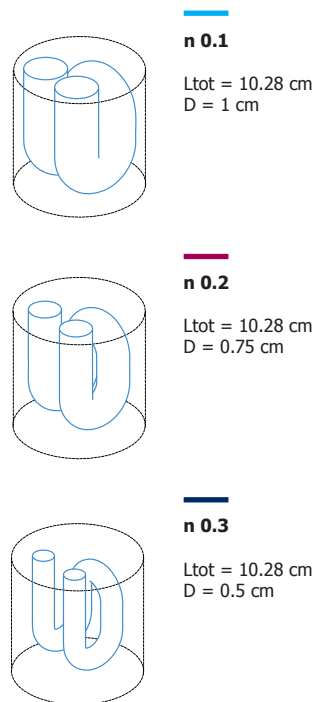
Taking into consideration the measured peak frequencies, it is easy to extract ΔL :

$$\Delta L = \frac{(2n - 1)c}{2f}$$

- [f] measured resonance frequency

The diagrams on this page indicate the location of the interference point when calculated with the above mentioned method.

When destructive interference occurs on the surface of the absorbers [samples 0.1/ 0.3/ 0.4/ 0.7], the ratio $\Delta L/L_{tot}$ equals 1 and the peak coincides with the first boundary of the interference frequency band. When the ratio $\Delta L/L_{tot}$ equals 0.5 [samples 0.4/ 0.6/ 0.7], the peak relates to the second boundary of destructive interference or to quarter wavelength tube principles; in this case interference occurs at the 1/4 of the total length of the air path. It is notable that in most of the cases the interference point lies between the 1/4 of the total length of the air path and the surface. Several attempts took place in order to relate the measured interference frequencies to the ratios of L/D [Length/ Diameter] and S/V [Surface/ Volume] without any satisfying result. [see also: p.]



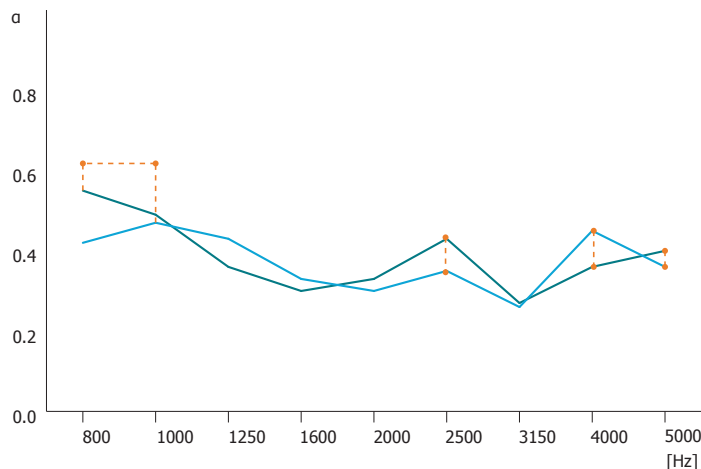
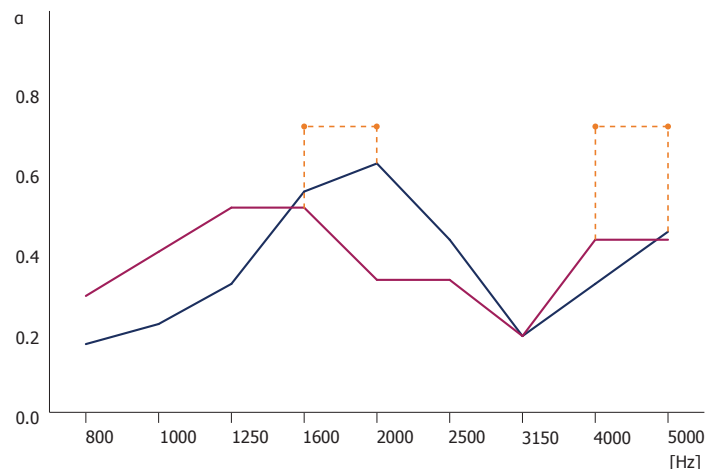
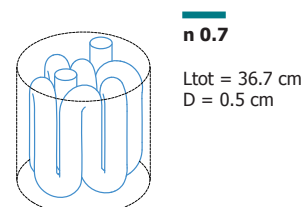
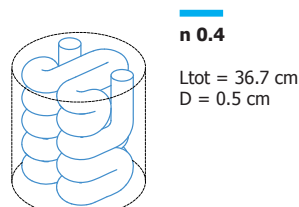
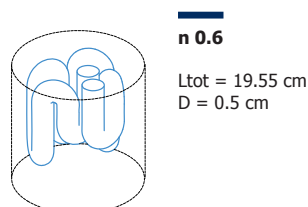
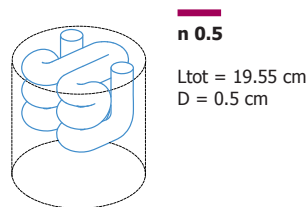
The samples with the codes 0.1, 0.2 and 0.3 have the same air-tube length [=10.28cm] and geometry, but their diameter varies from 1.00 to 0.50cm. The comparison of the measurement results, show that performance is affected by the diameter of the air-path.

According to the theory of passive destructive interference, it was expected that the three samples would perform their peaks at the same frequencies. More specifically, at 1668Hz ($n = 1$) and 5004Hz ($n = 2$). The measured performance of samples 0.1

and 0.3 is aligned with this estimation. In contrary, sample's 0.2 performance has not been in accordance with theory. Inaccuracy during the measurements or the fabrication process could possibly explain this fact.

Observing the performance of this set of samples, it can be argued that the three samples belong to the same family. They execute a first peak value between 1250 and 1600 Hz, a dip at 3150 Hz and a second peak between 4000 and 5000Hz.

In general, we notice that the values of the normal absorption coefficient get lower when the diameter gets smaller. This means that the sample 0.1 with a diameter of 1cm performs better than the samples 0.2 and 0.3. In the same logic, sample 0.2 performs better than sample 0.3.



The samples with the codes **0.5** and **0.6** have the same air-path length and diameter, but they differ in geometry: sample's 0.5 air-path, is horizontally oriented, while 0.6's vertically oriented. The total length of the air-path of each sample equals 19.55cm and the diameter is 0.5cm.

The two samples were expected to perform three peaks at the same frequencies: 877 Hz ($n=1$), 2631 Hz ($n=2$) and 4386 Hz ($n=3$). Apparently, the measured performance does not relate to the estimations. Despite this fact, the corresponding comparative graph shows that the two samples belong to the same "family". It is hard to identify which sample is performing better. Sample 0.6 with its vertically oriented geometry, gives the highest normal absorption coefficient for all frequencies and for both samples at 2000Hz.

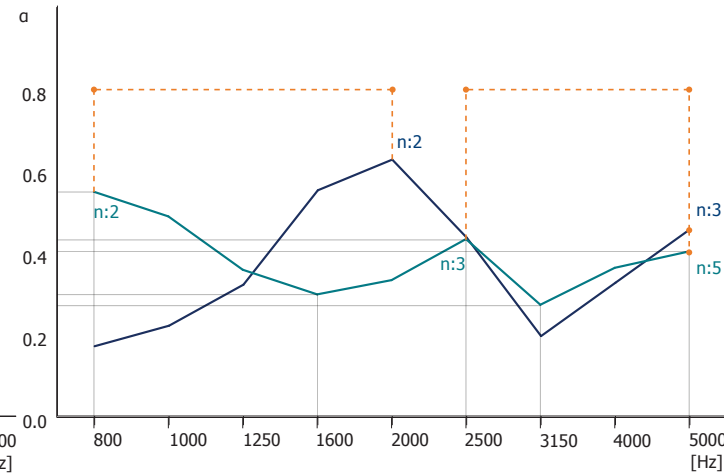
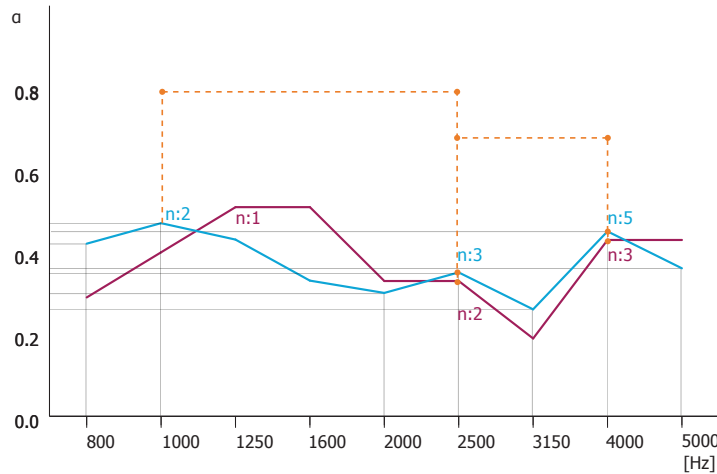
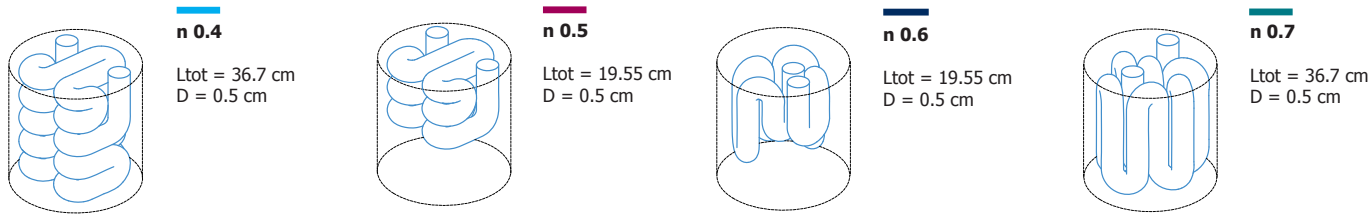
The samples with the numbers **0.4** and **0.7** have the same length and diameter, but they differ in geometry. Sample's 0.4 air path, is horizontally oriented, while 0.7's vertically oriented. The total length of the air-path of each sample equals 36.7cm and their diameter is 0.5cm.

The two samples were expected to perform five peaks at the same frequencies: 1402Hz ($n=2$), 2337Hz ($n=3$), 3272Hz ($n=4$), 4206Hz ($n=5$) and 5140 Hz ($n=6$). By observing the corresponding graph, it is suggested that the two samples belong to the same "family" and that they perform almost identically. Sample 0.7 with its vertically oriented geometry, has the highest direct absorption coefficient for all frequencies and for both samples at 800Hz.

Remarks

The purpose of this set of comparisons, was to better understand how the geometry of the air path affects performance.

Since the air path length and diameter per pair are identical, it was expected that the samples would perform similarly. The measurements show some small differences between the compared absorbers. This fact might be explained by the differentiated geometry and orientation of the air paths. However, the dissimilarities of the results might also have been caused by inaccuracy in the measurement procedure or by fabrication failures [difficulties in the post-processing, etc].



The samples **0.4** and **0.5** have the same diameter [=0.5cm] and geometry, but differ in the air-path length. Since the length of 0.5 (19.55cm) is almost half the length of 0.4 (36.7cm), it is expected that its corresponding peak frequencies when $n_{04}=n_{05}$, will almost double:

$$2 * f_{04(n=1)} = f_{05(n=1)} = 900\text{Hz}$$

$$2 * f_{04(n=2)} = f_{05(n=2)} = 2500\text{Hz}$$

$$2 * f_{04(n=3)} = f_{05(n=3)} = 4000\text{Hz}$$

Additionally, it is expected that peak frequencies will coincide at:

$$f_{04(n=3)} = f_{05(n=2)} = 2500\text{Hz}$$

$$f_{04(n=5)} = f_{05(n=3)} = 4000\text{Hz}$$

The samples perform exactly as expected: for similar n, frequency is almost double and at higher frequencies peaks coincide.

Samples with the code **0.6** and **0.7** have the same diameter [=0.5cm] and geometry, but differ in length. Since the length of 0.6 (19.55cm) is almost half the length of 0.7 (36.7cm), it is expected that its corresponding peak frequencies when $n_{06}=n_{07}$, will almost double:

$$2 * f_{07(n=1)} = f_{06(n=1)}$$

$$2 * f_{07(n=2)} = f_{06(n=2)}$$

$$2 * f_{07(n=3)} = f_{06(n=3)}$$

Additionally, it is expected that peak frequencies will coincide at:

$$f_{07(n=3)} = f_{06(n=2)}$$

$$f_{07(n=5)} = f_{06(n=3)}$$

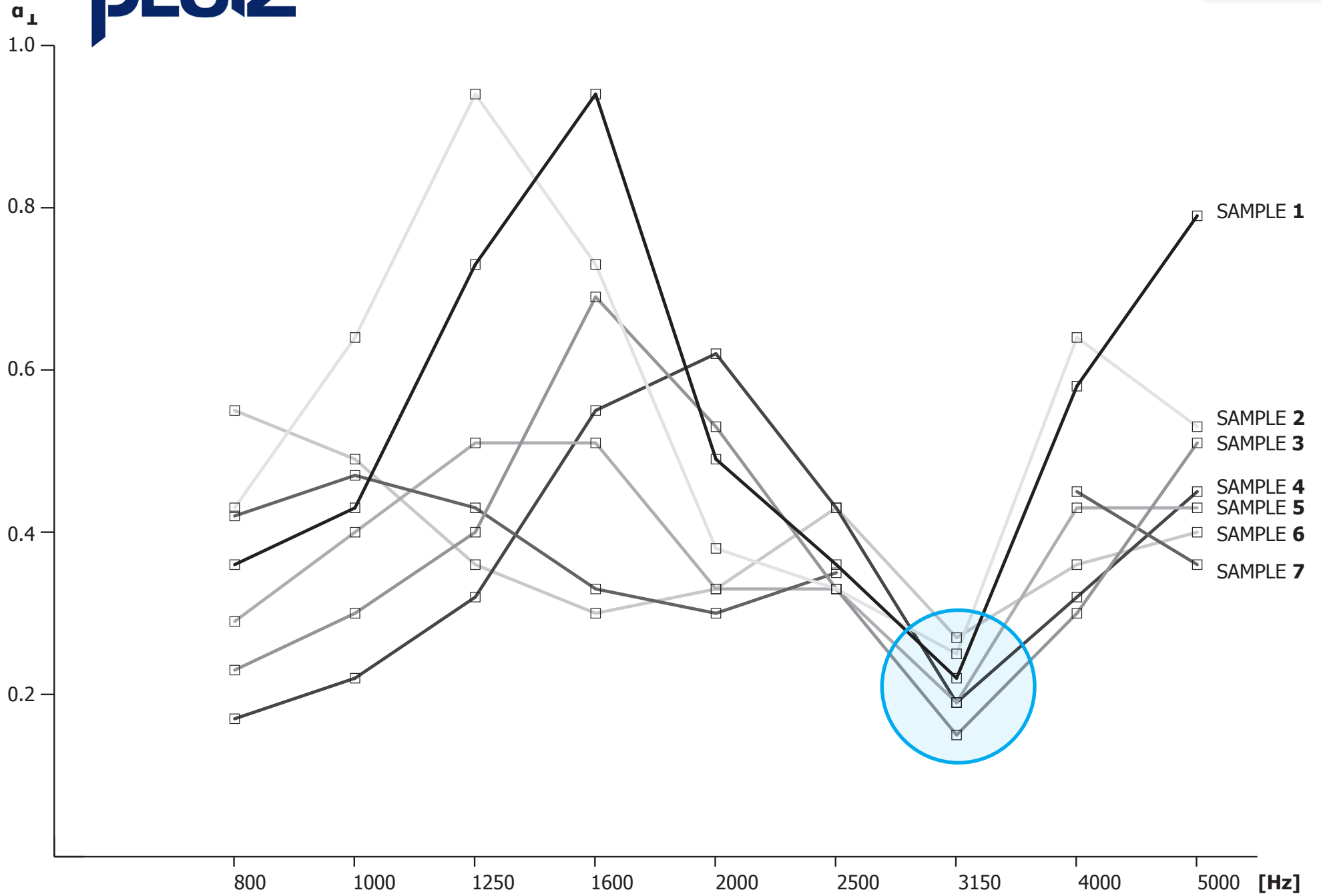
The samples perform almost as expected: for similar n, frequency is almost double and at higher frequencies peaks coincide.

Remarks

The objective of this section, was to test in which manner affects the length of the air path acoustic performance.

Since the compared samples obtained a ratio $L_{05/06} / L_{04/07}$ equal 0.5, it was expected that the corresponding peak frequencies for equal n would almost double. Additionally, at higher frequencies peaks were expected to coincide.

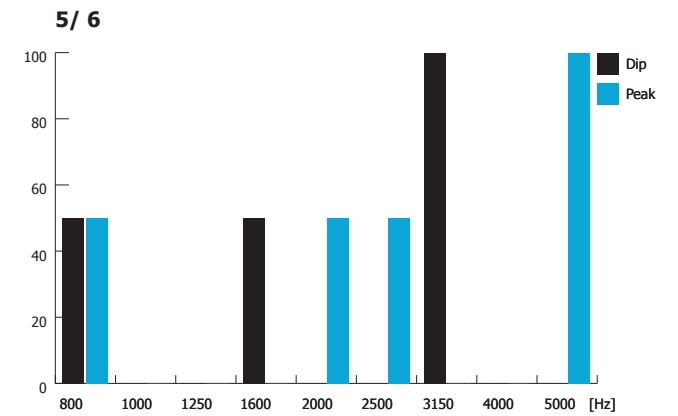
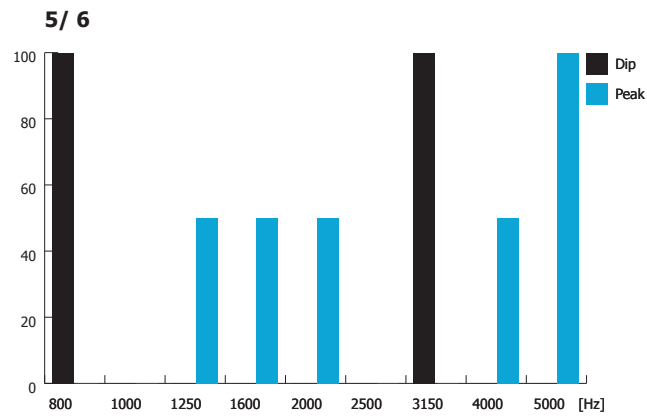
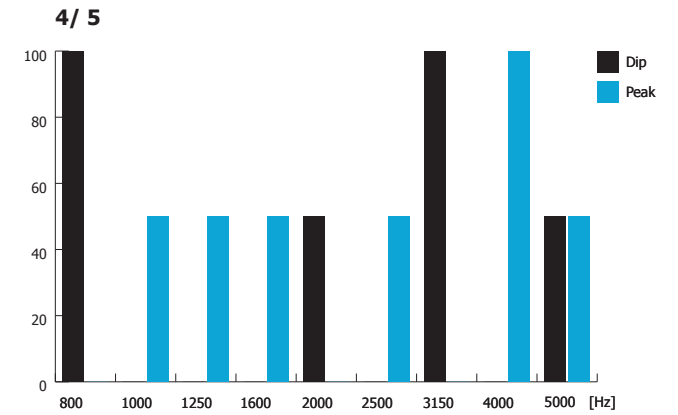
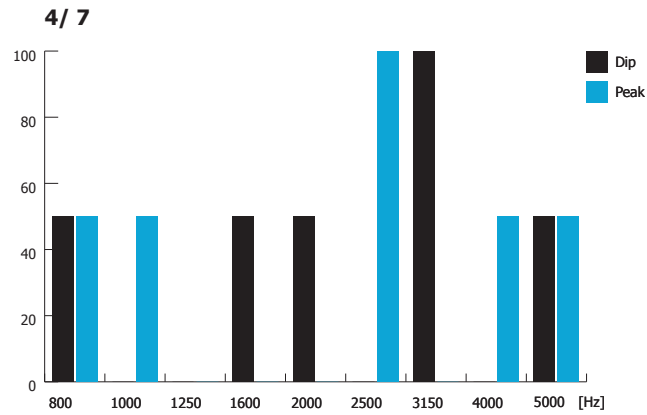
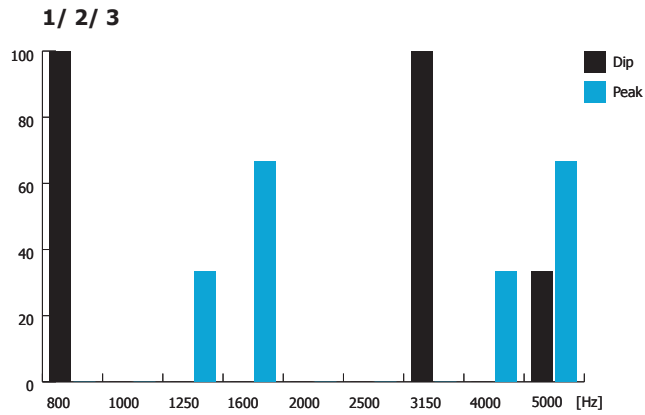
In general, both comparisons performed as expected.

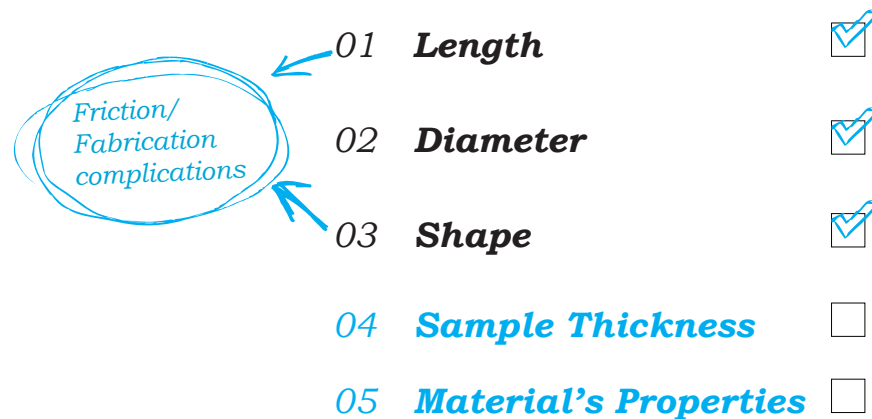


Diameter

Length

Geometry





The preliminary physical tests have been based mostly on the boolean logic. According to the results, it is proved that the acoustic performance is indeed affected by length and diameter of the air paths. More specifically:

Length

The analysis suggests that differentiation in length might cause a shift of the peak frequencies. The discussed shift relates to the ratio of the compared lengths.

It is assumed that the combination of various lengths might give fruitful results in the case of a broad band absorber.

Diameter

The diameter is affecting performance in a constructive way. There is an indication that for diameters between 0.5 and 1cm, the increase of their size, improves the direct absorbing coefficient values.

Shape/ Orientation

The measurement results show that different geometrical configurations might affect acoustic performance. Additionally, there is an indication that samples with simpler geometry perform better.

Coherence to theory

The peak frequencies of six samples are aligned with destructive interference theory. There is an indication that four samples might behave also alike quarter wavelength tube. The performance of sample 0.2 was not possible to be linked with a known acoustic behaviour. None of the tested absorbers performs as a Helmholtz resonator.

Several attempts took place in order to relate the measured resonant and interference frequencies to parameters such as length, diameter, surface, volume and their ratios without getting any satisfying result.

Interference point

During this analysis, it was possible to define the position of the interference point. In all the tested cases, the interference point lies between the 1/4 of the total length of the air path and the surface:

$$\frac{1}{4}L_{\text{tot}} < \Delta L < L_{\text{tot}}$$

Sample Thickness

It is notable that all tested samples perform a dip at 3150 Hz, which corresponds to their lower absorbing coefficient value. This might be caused by the material properties of the sintered powder.

Suggestions

Material/ Fabrication

It is suggested to measure a solid cylinder out of the same material to detect if the material has absorbing properties. In this case, the absorbing coefficient affects the discussed results and defines the minimum value of the measured samples. For future experiments it is better to use an air-tight, non-porous material. The roughness in material and the irregularities of the finished surface are characterising the parts of phase 1. This fact might have affected the results both in a positive and negative way.

Geometry

For the future measurements it is suggested to choose simpler geometries for the air paths.

All the remarks relate to the specific set of measurements and give hints on how to proceed in the future. The amount of samples is too small to generalise facts. Additional measurements will be needed in order to make more reliable conclusions.



The results of the first experiments have been encouraging and have defined the guidelines for the next step. In Phase 2, a total amount of 23 samples were designed, fabricated and measured. It is notable, that a new material is applied to the absorbers of the second experiment. The samples are categorised in two groups according to their global diameter:

- 8 samples have a diameter of 3 cm

This set of samples is supposed to support the calibration of the results of Phase 1 and 2. Their performance will be measured for frequencies between 800 and 5000Hz.

-15 samples have a diameter of 10cm

This set of absorbers will examine the principle of passive destructive interference in frequencies between 100 and 1600Hz.

Fabrication

The samples of phase 2, were fabricated at a company specialised in AM with the name Materialise [www.materialise.com]. The applied technique was **selective laser sintering** [SLS].

The basic material consists of powder with particle sizes in the order of magnitude of 50 µm. Powder

layers are spread on top of each other. After deposition, a computer controlled CO₂ laser beam scans the surface and selectively binds together the powder particles of the corresponding cross section of the product. During laser exposure, the powder temperature rises above the glass transition point after which adjacent particles flow together. The surface of the samples is smoother this time.

The technique is economical and fast. The standard accuracy equals to ± 0.3% (with lower limit on ± 0.3 mm) and the minimum wall thickness is 1 mm [in some occasions: 0.3 mm]¹.

Material [see also: APPENDIX]

Polyamide (PA12) is a solid material, the powder has the attractive feature of being self-supporting for the generated product sections. This makes supports redundant. The polyamide material allows the production of fully functional prototypes with high mechanical and thermal resistance.

The sound absorption performance of the material PA12 itself is expected to be low. This fact will assist in extracting more coherent conclusions on destructive interference. Additionally, the samples of this set are more solid and have a smoother surface that

might cause narrower peaks.

Measurements

The measurements of phase 2 took place in the laboratories of Peutz bv [Mook/ Molenhoek/ http://www.peutz.nl/] on the 23rd of April.

For the measurements, the impedance tube was used with two testing diameters: 3cm and 9.8cm [Briel & Kjaer]. With this tool, the direct absorption coefficient was measured at the following frequencies: 800/ 1000/ 1250/ 1600/ 2000/ 2500/ 3150/ 4000/ 5000 Hz [smaller tube] and 100/125/160/200/250/ 315/ 400/ 630/ 800/ 1000/ 1250/ 1600 Hz [bigger tube].

The **normal sound absorption coefficient** follows the measured amplitudes |P_{max}| and |P_{min}| at a given frequency. If the sound pressure in the impedance tube is measured in a logarithmic scale (in decibels), and the difference in level between the pressure maximum and the pressure minimum is ΔL dB, then:

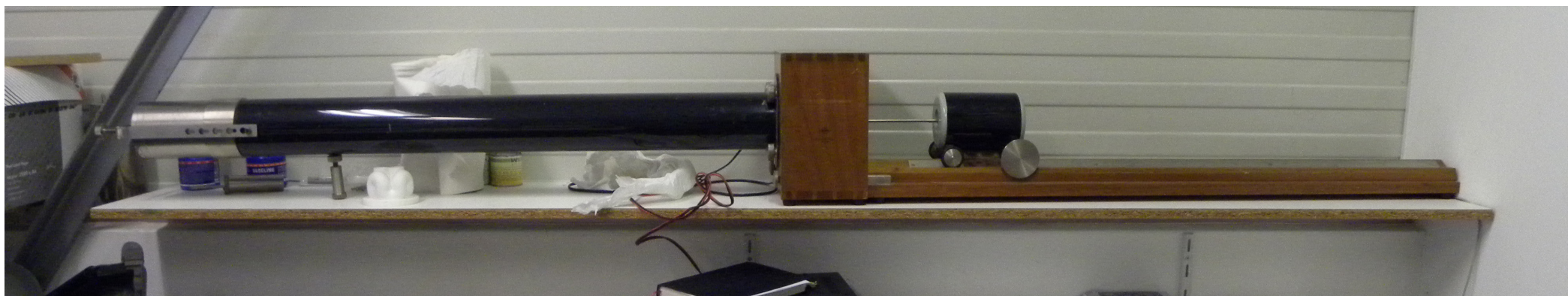
$$S = 10^{\Delta L/20}$$

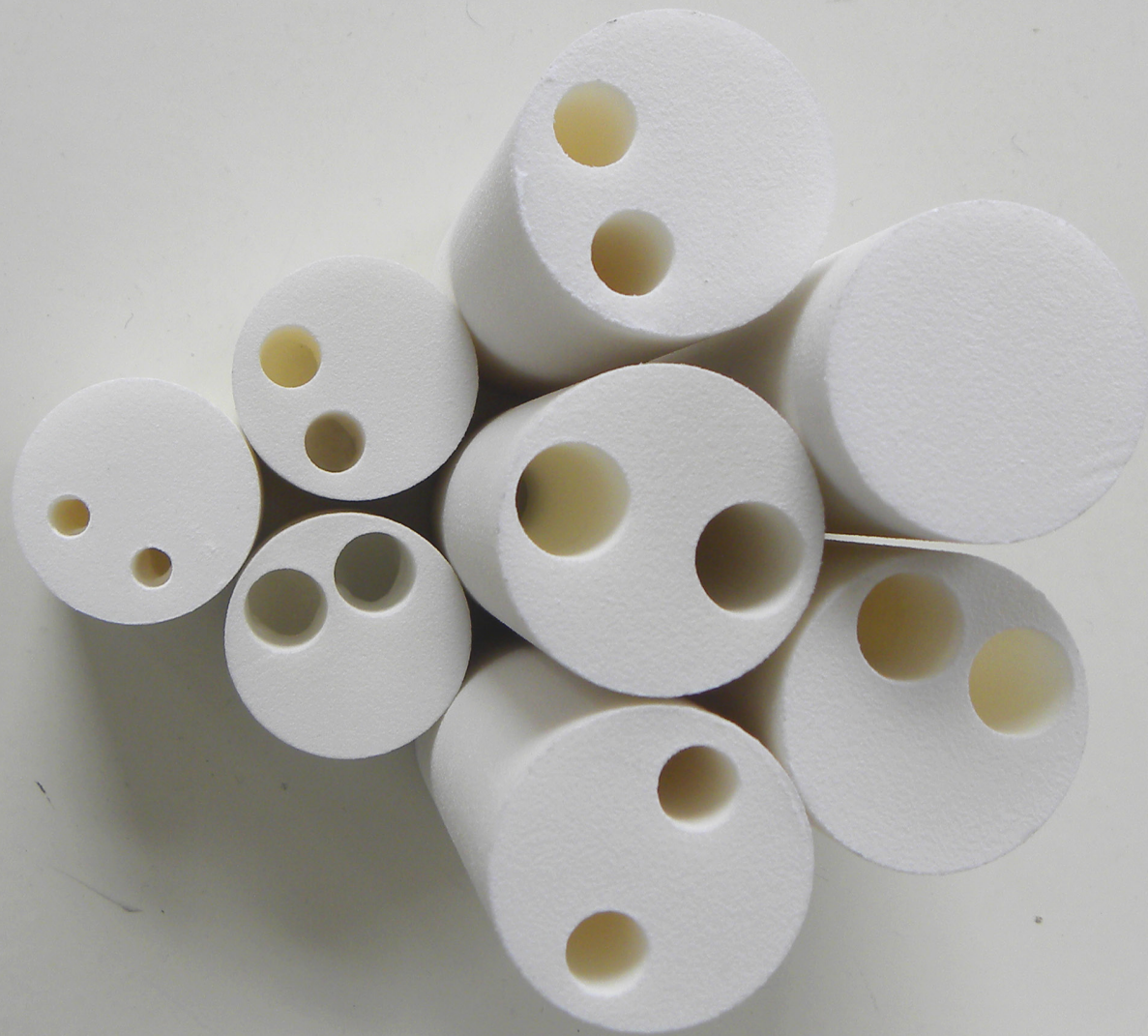
The sound absorption coefficient then follows from:

$$\alpha = 4 * 10^{\Delta L/20} / (10^{\Delta L/20} + 1)^2$$

The measurements followed the international standards as defined in ISO 10534-1:1996.

¹ www.materialise.com

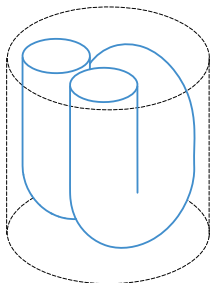




D = 3.00cm
H = 3.00/ 9.00/ 10.00cm

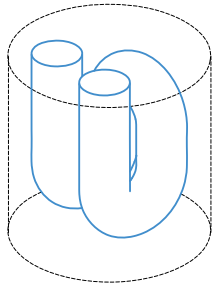
n1.1

$L_{tot} = 10.28\text{cm}$
D = 1.00cm



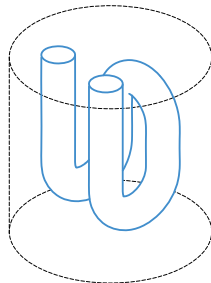
n1.2

$L_{tot} = 10.28\text{cm}$
D = 0.75 cm



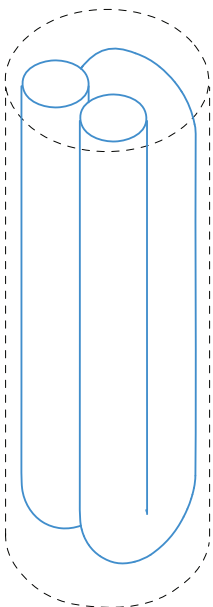
n1.3

$L_{tot} = 10.28\text{cm}$
D = 0.5 cm



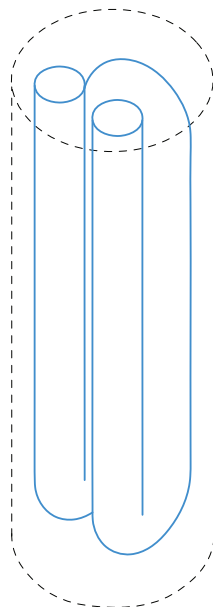
n2.1

$L_{tot} = 34.30\text{cm}$
D = 1.00cm



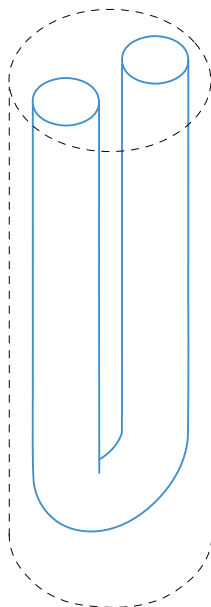
n2.2

$L_{tot} = 34.30\text{cm}$
D = 0.75cm



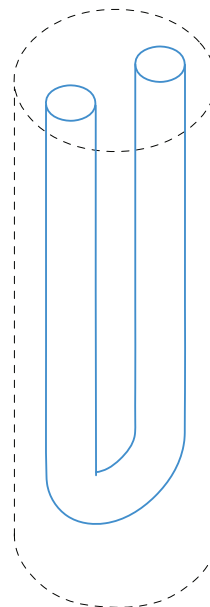
n2.4

$L_{tot} = 17.15\text{cm}$
D = 1.00cm



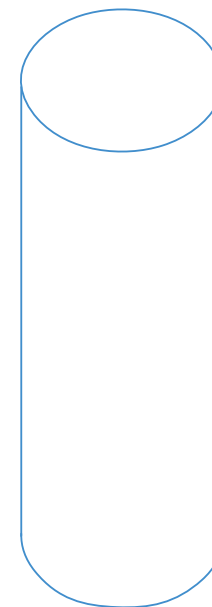
n2.5

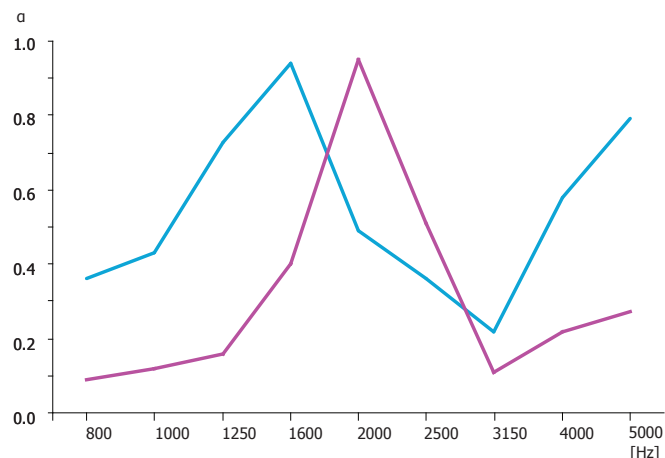
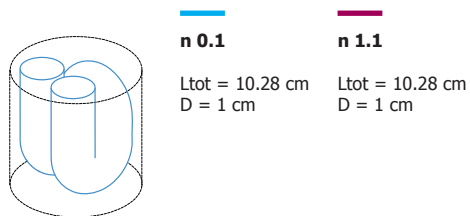
$L_{tot} = 17.15\text{cm}$
D = 0.75cm



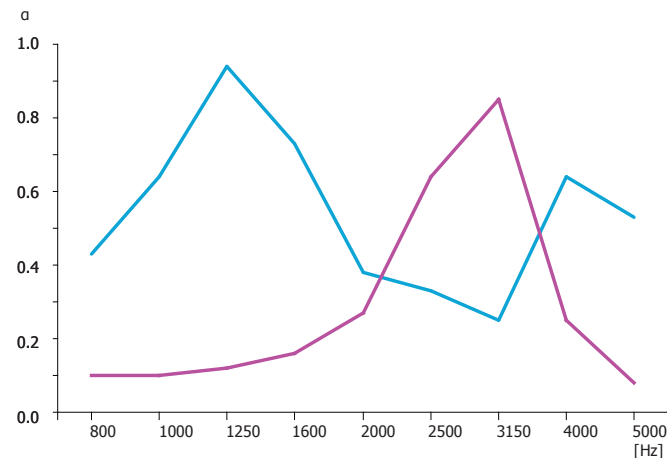
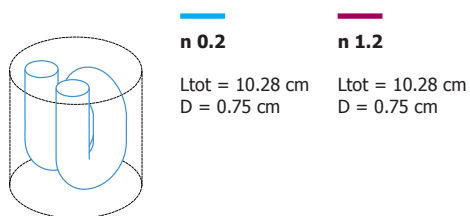
n2.3

SOLID



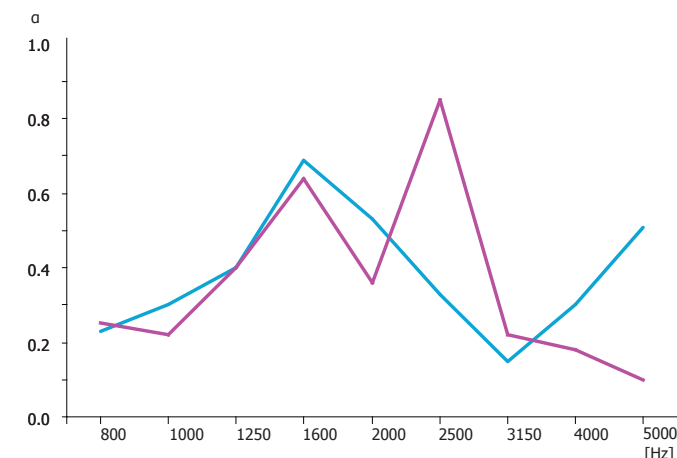
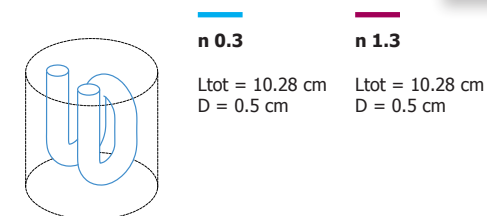


As mentioned before, during the second set of measurements a new material -called PA12- is tested. The new material is less porous and allows for a smoother surface. For this reason we re-fabricated 3 samples that were measured also in phase 1. In this manner, the measurements of the two phases will be calibrated. Additionally, it will be found out if material affects the results and in which manner. The assumption is that the tested principal of passive destructive interference is based upon geometrical characteristics. If this is the case, the results should not be dramatically affected by the material change. Additionally, it is expected that the smoothness of the new material will cause narrower peaks.



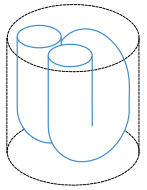
Samples 0.1 [Phase1] and 1.1 [Phase2]
Comparing the samples 0.1 and 1.1, some similarities are observed in their performance: equal amount of peaks and at similar frequencies. In the case of 1.1 the differences between higher and lower values become bigger and as follows the curve describing the absorbing coefficient becomes steeper. There is also a small shift in the peak towards higher frequencies.

Samples 0.2 [Phase1] and 1.2 [Phase2]
Sample 0.2 performs 2 peaks at 1250 and 4000Hz. Whereas sample 1.2 performs only one peak at 3150Hz, which constitutes the lowest performance of 0.2 The two samples have different amounts of peaks at distinct interference frequencies.



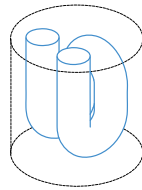
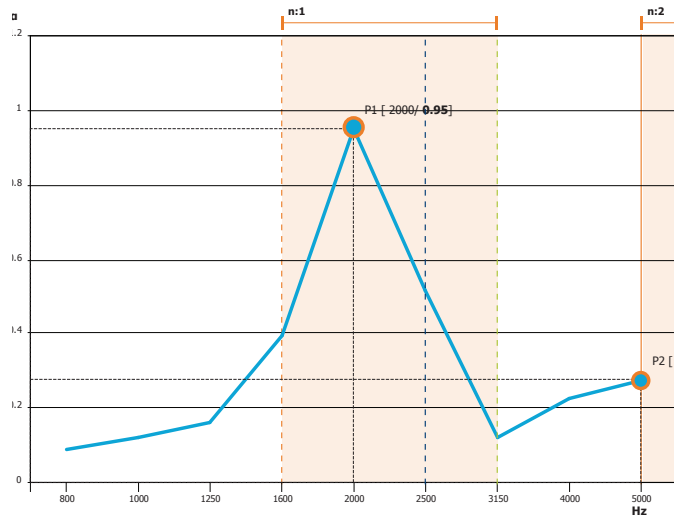
Samples 0.3 [Phase1] and 1.3 [Phase2]
The interference frequencies of sample 0.3 are at 1600 and 5000Hz. Whereas sample 1.3 performs 2 peaks at 1600 and 2500Hz. The two samples have the same amount of peaks at distinct interference frequencies. The peak of 1.3 might be just one peak with a measurement error around 2000 Hz.

At this part of the analysis, it is suggested that material properties and surface smoothness might influence acoustic performance. In the case of the samples 0.2/1.2, these parameters seem to affect the width of the peaks - which become narrower-, as well as their position and performance. However, the rest of the samples have closer correspondence. More tests are needed to unambiguously conclude whether material affects performance and in what way.



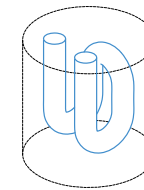
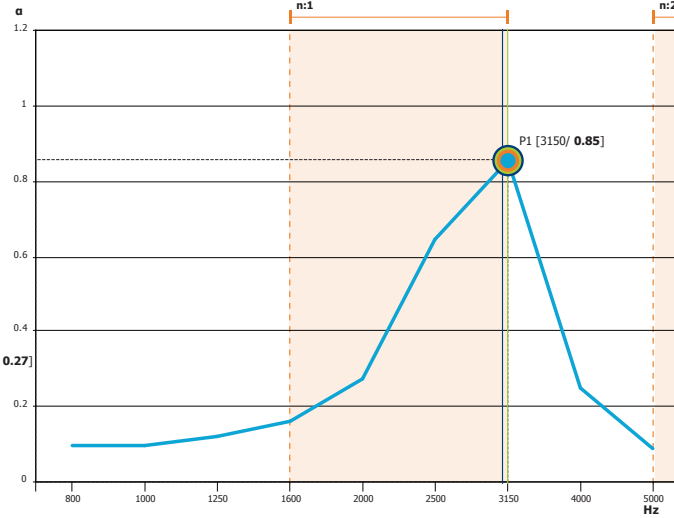
n 1.1

Ltot = 10.28 cm
D = 1 cm



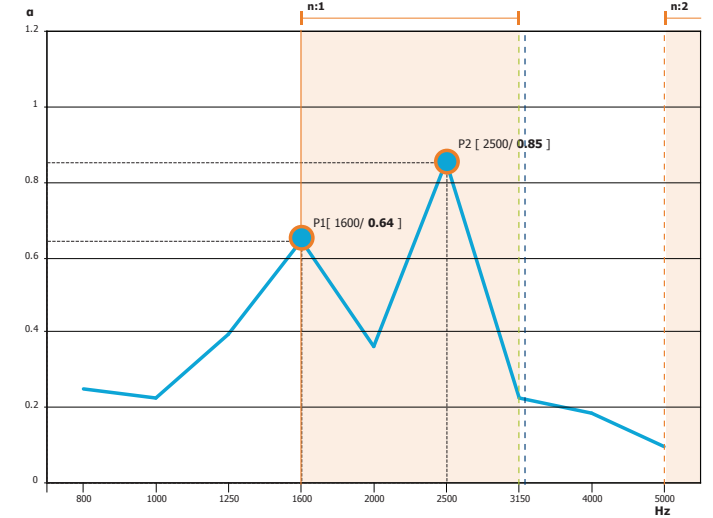
n 1.2

Ltot = 10.28 cm
D = 0.75 cm



n 1.3

Ltot = 10.28 cm
D = 0.5 cm



- Destructive Interference
- Quarter Wavelength tube
- Helmholtz Resonator

Sample 1.1

Sample 1.1 has a global diameter of 2.8 cm and height 3cm. It contains one air-path with length that equals to 10.28cm and diameter of 1cm. The analysis suggests 2 frequency bands where interference might take place: 1668-3336 Hz (n=1) and 5004-10009 Hz (n=2).

The measurements identified 2 peaks at 2000Hz ($\alpha = 0.95$) and at 5000Hz ($\alpha = 0.27$) correspondingly. The peaks lie within the suggested frequency bands. Therefore, the measured results are considered as aligned with theory of **destructive interference**. Further calculations prove that the sample is not behaving as a Helmholtz resonator ($f=2613\text{Hz}$), nor as a quarter wavelength tube ($f=3336\text{Hz}$).

Sample 1.2

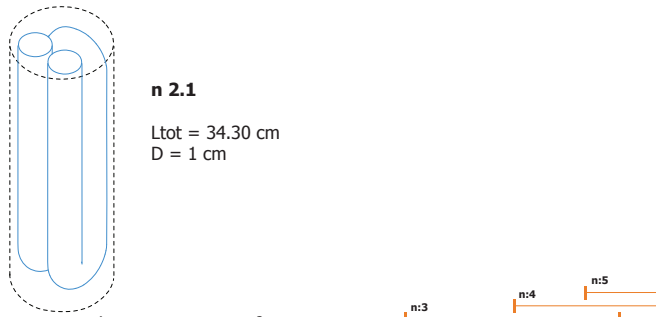
Sample 1.2 has a global diameter of 2.8 cm and height 3cm. It contains one air-path with length that equals to 10.28cm and diameter of 0.75cm. The analysis suggests 2 frequency bands where interference might take place: 1668-3336 Hz (n=1) and 5004-10009 Hz (n=2).

The measurements identified 1 peak at 3150Hz ($\alpha = 0.85$). The peak lies within the suggested **destructive interference** frequency band. Additionally, it might be caused by quarter wavelength tube ($f=3336\text{Hz}$) or Helmholtz resonator ($f=3017\text{Hz}$) principles. It is notable that the performance of the absorber is similar to the performance of sample 2.3 (solid cylinder).

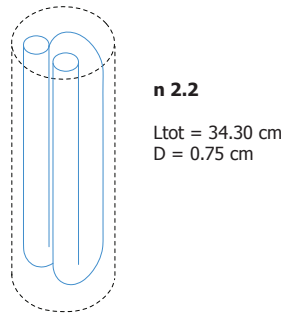
Sample 1.3

Sample 1.3 has a global diameter of 2.8 cm and height 3cm. It contains one air-path with length that equals to 10.28cm and diameter of 0.50cm. The analysis suggests 2 frequency bands where interference might take place: 1668-3336 Hz (n=1) and 5004-10009 Hz (n=2).

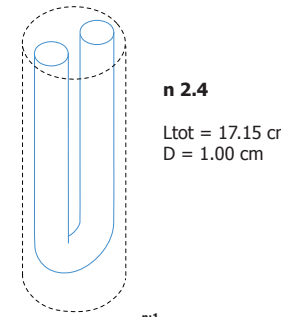
The measurements identified 2 peaks at 1600Hz ($\alpha = 0.64$) and 2500Hz ($\alpha = 0.85$). Both peaks are located within the first frequency band. This fact might be an indication, that there is a measurement error around 2000Hz. The measured results are partially aligned with theory of **destructive interference**. Further calculations prove that the sample is not behaving as a Helmholtz resonator ($f=3698\text{Hz}$), nor as a quarter wavelength tube ($f=3336\text{Hz}$).



n 2.1
Ltot = 34.30 cm
D = 1 cm

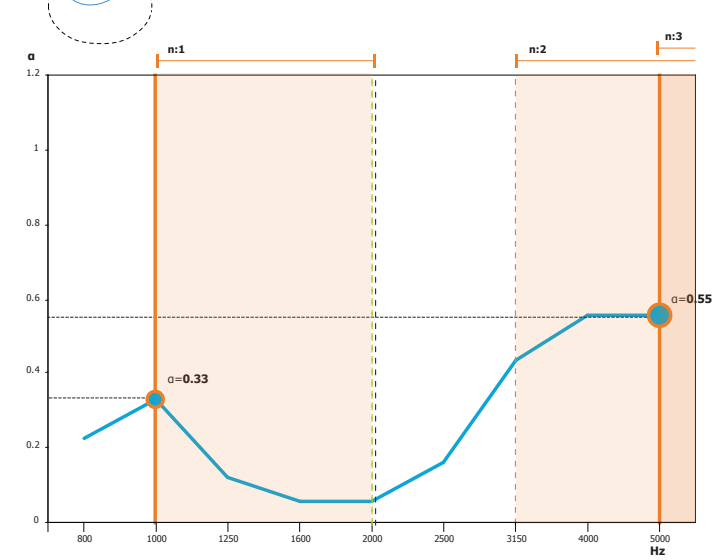
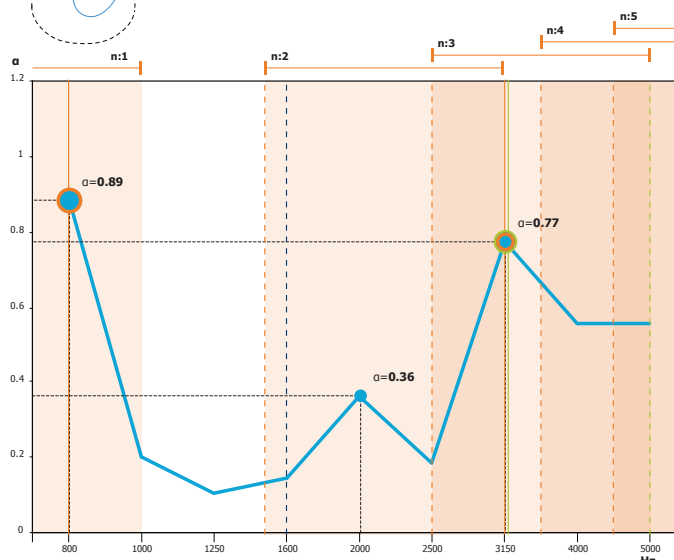
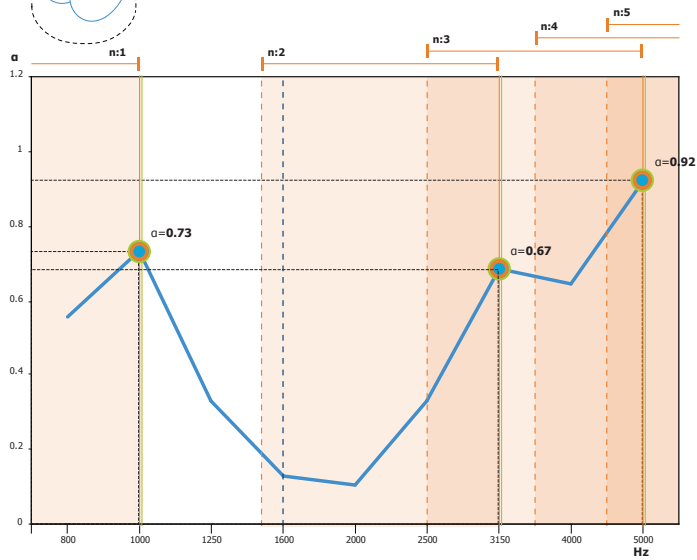


n 2.2
Ltot = 34.30 cm
D = 0.75 cm



n 2.4
Ltot = 17.15 cm
D = 1.00 cm

- Destructive Interference
- Quarter Wavelength tube
- Helmholtz Resonator



Sample 2.1

Sample 2.1 has a global diameter of 2.8 cm and height 9cm. It contains one air path with length that equals 34.3cm and diameter of 1.00cm. The analysis suggests 5 frequency bands where interference might take place: 500-1000 Hz (n=1), 1500-3000 Hz (n=2), 2500-5000 Hz (n=3), 3500-7000 Hz (n=4) and 4500-9000 Hz (n=5).

The measurements identified 3 peaks at 1000Hz ($\alpha = 0.73$), 3150Hz ($\alpha = 0.67$) and 5000Hz ($\alpha = 0.92$). All the peaks lie closer to the second boundaries of the suggested **destructive interference** frequency bands. Therefore, they also coincide with the interference frequencies of quarter wavelength tube. Further calculations prove that the sample is not behaving as a Helmholtz resonator ($f=1430\text{Hz}$).

Sample 2.2

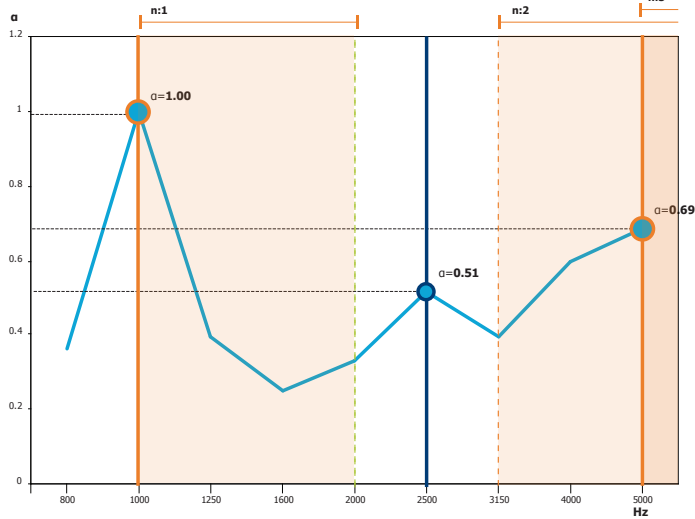
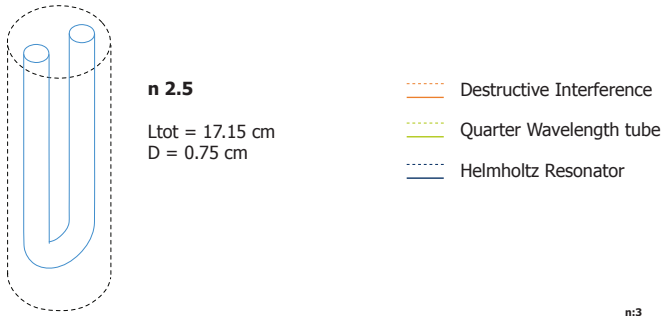
Sample 2.2 has a global diameter of 2.8 cm and height 9cm. It contains one air path with length that equals 34.3cm and diameter of 0.75cm. The analysis suggests 5 frequency bands where interference might take place: 500-1000 Hz (n=1), 1500-3000 Hz (n=2), 2500-5000 Hz (n=3), 3500-7000 Hz (n=4) and 4500-9000 Hz (n=5).

The measurements identified 3 peaks at 800Hz ($\alpha=0.89$), 2000Hz ($\alpha=0.36$) and 3150Hz ($\alpha=0.77$). All the peaks lie within the suggested **destructive interference** frequency bands. The third peak coincides also with the interference frequency of quarter wavelength tube. Further calculations prove that the sample is not behaving as a Helmholtz resonator. ($f=1652\text{Hz}$).

Sample 2.4

Sample 2.4 has a global diameter of 2.8 cm and height 9cm. It contains one air-path with length that equals to 17.15cm and diameter of 1.00cm. The analysis suggest 5 frequency bands where interference might take place: 1000-2000 Hz (n=1), 3000-6000 Hz (n=2) and 5000-10000 Hz (n=3).

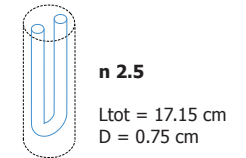
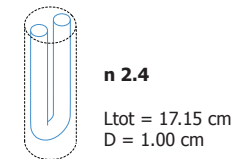
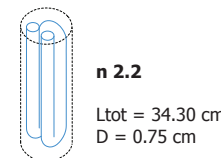
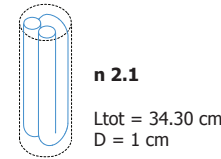
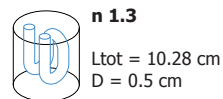
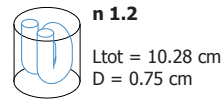
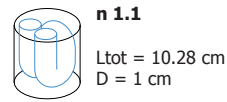
The measurements identified 2 peaks at 1000Hz ($\alpha=0.33$) and 5000Hz ($\alpha=0.55$). Both peaks are located within the suggested **destructive interference** frequency bands. Further calculations prove that the sample is not behaving as a Helmholtz resonator ($f=2023\text{Hz}$), nor as a quarter wavelength tube ($f=2000/ 6000\text{Hz}$).



Sample 2.5

Sample 2.5 has a global diameter of 2.8 cm and height 9cm. It contains one air-path with length that equals to 17.15cm and diameter of 0.75cm. The analysis suggests 5 frequency bands where interference might take place: 1000-2000 Hz ($n=1$), 3000-6000 Hz ($n=2$) and 5000-10000 Hz ($n=3$).

The measurements identified 3 peaks at 1000Hz ($\alpha = 1.00$), 2500Hz ($\alpha = 0.51$) and 5000Hz ($\alpha = 0.69$). The first and the third peak are located within the boundaries of the **destructive interference** frequency bands. Further calculations indicate that the peak at 2500Hz might be caused by Helmholtz resonator principles ($f=2336\text{Hz}$).

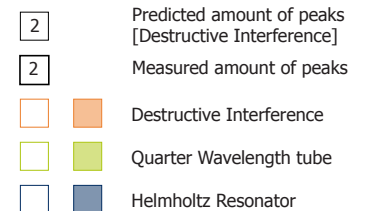


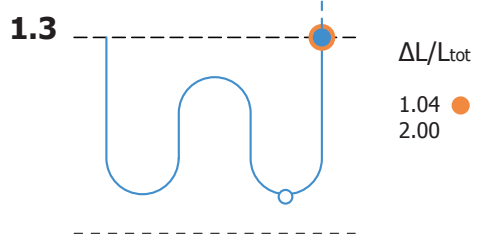
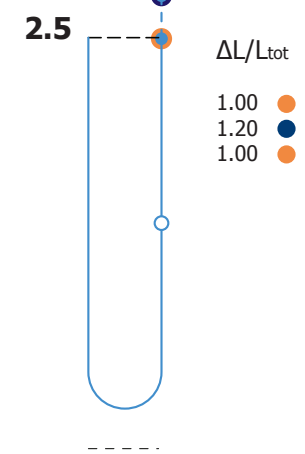
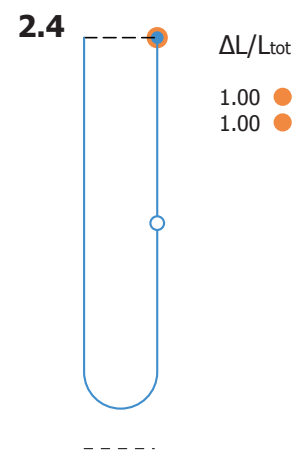
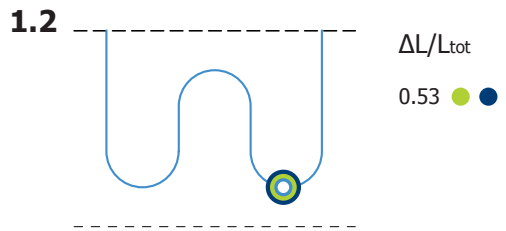
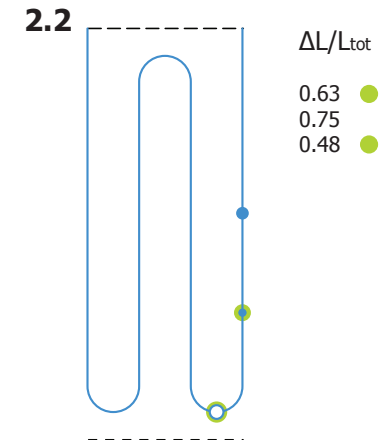
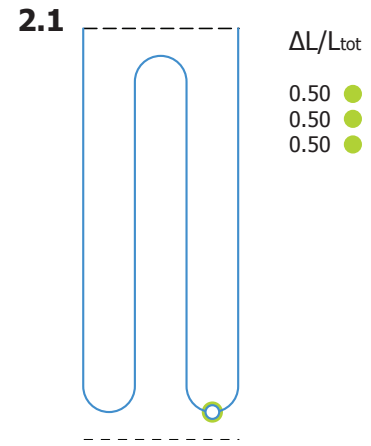
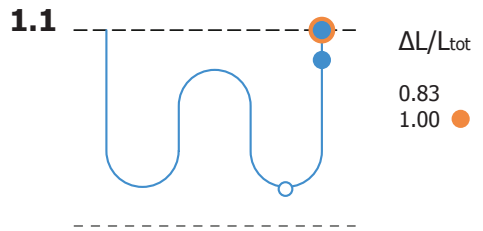
Summary

In this section, the focus was on analysing and further comprehending the measured performance of the 7 samples by linking it to related theories on resonant and interference absorption.

The majority of the measured peaks lies within the suggested destructive interference frequency bands. When the peak lies close to the second boundary of the band, it coincides also with the interference frequency of the quarter wavelength tube [1.2/ 2.1/ 2.2]. Finally, samples 1.2 and 2.5 might perform as a Helmholtz resonator. It seems that samples with a diameter of 1cm, perform closer to the predictions based on theory.

Furthermore, there was an attempt to relate performance to geometrical characteristics, but it was not possible to define clear and safe points.





- Surface
- Quarter length
- **Interference point** due to destructive interference on the surface
- **Interference point** due to destructive interference second boundary or quarter wavelength tube

The objective of this part of the analysis, is to define the position of the interference point along the tested air-paths. As mentioned earlier in this report, the equation of passive destructive interference is:

$$f = \frac{(2n - 1)c}{2\Delta L}$$

- [f] interference frequency
- [c] speed of sound in air
- [n] random integer 1, 2, 3, ...
- [ΔL] length difference

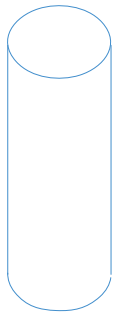
Taking into consideration the measured peak frequencies, it is easy to extract ΔL:

$$\Delta L = \frac{(2n - 1)c}{2f}$$

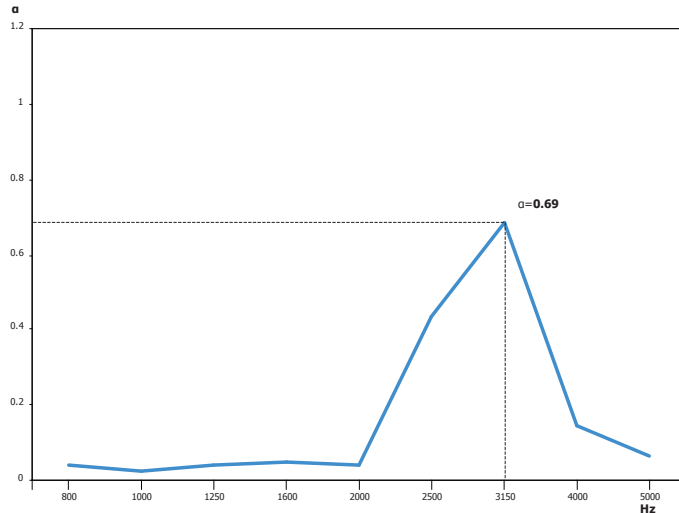
- [f] measured interference frequency

The diagrams on this page indicate the location of the interference point when calculated with the above mentioned method.

When destructive interference occurs on the surface of the absorbers [samples 1.1/ 1.3/ 2.4/ 2.5], the ratio $\Delta L/L_{tot}$ equals 1 and the peak coincides with the first boundary of the interference frequency band. When the ratio $\Delta L/L_{tot}$ equals 0.5 [samples 1.2/ 2.1/ 2,2], the peak relates to the second boundary of destructive interference or to quarter wavelength tube principles; in this case interference occurs at the 1/4 of the total length of the air path. It is notable that in most of the cases the interference point lies between the 1/4 of the total length of the air path and the upper surface. Furthermore, several attempts took place in order to relate the measured peak frequencies to the ratios of L/D [Length/ Diameter] and S/V [Surface/ Volume] without any satisfying result.



n 2.3
SOLID CYLINDER



Sample 2.3

Sample 2.3 has a global diameter of 2.8 cm and height 10cm. It constitutes a solid cylinder. It was important to measure the material properties itself, in order to extract more detailed conclusions about the rest of the samples.

The measurements identified very low acoustic performance of the material itself for most of the tested frequencies. Paradoxically, it performs one relatively high and wide peak at 3150Hz ($\alpha = 0.69$).

In this section, it is attempted to analyse the possible reasons behind this peak. Consequentially, several potential explanations are tested and evaluated:

-Standing waves

A sound wave that is travelling inside the material perpendicular to the surfaces and is reflected by the surfaces of the material back and forth. Because of interference a standing wave is created where one surface inside the material is at one moment a point with high pressure and at the next moment a point with low pressure. The frequency of standing wave is given by:

$$f = \frac{nc}{2h} = \frac{n\sqrt{\frac{E}{\rho}}}{2h}$$

- [n] integer 1, 2, 3, etc
- [c] speed of sound in m/s
- [h] height of the cylinder in m
- [E] Young's modulus
- [ρ] Material density

The material specifications for sintered PA12, are:

$$E = 1650 \pm 150 \text{ MPa}$$

$$\rho = 0.9 - 0.97 \text{ g/cm}^3$$

$$h = 0.1 \text{ m}$$

When applied to the equation, standing waves would occur between 5838 and 6396Hz.

Based on this calculation it seems that the peak is not caused by a standing wave. According to the source of the material data, the actual values of the properties might vary significantly as they are dramatically affected by part geometry and process parameters. In this sense, standing wave remains a possible explanation of the issued peak.

-Resonance of small air gap

During the measuring process, samples were carefully sealed with vaseline before measured at the impedance tube. Despite this fact, the peak might be caused by a small air gap at the cylinder's boundaries.

-Standing wave in the cross-sectional direction of the tube. This explanation is mostly improbable, since the measurements followed the standards.

$$f = \frac{nc}{2d}$$

- [n] integer 1, 2, 3, etc
- [c] speed of sound in air
- [d] diameter of the cylinder in m

Applying the values to the equation, suggest a peak frequency at 5716Hz.

-Mass-spring system of mass on top of small air gap

$$f = \frac{1}{2\pi} \sqrt{\frac{E_{air}}{d_{spr}m}} = \frac{1}{2\pi} \sqrt{\frac{E_{air}}{d_{spr}\rho_m d_m}}$$

- [E] Bulk modulus of air
- [d_{spr}] air gap diameter
- [ρ_m] material thickness
- [d_m] material density

Knowing that the peak frequency is at 3150Hz, it can easily be calculated that the size of the gap would be approximately 3µm. Moreover, for such a mass-spring system with these properties the peak would be small and low.

-Mass-spring-mass system because of layered production system with small deviations in density

$$f = \frac{1}{2\pi} \sqrt{\frac{E_{dyn}}{d_{spr}} \left(\frac{2}{\rho_m d_m} \right)} = \frac{C_M}{2\pi} \sqrt{\frac{2}{d_{spr} d_m}}$$

Performing the calculation for $f = 3150\text{Hz}$ and $C_M = 1167\text{m/s}$, it comes out that d_{spr} and d_m should be approximately 0.26m. This value excites the sample's size.

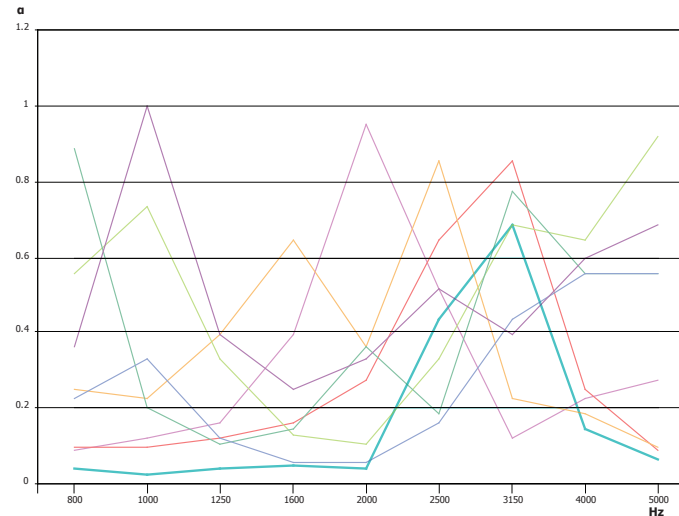
Conclusions:

Standing waves inside the material are possible. However, the material properties of PA12 should be different from the tabulated values. This explanation remains possible, since the material specifications might vary because of the fabrication technique.

For the same reason [uncertified actual material specifications] the proposed mass-spring-mass system might be possible.

Alternatively, the peak might be caused by insufficient sealing during the measurement process.

The rest of the options seem to be most unlikely.



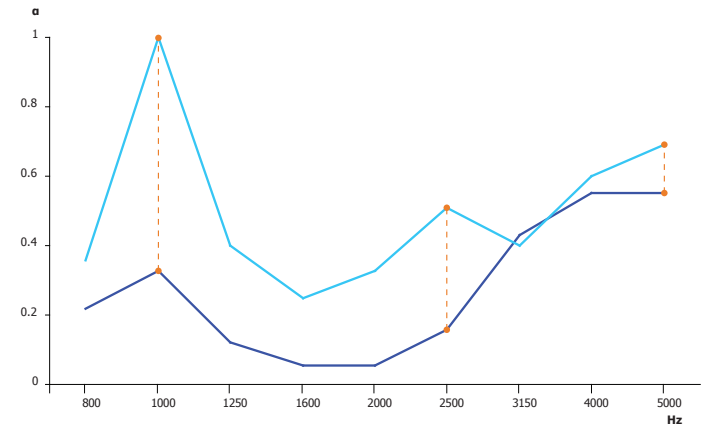
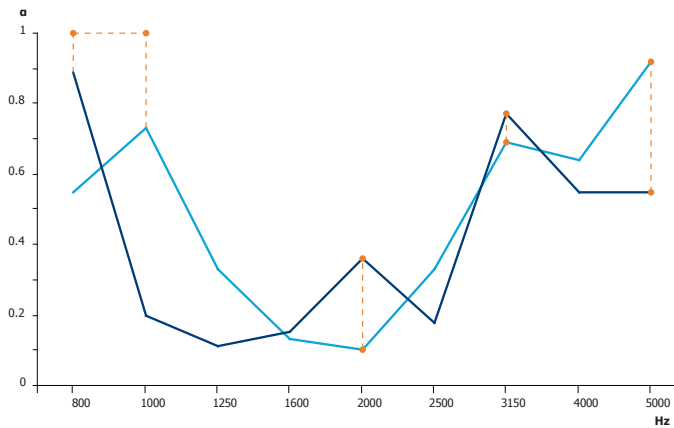
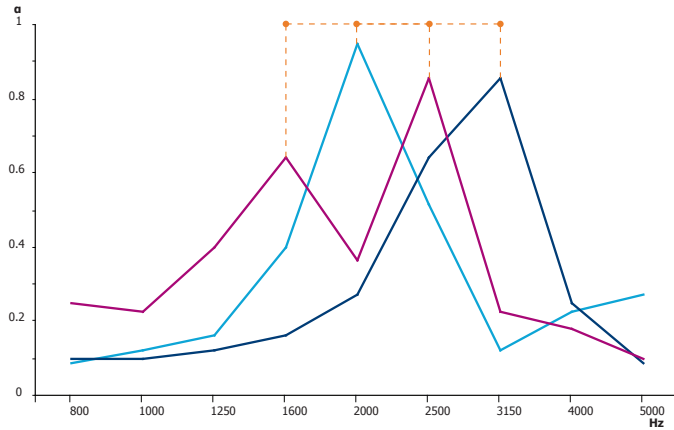
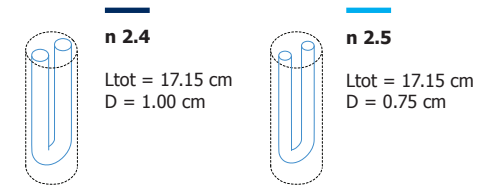
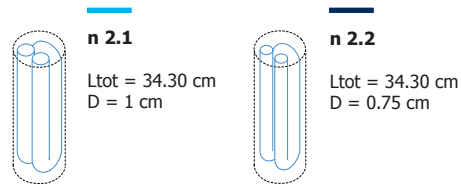
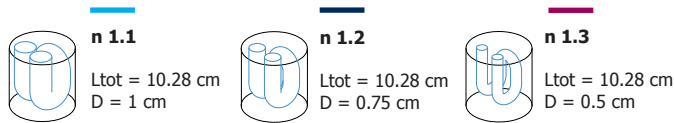
When the graph of the performance of the solid cylinder is overlaid with the rest of the tested samples, it is observed that:

-At frequencies between 800 and 2000 Hz, as well as between 4000 and 5000Hz, the material sample has a low sound absorption coefficient. This means that at least here the results of the passive destructive absorbers will not be affected by the material as shown with the solid cylinder.

-At 2500Hz, samples 2.1 [L=34.3cm, D=1cm], 2.2 [L=17.15cm, D=0.75cm] and 2.4 [L=17.15cm, D=1cm] perform lower than the material itself.

-at 3150Hz, samples 2.4 [L=17.15cm, D=1cm], 2.5 [L=17.15cm, D=0.75cm], 1.1 [L=10.28cm, D=1cm] and 1.3 [L=10.28cm, D=0.75cm] perform lower than the material itself.

An additional remark is that when the graphs of the samples are overlaying there is no frequency that their performance is "synchronised" [as it was the case in Phase 1].



Samples 1.1, 1.2 and 1.3

In this set, all samples have the same length (=10.28cm) and shape of air-path. The only characteristic that is changing is the diameter.

1.1: Diameter=1cm > 2000 Hz > $\alpha = 0.95$

1.2: Diameter=0.75cm > 3150 Hz > $\alpha = 0.85$

1.3: Diameter=0.5cm > 1600/ 2500 Hz > $\alpha = 0.64/ 0.85$

The highest value for normal absorption coefficient is measured for sample 1.1, which has a diameter of 1cm. All samples perform relatively well at specified frequencies.

The peak frequencies occur between 1250 and 3150 Hz. There is no clear relation detected between radius, length and interference frequency.

According to the analysis of the previous chapter, samples 1.1 performs closer to the predictions based on theory of destructive interference.

Samples 2.1 and 2.2

In this set, all samples have the same length (=34.30cm) and shape of air-path. The only characteristic that is changing is the diameter.

2.1: Diameter = 1cm > 1000/ 3150/ 5000 Hz > $\alpha = 0.73/ 0.68/ 0.92$

2.2: Diameter = 0.75cm > 800/ 2000/ 3150 Hz > $\alpha = 0.89/ 0.36/ 0.77$

The highest value for normal absorption coefficient is measured for sample 2.1, which has a diameter of 1cm. Both samples, perform relatively well at specific frequencies.

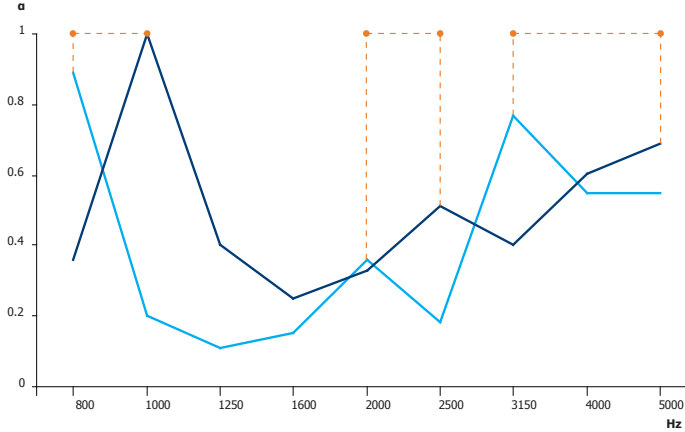
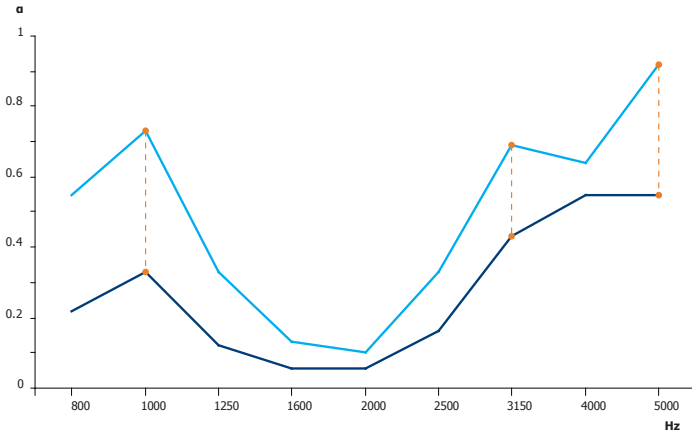
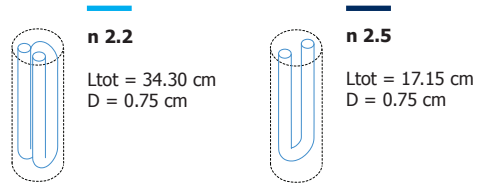
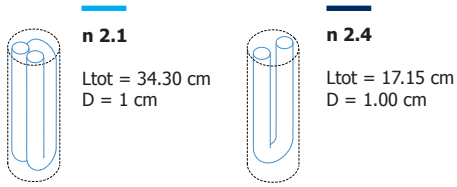
Sample 2.4 and 2.5

In this set, all samples have the same length (=17.15cm) and shape of air-path. The only characteristic that is changing is the diameter.

2.4: Diameter = 1cm > 1000/ 5000 Hz > $\alpha = 0.33/ 0.55$

2.5: Diameter = 0.75cm > 1000/ 2500/ 5000 Hz > $\alpha = 1.00/ 0.51/ 0.69$

In this case, the sample with the smaller diameter [2.5] performs better than the sample with the bigger diameter. Consequently, the biggest absorption coefficient [best acoustic performance] is measured on the sample 2.5 which has a diameter of 0.75cm. The difference in diameter does not affect the global peak frequency, which occurs for both samples at 1000Hz.



Samples 2.1 and 2.4

In this set, all samples have the same diameter (=1cm) and shape of air path. The only characteristic that is changing is the length. Since the length of 2.4 (17.15cm) is half the length of 2.1 (34.3cm), it is expected that its corresponding peak frequencies when $n_{2.4} = n_{2.1}$, will almost double:

$$\begin{aligned} 2 * f_{2.1(n=1)} &= f_{2.4(n=1)} = 1000\text{Hz} \\ 2 * f_{2.1(n=2)} &= f_{2.4(n=2)} = 3000\text{Hz} \\ 2 * f_{2.1(n=3)} &= f_{2.4(n=3)} = 5000\text{Hz} \end{aligned}$$

In this case, no shift of the peak frequencies is observed. In contrary, both samples perform their global peaks at the same frequencies. The sample with the longer path performs clearly better.

Samples 2.2 and 2.5

In this set, all samples have the same diameter (=0.75cm) and shape of air path. The only characteristic that is changing is the length. Since the length of 2.5 (17.15cm) is half the length of 2.2 (34.3cm), it is expected that its corresponding peak frequencies when $n_{2.4} = n_{2.1}$, will almost double:

$$\begin{aligned} 2 * f_{2.2(n=1)} &= f_{2.5(n=1)} = 1000\text{Hz} \\ 2 * f_{2.2(n=2)} &= f_{2.5(n=2)} = 3000\text{Hz} \\ 2 * f_{2.2(n=3)} &= f_{2.5(n=3)} = 5000\text{Hz} \end{aligned}$$

Even though the difference in length causes peaks at different frequencies, the shift is much smaller than expected. Additionally, the sample with the shorter length results to higher values of normal absorbing coefficient.

Conclusions

The objective of this section, was to examine how length and diameter affect acoustic performance through the comparative analysis of the tested absorbers.

In most of the cases, the samples with bigger diameter result to higher absorbing coefficient values, which is measured along the vertical axis of the graph. Additionally, the samples with bigger diameter [1 or 0.75 cm] perform in a more predictable manner. In some cases, it is observed that a change in diameter can cause also peaks at different frequencies.

In this set of measurements, the length appears less effective. The tested absorbers had a length difference with a factor 2; this corresponds to a frequency difference with a factor 2 as well. This was not exactly the case here. There is an indication that longer air-paths can improve the acoustic performance of the samples.

In this chapter, the results of the second phase's measurements at mid and high frequencies are discussed. The small amount of samples leads to a series of observations and assumptions, thus does not allow to more general rules/ statements.

Observations:

1_ The measured performance of the samples has been successfully related to the **theory** on interference and resonant absorbers: passive destructive interference, Helmholtz absorbers and quarter wave-length tube.

2_ It is observed that the position of the **interference point** is located between the 1/4 [one quarters] of the total length of the air-path and the upper surface of the absorber:

$$\frac{1}{4}L_{\text{tot}} < \Delta L < L_{\text{tot}}$$

3_ The **material properties** and **surface smoothness** seem to affect acoustic performance. In the case of the samples 0.2/1.2, these parameters seem

to affect the width of the peaks - which become narrower-, as well as their position and performance. However, the rest of the samples have closer correspondence. More tests are needed to unambiguously conclude whether material affects performance and in what way.

4_The **material** itself was expected to have low acoustic performance at all frequencies. Despite this fact, it performs a peak at 3150Hz ($\alpha = 0.69$) when measured. Several attempts to explain this peak are not confirmed yet. Standing waves inside the material are possible. However, the material properties of PA12 should be different from the tabulated values. This explanation remains possible, since the material specifications might vary because of the fabrication technique. For the same reason [uncertified actual material specifications] the proposed mass-spring-mass system might be possible. Alternatively, the peak might be caused by insufficient sealing during the measurement process.

It appears that the geometrical rules of the passive

destructive interference when applied on the majority of the samples, improve the acoustic performance of the material.

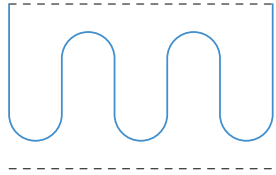
6_The **diameter** of the air-paths affects the results. In most of the cases, the samples with bigger diameter result to higher absorbing coefficient values. In some cases, it is observed that a change in diameter can cause also peaks at different frequencies. Additionally, samples with a tube diameter closer to 1 cm, perform in a more predictable manner.

7_ In this set of measurements, the **length** appears less effective. There is an indication that longer air-paths can improve the acoustic performance of the samples.

8_ The samples give high values for absorbing coefficients, but on the same time very low dips. The following table is summarizing the highest values performed:

Sample Code	1.1	1.2	1.3	2.1	2.2	2.4	2.5
Length [cm]	10.28	10.28	10.28	34.30	34.30	17.15	17.15
Diameter [cm]	1.00	0.75	0.50	1.00	0.75	1.00	0.75
Frequency [Hz]	2000	3150	1600/ 2500	1000/ 3150/ 5000	800/ 3150	5000	1000/ 2500/ 5000
Absorbing Coefficient	0.95	0.85	0.64/ 0.85	0.73/ 0.68/ 0.92	0.89/ 0.77	0.55	1.00/ 0.51/ 0.69





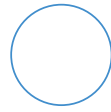
D = 10.00cm
H = 10.00cm

BIG SAMPLES: **DIAMETER**
MEASUREMENT'S ACCURACY



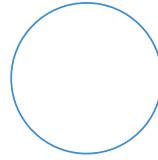
n3.1.A 3.1.B

L_{tot} = 52.13cm
D = 1.00cm



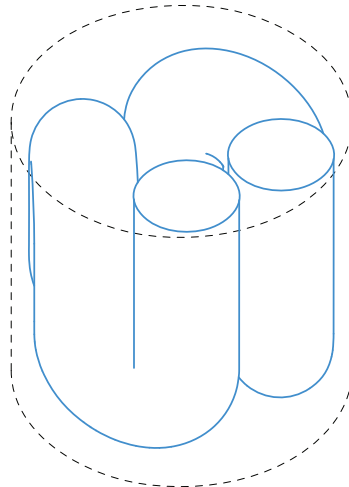
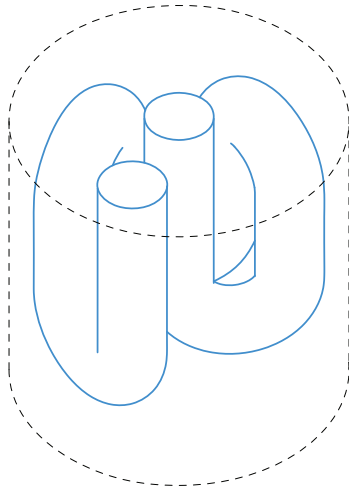
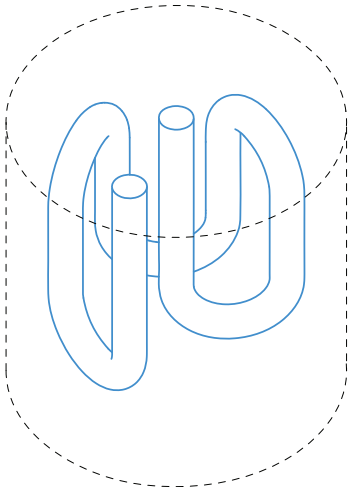
n3.2.A 3.2.B

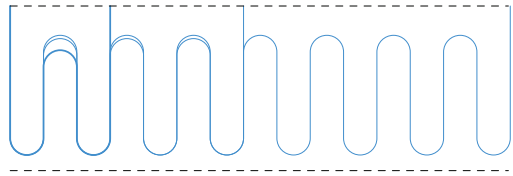
L_{tot} = 52.13cm
D = 2.00cm



n3.3.A 3.3.B

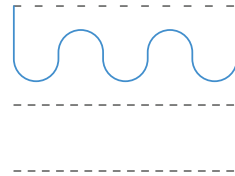
L_{tot} = 52.13cm
D = 3.00cm





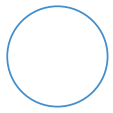
D = 10.00cm
H = 10.00cm

BIG SAMPLES: LENGTH



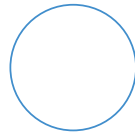
D = 10.00cm
H = 10.00cm
6.00cm

BIG SAMPLES: THICKNESS / [NO]CAP/ GEOMETRY



n3.4

L_{tot} = 34.30cm
D = 2.00cm



n3.6

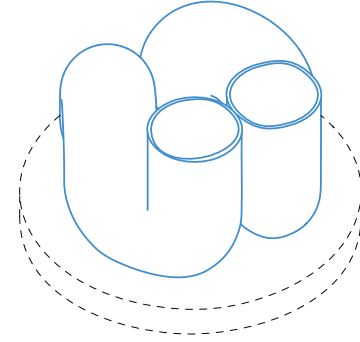
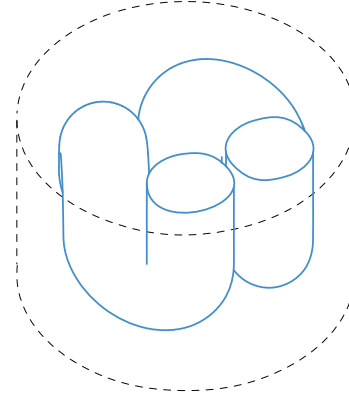
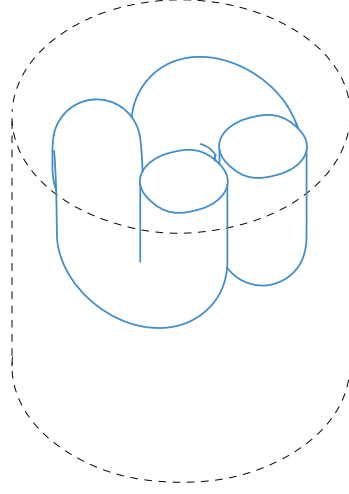
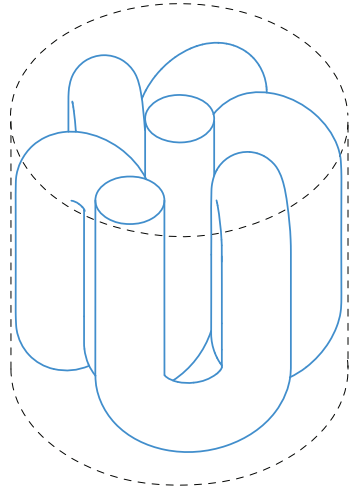
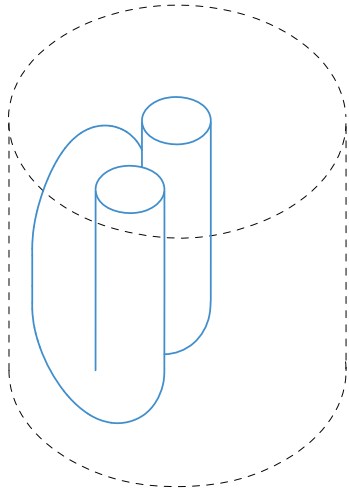
L_{tot} = 29.21cm
D = 2.50cm

n3.7

L_{tot} = 29.21cm
D = 2.50cm

n3.8

L_{tot} = 29.21cm
D = 2.50cm

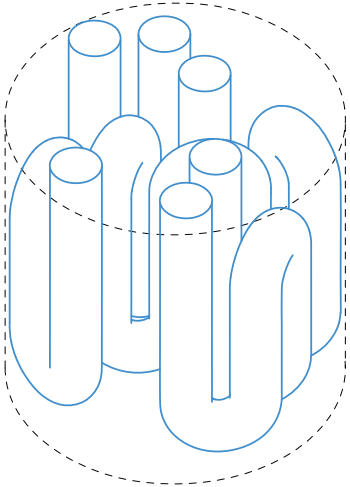


BIG SAMPLES: COMBINATIONS/ DIAMETER SCALING



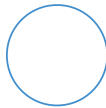
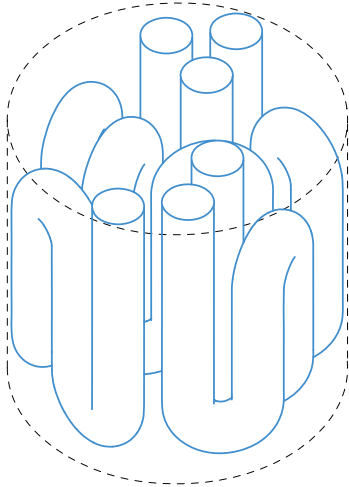
n4.1

2*L1 + L2
 L1 = 34.3cm
 L2 = 68.6cm
D = 1.50cm



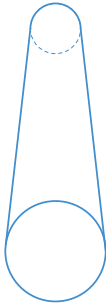
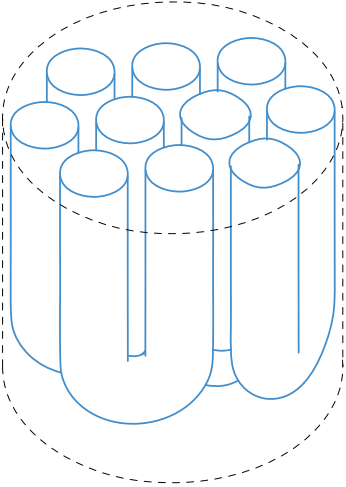
n4.2

L1 + L2 + L3
 L1 = 34.3cm/ L2 = 68.6cm
 L3 = 51.5cm
D = 1.50cm



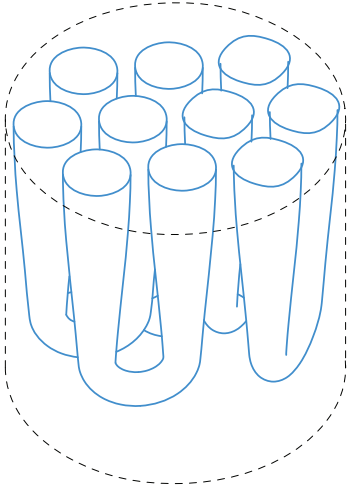
n4.3

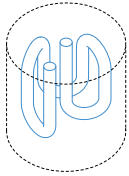
5*D
 Ltot = 19.28cm
D = 2.00cm



n4.4

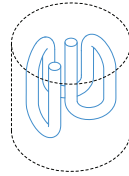
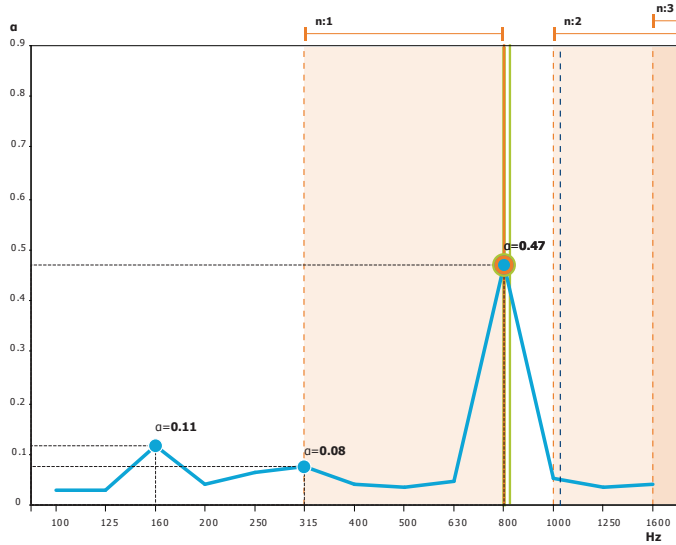
5*L
 Ltot = 52.13cm
D = 2.00 - 1.00cm





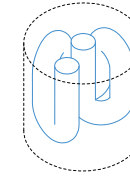
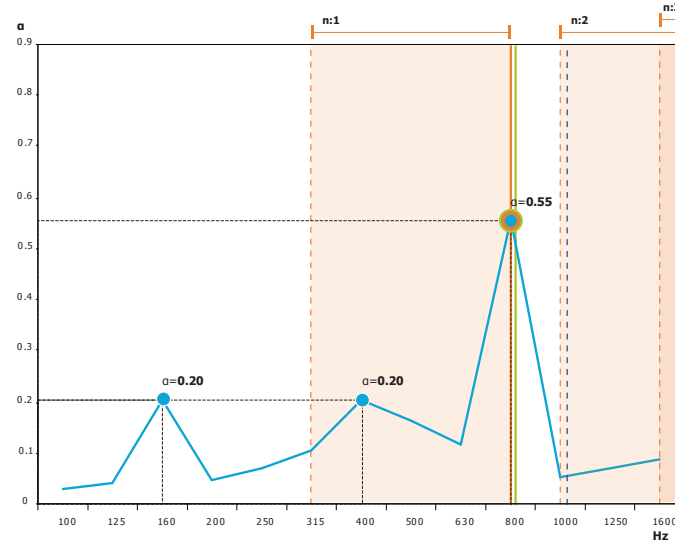
n 3.1.A

Ltot = 52.13 cm
D = 1 cm



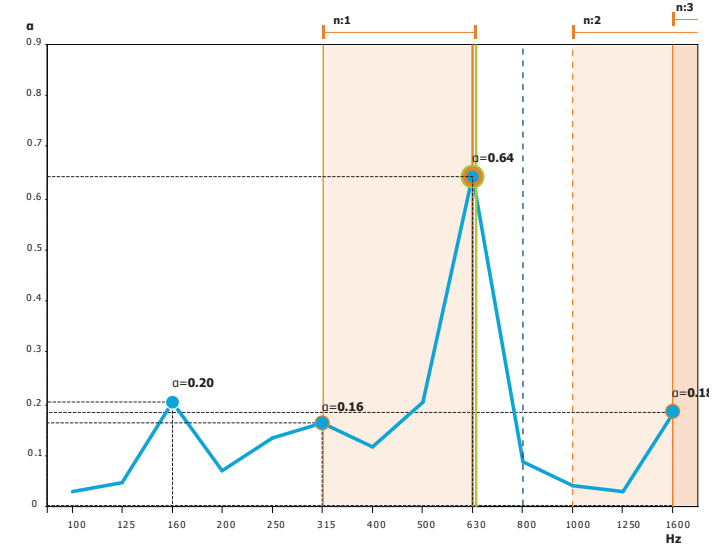
n 3.1.B

Ltot = 52.13 cm
D = 1 cm



n 3.2.A

Ltot = 52.13 cm
D = 2 cm



- Destructive Interference
- Quarter Wavelength tube
- Helmholtz Resonator

Sample 3.1.A

The sample 3.1.A has a global diameter of 9.8 cm and height 10cm. It contains one air path with a total length of 52.13 cm and diameter of 1 cm. The analysis suggests 3 frequency bands where interference might occur: 328-657 Hz (n=1), 986-1973 Hz (n=2) and 1644-3288 Hz (n=3).

The measurements identify 3 peak frequencies at 160Hz ($\alpha=0.11$), 315Hz ($\alpha=0.08$) and 800Hz ($\alpha=0.47$). The performance of the sample is relatively low. All the peaks over 315 Hz match with destructive interference. The global peak lies close to the second boundary of the suggested **destructive interference** frequency band for n=1. So, it coincides also with the interference frequency of quarter wavelength tube. Further calculations show that the sample is not behaving as a Helmholtz resonator.

Sample 3.1.B

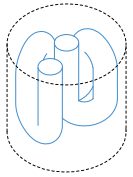
The sample 3.1.B has a global diameter of 9.8 cm and height 10cm. It contains one air-path with a total length of 52.13 cm and diameter of 1 cm. The analysis suggests 3 frequency bands where interference might take place: 328-657 Hz (n=1), 986-1973 Hz (n=2) and 1644-3288 Hz (n=3).

The measurements show 3 peak frequencies at 160Hz ($\alpha=0.20$), 400Hz ($\alpha=0.20$) and 800Hz ($\alpha=0.55$). The performance of the sample is relatively low. All the peaks over 400 Hz match with destructive interference. The global peak lies close to the second boundary of the suggested **destructive interference** frequency band for n=1. So, it coincides also with the interference frequency of quarter wavelength tube. Additional calculations show that the sample is not behaving as a Helmholtz resonator.

Sample 3.2.A

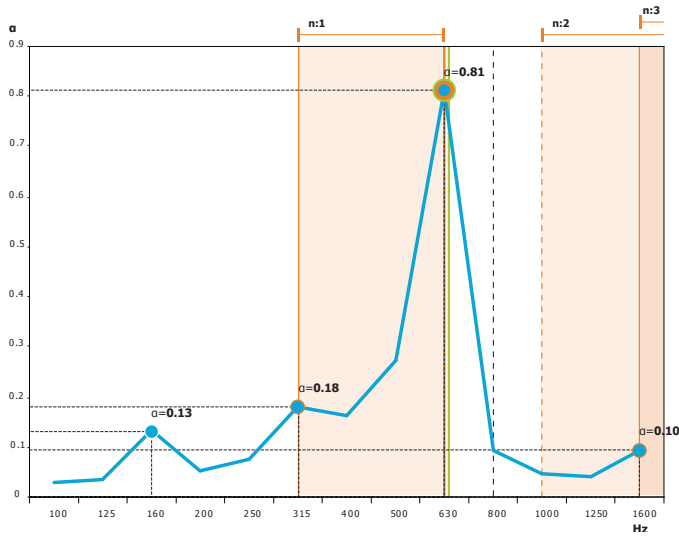
Sample 3.2.A has a global diameter of 9.8 cm and height 10cm. It contains one air-path with a total length of 52.13 cm and diameter of 2 cm. The analysis suggests 3 frequency bands where interference might take place: 328-657 Hz (n=1), 986-1973 Hz (n=2) and 1644-3288 Hz (n=3).

The measurements identified 4 peaks at 160Hz ($\alpha=0.20$), 315Hz ($\alpha=0.16$), 630Hz ($\alpha=0.64$) and 1600Hz ($\alpha=0.11$). All the peaks over 315Hz match with **destructive interference**. The analysis shows that the global peak lies close to the second boundary of the suggested frequency band for n=1. Hence, it coincides also with the interference frequency of quarter wavelength tube. Further calculations show that the absorber is not performing as a Helmholtz resonator ($f=820$ Hz).



n 3.2.B

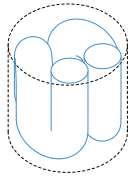
Ltot = 52.13 cm
D = 2 cm



Sample 3.2.B

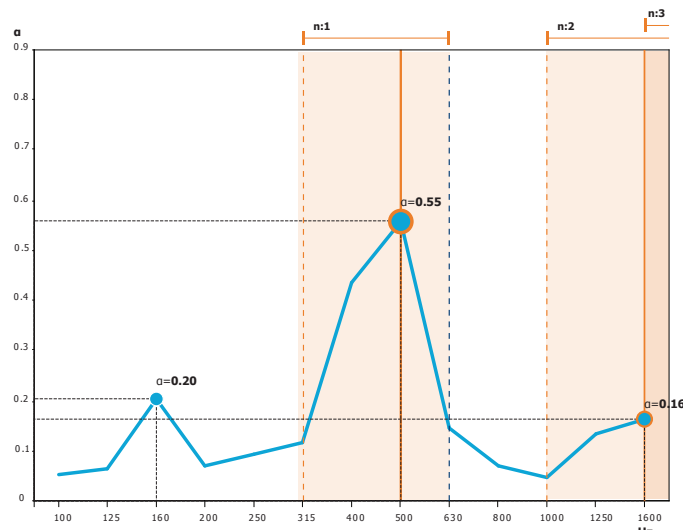
Sample 3.2.B has a global diameter of 9.8 cm and height 10cm. It contains one air-path with a total length of 52.13 cm and diameter of 2 cm. The analysis suggest 3 frequency bands where interference might take place: 328-657 Hz (n=1), 986-1973 Hz (n=2) and 1644-3288 Hz (n=3).

During the measurements 4 peaks are identified at 160 Hz ($\alpha=0.13$), 315 Hz ($\alpha=0.18$), 630 Hz ($\alpha=0.81$) and 1600 Hz ($\alpha=0.10$). All the peaks over 315Hz match with **destructive interference**. The analysis of the results shows that the global peak lies close to the second boundary of the suggested frequency band for n=1. Therefore, it coincides also with the interference frequency of quarter wavelength tube. Further calculations show that the absorber is not performing as a Helmholtz resonator ($f=820\text{Hz}$).



n 3.3.A

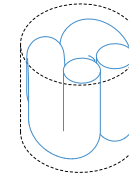
Ltot = 52.13 cm
D = 3 cm



Sample 3.3.A

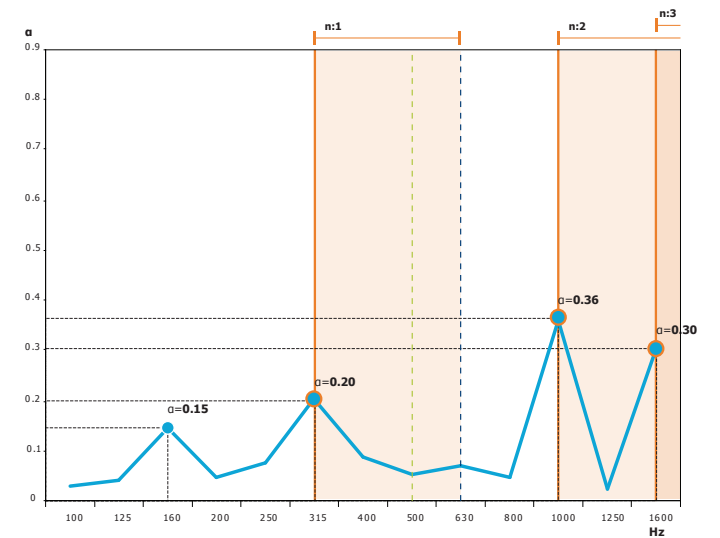
Sample 3.3.A has a global diameter of 9.8 cm and height 10cm. It contains one air-path with a total length of 52.13 cm and diameter of 3 cm. The analysis suggest 3 frequency bands where interference might take place: 328-657 Hz (n=1), 986-1973 Hz (n=2) and 1644-3288 Hz (n=3).

According to the measurements, there were 3 peak frequencies, namely at 160 Hz ($\alpha = 0.20$), 500 Hz ($\alpha = 0.55$) and 1600 Hz ($\alpha = 0.16$). All the peaks over 500Hz match with destructive interference. The performance of the sample is relatively low. The global peak lies within the suggested **destructive interference** frequency band for n=1. Further calculations show that the absorber is not performing as a Helmholtz resonator ($f=670\text{Hz}$).



n 3.3.B

Ltot = 52.13 cm
D = 3 cm

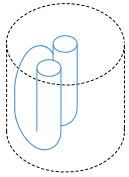


Sample 3.3.B

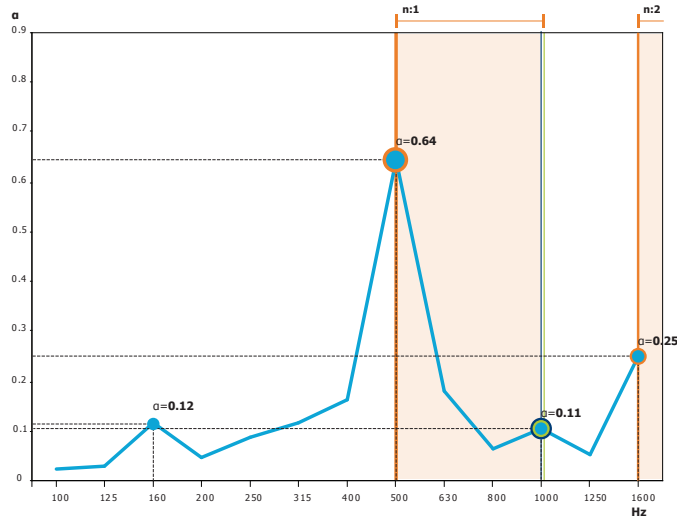
Sample 3.3.B has a global diameter of 9.8 cm and height 10cm. It contains one air-path with a total length of 52.13 cm and diameter of 3 cm. The analysis suggest 3 frequency bands where interference might take place: 328-657 Hz (n=1), 986-1973 Hz (n=2) and 1644-3288 Hz (n=3).

During measurements, there were 4 peak frequencies identified, at 160 Hz ($\alpha=0.15$), 315 Hz ($\alpha=0.20$), 1000 Hz ($\alpha=0.36$) and 1600 Hz ($\alpha=0.30$). The performance of the sample is relatively low. All the peaks over 315 Hz, lie within the suggested **destructive interference** frequency bands. Further calculations show that the absorber is not performing as a Helmholtz resonator ($f=670\text{Hz}$).

- Destructive Interference
- Quarter Wavelength tube
- Helmholtz Resonator



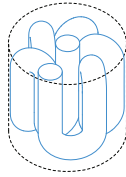
n 3.4
Ltot = 34.30 cm
D = 2 cm



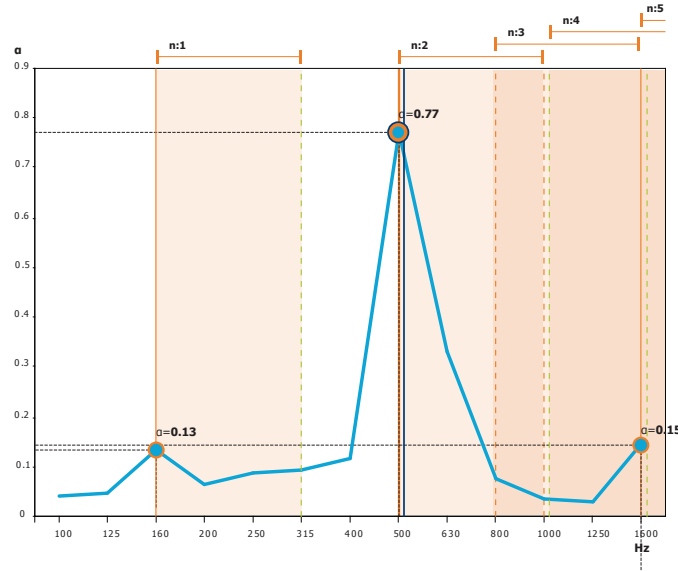
Sample 3.4

Sample 3.4 has a global diameter of 9.8 cm and height 10cm. It contains one air-path with a total length of 34.30 cm and with a diameter of 2 cm. The analysis suggests 2 frequency bands where interference might take place: 500-1000 Hz (n=1) and 1500-3000 Hz (n=2).

During measurements, 4 peaks are identified at 160 Hz ($\alpha=0.12$), 500 Hz ($\alpha=0.64$), 1000 Hz ($\alpha=0.11$) and 1600 Hz ($\alpha=0.25$). All the peaks over 500Hz match with destructive interference. The analysis of the results shows that the global peak lies within the suggested **destructive interference** frequency band for n=1. Further calculations show that the absorber's performance at 1000 Hz might also relate to Helmholtz resonator ($f=820\text{Hz}$) or quarter wavelength tube principles.



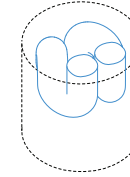
n 3.5
Ltot = 108.30 cm
D = 2 cm



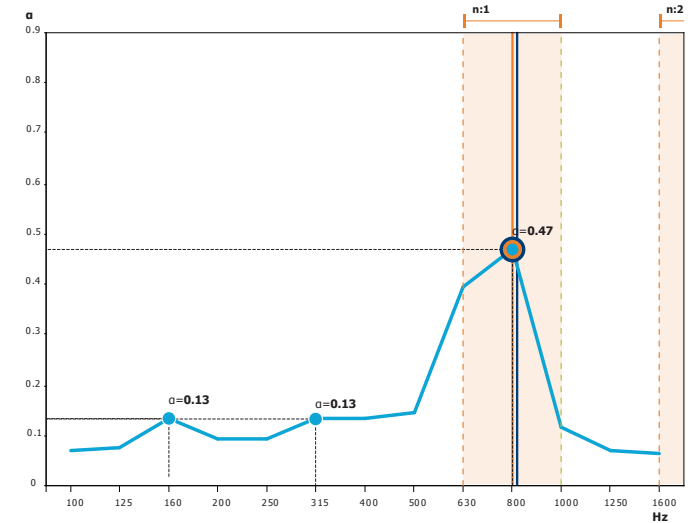
Sample 3.5

Sample 3.5 has a global diameter of 9.8 cm and height 10cm. It contains one air-path with a total length of 108.30 cm and with a diameter of 2 cm. The analysis suggests 5 frequency bands where interference might take place: 158-316 Hz (n=1), 475-950 Hz (n=2), 791-1583 Hz (n=3), 1108-2216 Hz (n=4) and 1425-2850 Hz (n=5).

During measurements, 3 peaks are identified at 160 Hz ($\alpha = 0.13$), 500 Hz ($\alpha = 0.77$) and 1600 Hz ($\alpha = 0.15$). All the peaks match with the suggested **destructive interference** frequency bands. There is an indication that the global peak might be caused by Helmholtz resonator principles.



n 3.6
Ltot = 29.21 cm
D = 2.5 cm



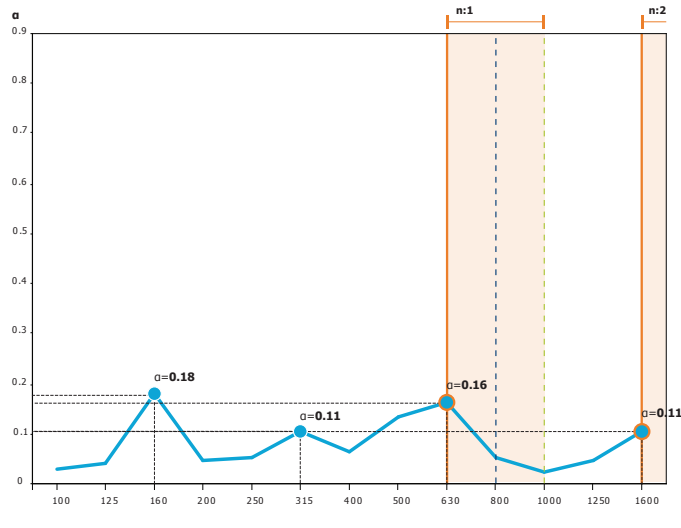
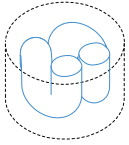
Sample 3.6

Sample 3.6 has a global diameter of 9.8 cm and height 10cm. It contains one air-path with a total length of 29.21 cm and with a diameter of 2.5 cm. The analysis suggests 2 frequency bands where interference might occur: 587-1174 Hz (n=1) and 1761-3522 Hz (n=2).

During measurements, 3 peaks are identified at 160 Hz ($\alpha = 0.13$), 315 Hz ($\alpha = 0.13$) and 800 Hz ($\alpha = 0.47$). The analysis of the results suggests that the global peak might be caused either by **destructive interference** or Helmholtz resonator principles.

- Destructive Interference
- Quarter Wavelength tube
- Helmholtz Resonator

n 3.7
L_{tot} = 29.21 cm
D = 2.5 cm

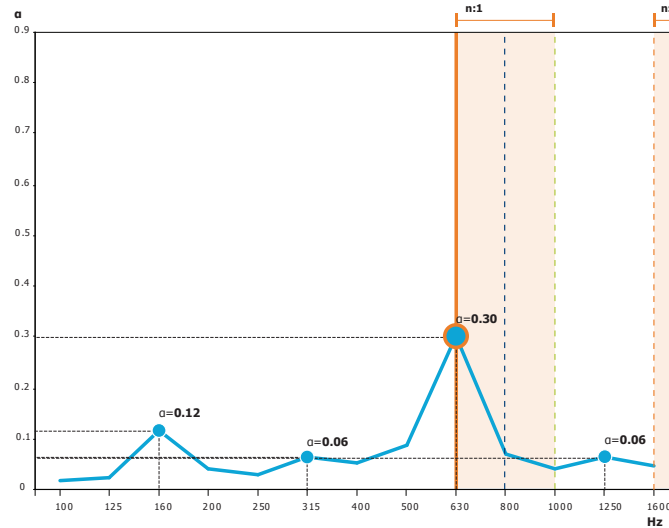
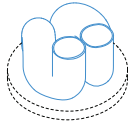


Sample 3.7

Sample 3.7 has a global diameter of 9.8 cm and height 6cm. It contains one air-path with a total length of 29.21 cm and with a diameter of 2.5 cm. The analysis suggests 2 frequency bands where interference might occur: 587-1174 Hz (n=1) and 1761-3522 Hz (n=2).

During measurements, 4 peaks are identified at 160 Hz ($\alpha = 0.18$), 315 Hz ($\alpha = 0.11$), 630 Hz ($\alpha = 0.16$) and 1600 Hz ($\alpha = 0.11$). The performance of this sample is very low. The peaks over 630Hz match with **destructive interference**. Further calculations show that the performance is not related to Helmholtz resonator ($f=980\text{Hz}$) or quarter wavelength tube principles.

n 3.8
L_{tot} = 29.21 cm
D = 2.5 cm

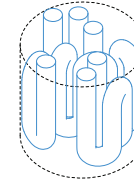


Sample 3.8

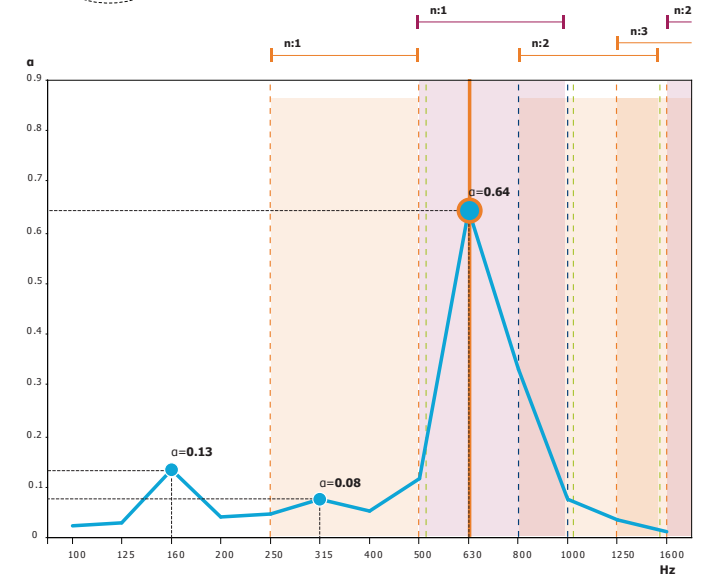
Sample 3.8 has a global diameter of 9.8 cm and height approximately 6cm. It contains one air-path with a total length of 29.21 cm and with a diameter of 2.5 cm. The sample shares the same characteristics with 3.7. Their main difference is that the air-path structure of the examined sample, is exposed. The analysis suggests 2 frequency bands where interference might occur: 587-1174 Hz (n=1) and 1761-3522 Hz (n=2).

During measurements, 4 peaks are identified at 160 Hz ($\alpha = 0.12$), 315 Hz ($\alpha = 0.06$), 630 Hz ($\alpha = 0.30$) and 1250 Hz ($\alpha = 0.06$). The performance of this sample is very low. The analysis suggests that the peak at 630 Hz is caused by **destructive interference**.

n 4.1
L_{tot,1} = 34.30 cm
L_{tot,2} = 68.60 cm
D = 1.5 cm



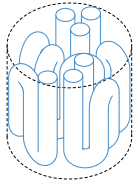
--- Destructive Interference
--- Quarter Wavelength tube
--- Helmholtz Resonator



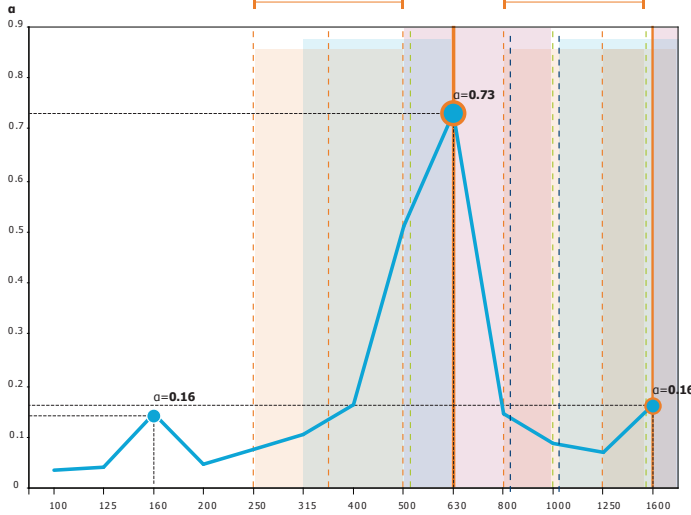
Sample 4.1

Sample 4.1 has a global diameter of 9.8 cm and height 10cm. It contains three air-paths: one with length of 68.6 cm and two with length of 34.3cm. All of them have a diameter of 1.5 cm. The analysis suggests 5 frequency bands where interference might occur; two caused by the short paths [500-1000 Hz (n=1)/ 1500-3000 Hz (n=2)] and 3 caused by the long path [250-500 Hz (n=1)/ 750-1500 Hz (n=2)/ 1250-2500 Hz (n=3)].

During measurements, 3 peaks are identified at 160 Hz ($\alpha = 0.13$), 315 Hz ($\alpha = 0.08$) and 630 Hz ($\alpha = 0.64$). The analysis suggests that the global peak is caused by **destructive interference**. Additional calculations show that performance is not related to Helmholtz resonator or quarter wave tube principles.



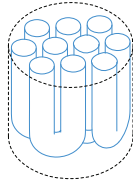
n 4.2
 $L_{tot,1} = 34.30$ cm
 $L_{tot,2} = 51.50$ cm
 $L_{tot,3} = 68.60$ cm
 $D = 1.5$ cm



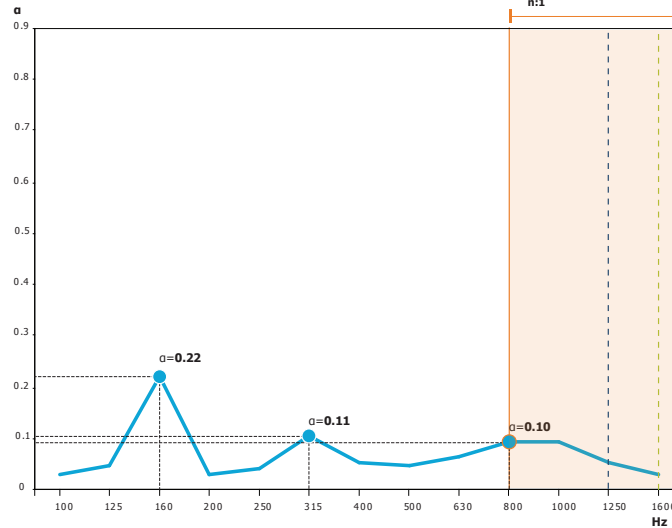
Sample 4.2

Sample 4.2 has a global diameter of 9.8 cm and height 10cm. It contains three air-paths with various lengths: 34.3cm, 51.5cm and 68.6 cm. All of them have a diameter of 1.5 cm. The analysis suggests 7 frequency bands where interference might occur; 2 caused by the short path [500-1000 Hz ($n=1$)/ 1500-3000 Hz ($n=2$)], 2 caused by the medium path [333-666 Hz ($n=1$)/ 999-1998 Hz ($n=2$)] and 3 caused by the long path [250-500 Hz ($n=1$)/ 750-1500 Hz ($n=2$)/ 1250-2500 Hz ($n=3$)].

During measurements, 3 peaks are identified at 160 Hz ($\alpha=0.16$), 630 Hz ($\alpha=0.73$) and 1600Hz ($\alpha=0.16$). The analysis suggests that peaks over 630Hz are caused by **destructive interference**. Further calculations show that performance is not related to Helmholtz resonator.

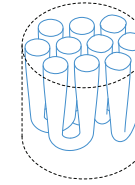


n 4.3
 $L_{tot} = 19.30$ cm
 $D = 2$ cm

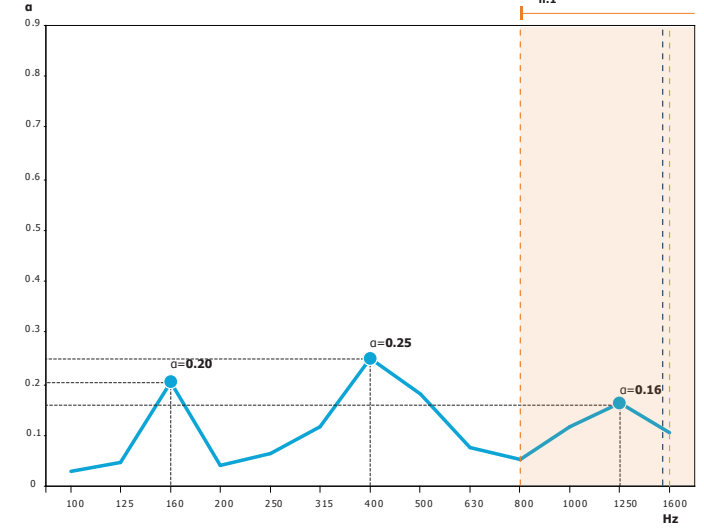


Sample 4.3

Sample 4.3 has a global diameter of 9.8 cm and height 10cm. It contains 5 air-paths with similar characteristics: length 19.3cm and diameter 2 cm. The analysis suggests 1 frequency band where interference might take place: 889-1779 Hz ($n=1$). During measurements, 3 peaks are identified at 160 Hz ($\alpha=0.22$), 315 Hz ($\alpha=0.11$) and 800Hz ($\alpha=0.10$). The performance of the sample is very low. The analysis suggests that the peak at 800 Hz is caused by **destructive interference**. Further calculations show that performance is not related to Helmholtz resonator nor to quarter wavelength tube principles.



n 4.4
 $L_{tot} = 19.30$ cm
 $D = 1-2$ cm

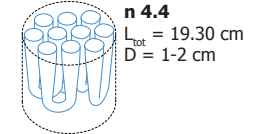
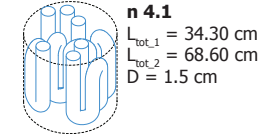
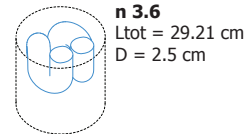
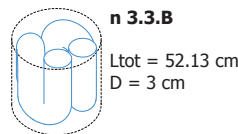
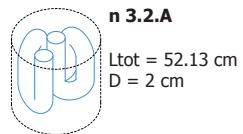
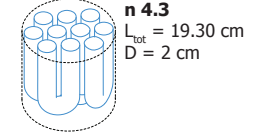
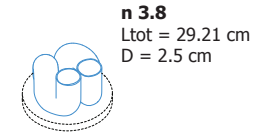
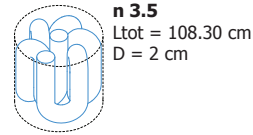
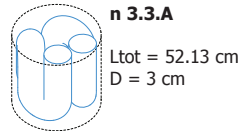
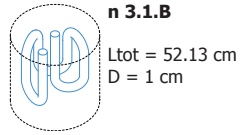
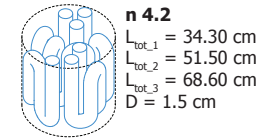
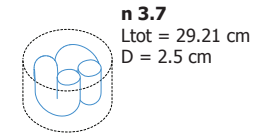
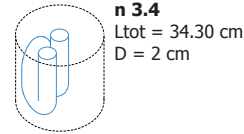
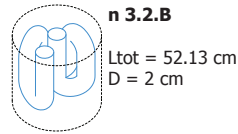
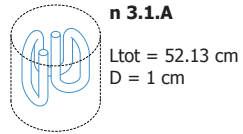


Sample 4.4

Sample 4.4 has a global diameter of 9.8 cm and height 10cm. It contains 5 air-paths with similar characteristics: length 19.3cm and diameter that shifts gradually from 2 cm to 1cm. The analysis suggests 1 frequency band where interference might take place: 889-1779 Hz ($n=1$).

During measurements, 3 peaks are identified at 160 Hz ($\alpha=0.20$), 400 Hz ($\alpha=0.25$) and 1250Hz ($\alpha=0.16$). The performance of the sample is very low. The analysis suggests that the peak at 1250 Hz is caused by **destructive interference**. The performance of the absorber is not related to destructive interference, Helmholtz resonator nor to quarter wavelength tube principles.

- Destructive Interference
- Quarter Wavelength tube
- Helmholtz Resonator



Summary

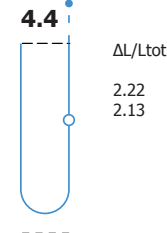
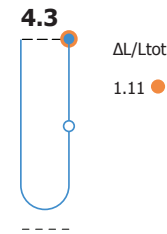
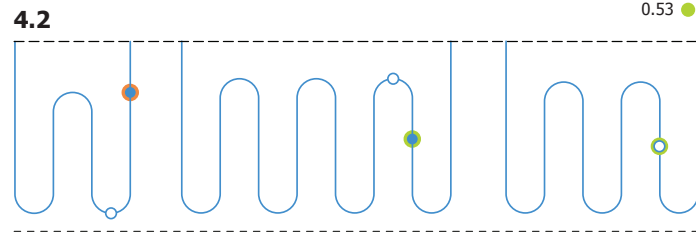
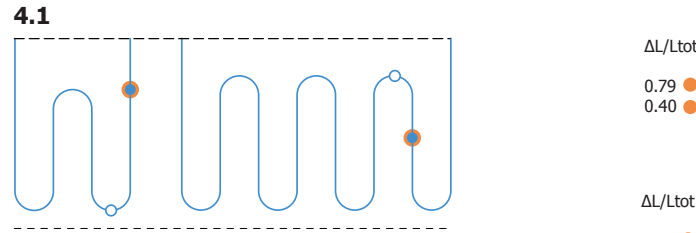
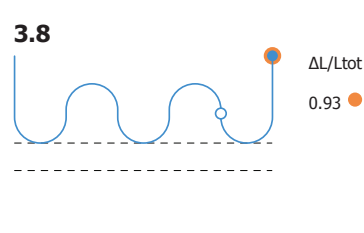
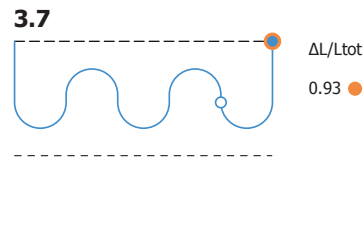
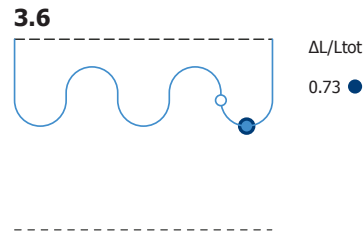
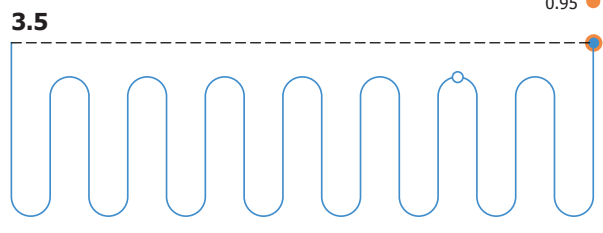
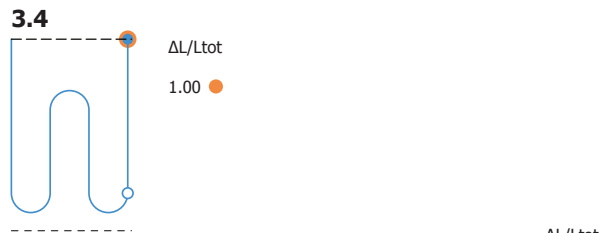
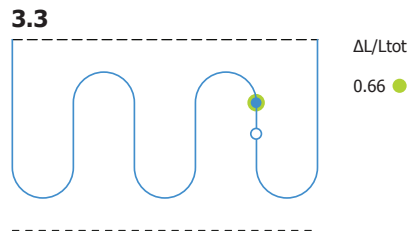
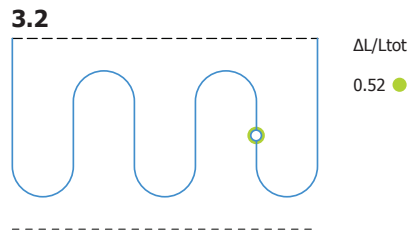
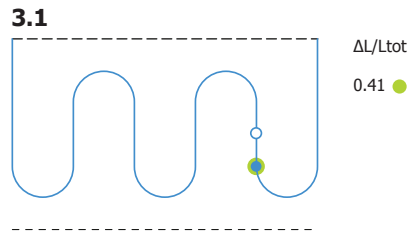
In this section, the focus was on analysing and further comprehending the measured performance of the 15 samples by linking it to related theories on interference and resonant absorption.

It is observed that the performance of every sample relates to destructive interference. Moreover, the global peaks of ten samples correspond to the discussed phenomenon [3.1.A/ 3.1.B/ 3.2.A/ 3.2.B/3.3.A/ 3.3.B/ 3.4/ 3.5/ 3.6/ 4.1/ 4.2]. Seven samples [3.1.A/ 3.1.B/ 3.2.A/ 3.2.B/ 3.3.A/ 3.4/ 4.2] might behave also similar to quarter wavelength tube. Finally, samples 3.4 and 3.6 might perform as a Helmholtz resonator.

It is observed that samples with a diameter between 1.5 and 3cm, perform closer to the predictions based on theory on passive destructive interference.

All samples perform a low peak at 160 Hz. It is assumed that this repetitive pattern in acoustic performance is caused by criteria such as material properties, global dimensions of the samples, etc. Most probably, this fact is not related to the phenomenon of passive destructive interference. Furthermore, there was an attempt to relate performance to geometrical characteristics, but it was not possible to define clear and safe conclusions.

- Predicted amount of peaks [Destructive Interference]
- Measured amount of peaks [G: Global/ L: Local]
- Destructive Interference
- Quarter Wavelength tube
- Helmholtz Resonator
- Surface
- Quarter length
- Interference point** due to destructive interference on the surface
- Interference point** due to destructive interference second boundary or quarter wavelength tube



The objective of this part of the analysis, is to define the position of the interference point along the tested air-paths. Based on the theory of passive destructive interference, it is simple to calculate the position of the interference point along the air-path. The diagrams on this page visualise the results of this analysis.

It is notable that **destructive interference** occurs:

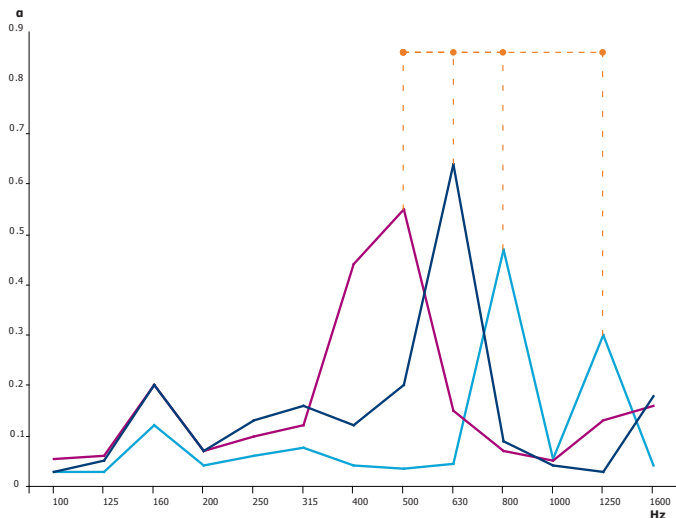
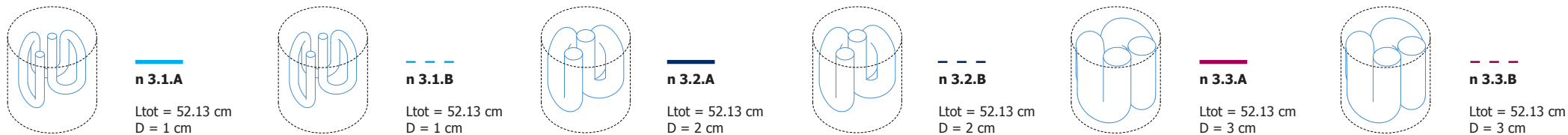
- on the surface of the absorbers if it contains one air-path [samples 3.4/ 3.5/ 3.7/ 3.8]. In this case, the ratio of $\Delta L/L_{tot}$ equals to 1 [$\Delta L = L_{tot}$].
- between $0.40 * L_{tot} < L_{IP} < 0.20 * L_{tot}$, if the absorber contains more than one air-paths [samples 4.1/ 4.2/ 4.3]. In this case, the ratio of $\Delta L/L_{tot}$ varies from 0.8 to 0.4. This fact, might constitute an indication that the measured performance of the multi-channelled samples, might be distorted by the short distance between the air-path entrances¹.

When the ratio $\Delta L/L_{tot}$ equals 0.5, the peak relates to the second boundary of destructive interference or to quarter wavelength tube principles; in this case interference occurs at the 1/4 of the total length of the air path. [samples 3.1/ 3.2/ 3.3/ 4.2].

It is notable that the interference point lies between the 1/4 of the total length of the airpath and the upper surface of the samples. This fact might play an important role when attempting to predict the performance of this specific type of absorbers.

Furthermore, several attempts took place at this stage in order to relate the measured resonant frequencies to the ratios of L/D [Length/ Diameter] and S/V [Surface/ Volume] without getting any satisfying result. [see also: p.]

¹ http://www.deicon.com/technote/adjacent_resonators_deicon.pdf



Samples 3.1.A/ 3.2.A/ 3.3.A

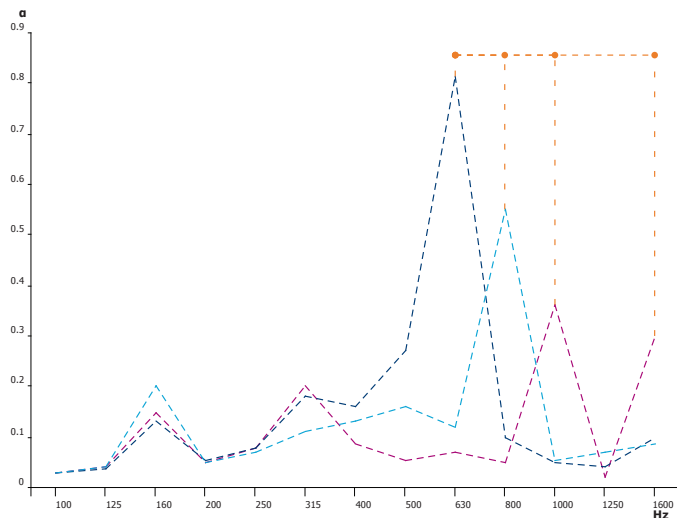
In this set, all samples have the same length (=52.13cm) and shape of air-path. The only characteristic that is changing is the diameter.

3.1.A: D=1cm > 800/ 1250 Hz > $\alpha = 0.47/ 0.30$

3.2.A: D=2cm > 630 Hz > $\alpha = 0.64$

3.3.A: D=3cm > 500 Hz > $\alpha = 0.55$

The highest value for the normal sound absorption coefficient is measured for sample 3.2.A, which obtains a diameter of 2cm. All samples perform relatively good at specified frequencies. The peak frequencies occur between 500 and 1250 Hz. There is no clear relation detected between radius, length and interference frequency.



Samples 3.1.B/ 3.2.B/ 3.3.B

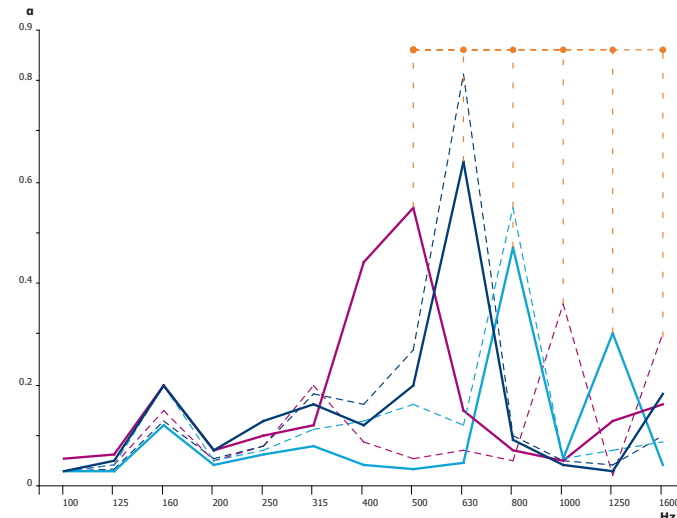
In this set, all samples have the same length (=52.13cm) and shape of air-path. The only characteristic that is changing is the diameter.

3.1.B: D=1cm > 800 Hz > $\alpha = 0.55$

3.2.B: D=2cm > 630 Hz > $\alpha = 0.81$

3.3.B: D=3cm > 1000/ 1600 Hz > $\alpha = 0.36/ 0.3$

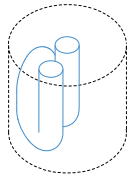
The highest value for the normal sound absorption coefficient is measured for sample 3.2.B, which obtains a diameter of 2cm. All samples perform relatively good at specified frequencies. The peak frequencies occur between 630 and 1600 Hz. There is no clear relation detected between radius, length and resonant frequency.



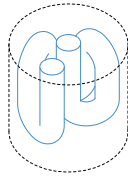
Samples 3.1.A/B 3.2.A/B 3.3.A/B

In this section, it is attempted to identify the influence of the diameter on acoustic performance. The examined samples have the same length (=52.13cm) and shape of air-path. The only characteristic that is changing is the diameter.

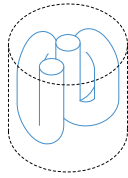
The samples with a diameter equal to 2 cm result to higher absorbing coefficient values, which are measured along the vertical axis of the graph. This fact suggests that there is no linear relation between diameter size and absorbing coefficient values. Besides the improvement of the performance, it seems that diversity in diameter might also cause variations in the frequencies where peaks occur. There is an indication that the increase in the size of the diameter causes peaks at lower frequencies. The only sample that does not comply with this rule is sample 3.3B.



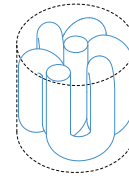
n 3.4
 $L_{tot} = 34.30$ cm
 $D = 2$ cm



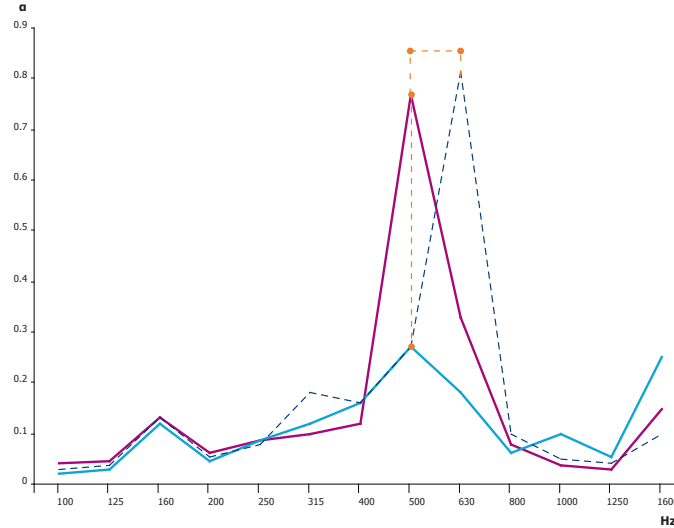
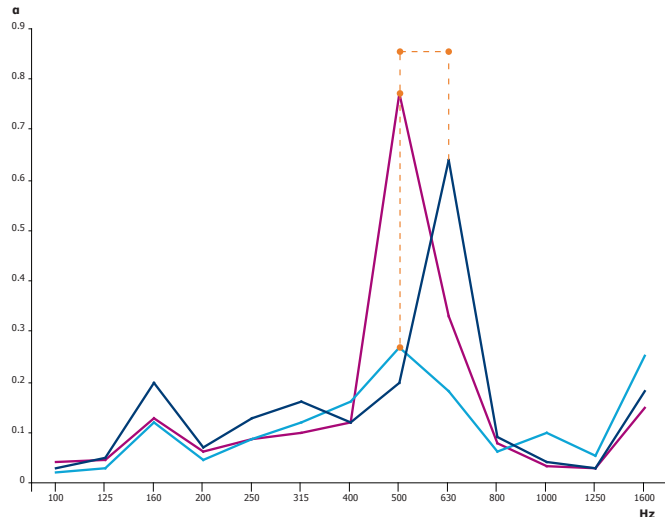
n 3.2.A
 $L_{tot} = 52.13$ cm
 $D = 2$ cm



n 3.2.B
 $L_{tot} = 52.13$ cm
 $D = 2$ cm



n 3.5
 $L_{tot} = 108.30$ cm
 $D = 2$ cm



Samples 3.4/ 3.2.A/ 3.5

In this set, all samples have the same diameter (=2cm) and shape of air-path. The only characteristic that is changing is the length.

- 3.4:** $L = 34.3\text{cm} > 500 \text{ Hz} > \alpha = 0.64$
- 3.2.A:** $L = 52.13\text{cm} > 630 \text{ Hz} > \alpha = 0.64$
- 3.5:** $L = 108.3\text{cm} > 500\text{Hz} > \alpha = 0.77$

The measurements of the compared samples identify equal amounts of global peaks. Samples 3.4 and 3.5 perform their global peaks at the same frequency. The sample with the longer path performs clearly better.

Samples 3.4/ 3.2.B/ 3.5

In this set, all samples have the same diameter (=2cm) and shape of air-path. The only characteristic that is changing is the length.

- 3.4:** $L = 34.3\text{cm} > 500 \text{ Hz} > \alpha = 0.64$
- 3.2.B:** $L = 52.13\text{cm} > 630 \text{ Hz} > \alpha = 0.81$
- 3.5:** $L = 108.3\text{cm} > 500\text{Hz} > \alpha = 0.77$

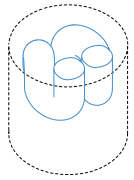
The measurements of the compared samples identify equal amounts of global peaks. Samples 3.4 and 3.5 perform their global peaks at the same frequency. In this case, the sample with the medium length performs better.

Conclusions

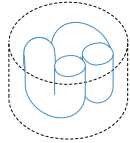
The objective of this section, was to examine how length might influence acoustic performance.

In this set of measurements, the length appears less effective. There is an indication that longer air-paths can improve the acoustic performance of the samples and potentially cause more peaks.

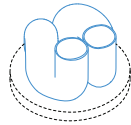
According to theory of destructive interference, it was expected that variation in lengths would cause wider distribution of the peaks. However, this speculation is not confirmed; all peak frequencies are gathered around 500Hz.



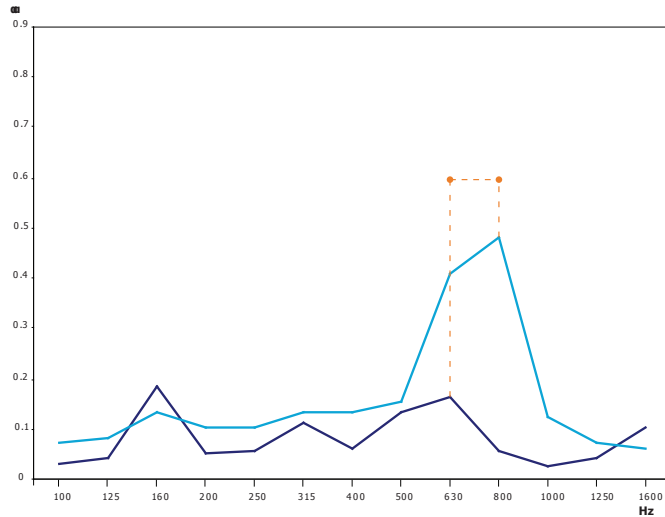
n 3.6
Ltot = 29.21 cm
D = 2.5 cm



n 3.7
Ltot = 29.21 cm
D = 2.5 cm



n 3.8
Ltot = 29.21 cm
D = 2.5 cm



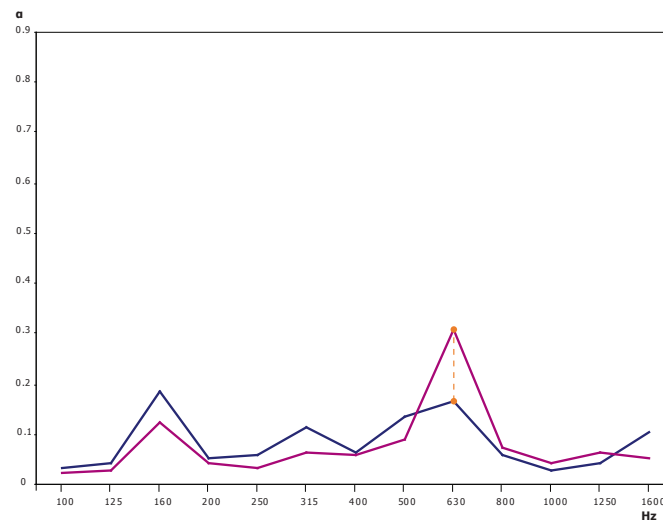
Samples 3.6/ 3.7

In this set of measurements, it is tested if the material thickness can affect the results. In this case, both samples have the same diameter (=2.5cm), length (=29.21cm) and shape of air-path. The only characteristic that is changing is the global height of the sample.

3.6: $H = 10\text{cm} > 800 \text{ Hz} > \alpha = 0.47$

3.7: $H = 6\text{cm} > 630 \text{ Hz} > \alpha = 0.16$

The measurements of the compared samples identify equal amounts of global peaks. The resonant frequency of the thicker sample is shifted towards higher frequencies and performs clearly better.



Samples 3.7/ 3.8

In this case, both samples have the same diameter (=2.5cm), length (=29.21cm) and shape of air-path. The structure of the air-path is for sample 3.7 enclosed in the geometry of the cylinder and for sample 3.8 exposed.

3.7: $H = 6\text{cm} > 630 \text{ Hz} > \alpha = 0.16$

3.8: $H = 6\text{cm} [\text{approximately}] > 630 \text{ Hz} > \alpha = 0.30$

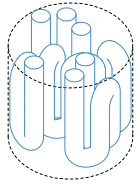
The position of the peak frequency is not shifted and the absorbing coefficient value is improved when the air-path is exposed. Both absorbers have almost identical behaviour, but is very low.

Conclusions

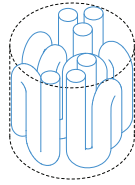
The objective of this section, was to examine how material thickness and exposed geometry might influence acoustic performance.

The analysis suggests that increasing the material thickness might influence performance in a positive way. Diversity in material thickness does not seem to affect the position of the peak frequencies.

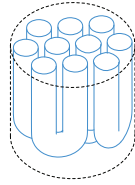
Exposed air-paths seem to improve the direct absorption coefficient values. Additionally, there is no shift in the peak frequency observed. Both samples [3.7 and 3.8] perform relatively low.



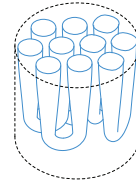
n 4.1
 $L_{tot,1} = 34.30$ cm
 $L_{tot,2} = 68.60$ cm
 $D = 1.5$ cm



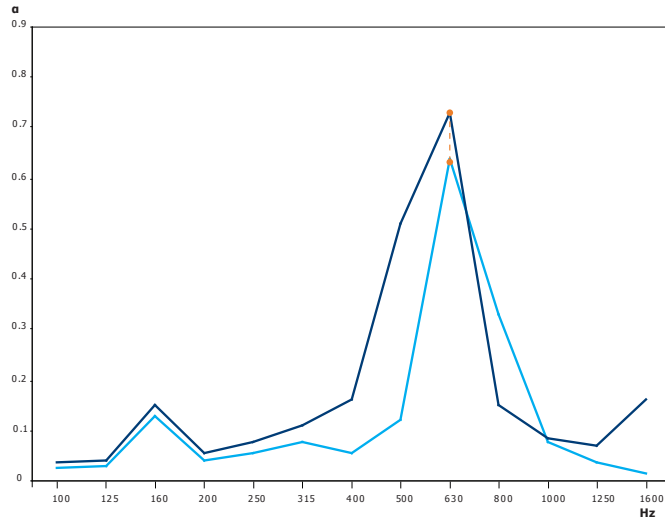
n 4.2
 $L_{tot,1} = 34.30$ cm
 $L_{tot,2} = 51.50$ cm
 $L_{tot,3} = 68.60$ cm
 $D = 1.5$ cm



n 4.3
 $L_{tot} = 19.30$ cm
 $D = 2$ cm



n 4.4
 $L_{tot} = 19.30$ cm
 $D = 1-2$ cm



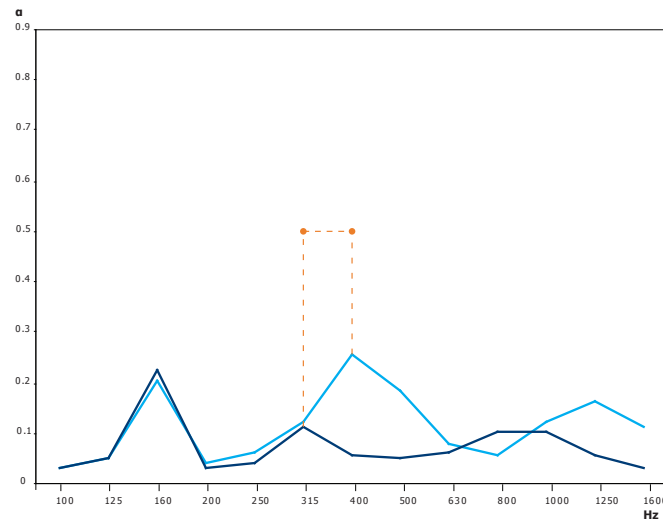
Samples 4.1 and 4.2

The two samples are designed with the goal to cover a broader band spectrum. For this reason, 3 air-paths with various lengths and similar diameter are included on each sample.

4.1: $L_1=34.3\text{cm}/ L_2=68.6\text{cm} > 630 \text{ Hz} > \alpha = 0.64$

4.2: $L_1=34.3\text{cm}/ L_2=68.6\text{cm} / L_3=51.46\text{cm} > 630 \text{ Hz} > \alpha = 0.73$

The measurements of the compared samples identify equal amounts of global peaks at the same frequency (630 Hz). The sample that includes more variations in length results to higher absorbing coefficient value, but the difference is not significant. The intention of covering a broad band spectrum is not satisfied.



Samples 4.3 and 4.4

The two samples are supposed to test if the geometry of the air-paths affects the acoustic performance. Each sample contains 5 air-paths with the same length (=19.28 cm). In sample 4.3, the air-paths have a constant diameter (= 2cm), whilst the air-paths of sample 4.4, have a gradually changing diameter (= 1 to 2cm).

4.3: $D = 2\text{cm} > 800 \text{ Hz} > \alpha = 0.1$

4.4: $D = 1-2\text{cm} > 400/ 1000 \text{ Hz} > \alpha = 0.25/ 0.16$

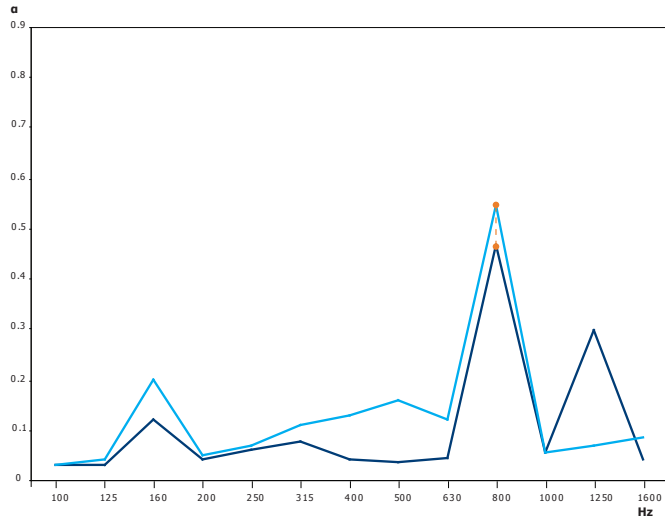
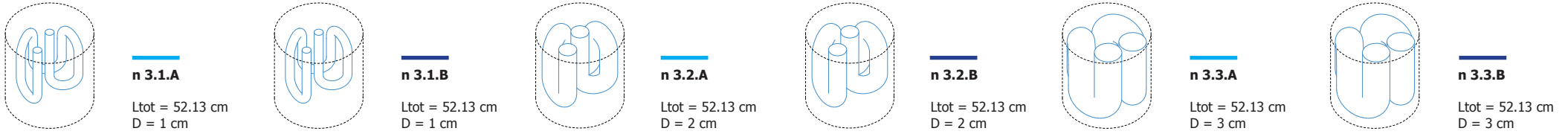
Both samples have very low acoustic performance. The peak of sample 4.4 is shifted towards lower frequencies and the absorbing coefficient value is improved.

Conclusions

The unexpected and low performance of the multi-channel samples may be caused by the close placement of the tubes which had a negative impact on their effectiveness. For this reason, it is suggested for future applications, that air-path entrances are not located too closely, otherwise the full benefit of multiple resonators may not be realized. It seems that the acoustic coupling between adjacent resonators produces a shift in the interference frequencies¹. The first attempt to produce a broad-band spectrum absorber constituted by multiple air-paths was not successful.

Furthermore, there is an indication that grading cross-sections might affect performance in a positive way. This however needs to be investigated further. The suggested geometry might be advantageous for more economic application of material [depending on fabrication technique].

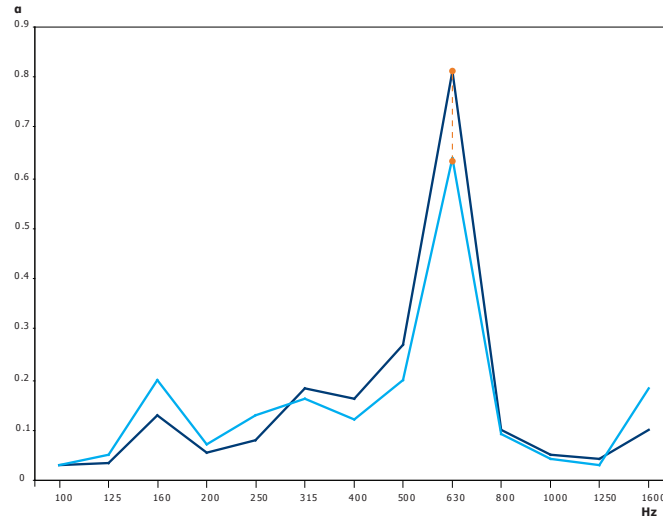
¹ http://www.deicon.com/technote/adjacent_resonators_deicon.pdf



Samples 3.1.A and 3.1.B

The objective of this section, is to examine the accuracy of the measurements. Since, the two samples are identical, it is highly expected that they will perform similarly when measured.

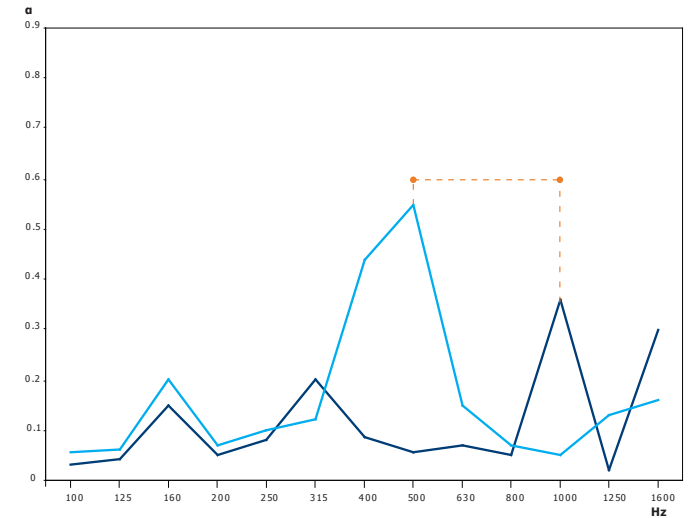
Comparing the results, we can argue that they perform in a similar way. The performed global peaks of the two samples occur at the same frequency; small differentiation is observed at the values of normal absorption coefficient. The percentage of the difference between the absorption coefficient values has been calculated and is always kept lower than 16%. It is notable that at 800Hz the deviation is limited to 8%. The measurement is considered **accurate** and reliable.



Samples 3.2.A and 3.2.B

Since, the two samples are identical, it is highly expected that they will perform similarly when measured.

Comparing the results, we can argue that they perform in a similar way. The performed global peaks of the two samples occur at the same frequency; small differentiation is observed at the values of normal absorption coefficient. The percentage of the difference between the absorption coefficient values has been calculated and is always kept lower than 18%. The measurement is considered **accurate** and reliable.



Samples 3.3.A and 3.3.B

Since, the two samples are identical, it is highly expected that they will perform similarly when measured. Comparing the results, we observe that they do not perform in a similar way. One possible explanation could be that the position of the "entrances" of the two samples, lie upon the perimeter. None of the two holes is in the centre, as it is the case for the samples 3.1.A, 3.1.B, 3.2.A and 3.2.B. This conclusion might play an important role in the design process. The holes should not be too close to an edge of the product.

They performed peaks occur at different frequencies. Additionally, both samples perform relatively poor. In this case, the results do not reproduce well.

In this chapter, the focus was on analysing the measured performance of 15 samples at low and mid frequencies. The conclusions and observations are summarised as follows:

1_ The measured performance of the samples has been successfully related to the **theory** on interference and resonant absorbers: passive destructive interference, Helmholtz absorbers and quarter wavelength tube.

It is observed that the performance of every sample relates to destructive interference. The global peaks of ten samples correspond to the discussed phenomenon. Moreover, Seven samples might behave also similar to quarter wavelength tube. There is an indication that a small percentage of the samples performs as a Helmholtz resonator. In general, it is observed that samples with a diameter between 1.5 and 3cm, perform closer to the predictions based on theory on passive destructive interference.

2_ It is observed that the **interference point** lies always between the 1/4 of the total length of the air path and the upper surface of the samples.

$$[\frac{1}{4}L_{tot} < L_{IP} < L_{tot}]$$

3_ It appears that **diameter** as a geometrical characteristic of the air-paths might influence the peak frequencies. The samples with a diameter equal to

2 cm result to higher absorbing coefficient values. Besides the improvement of the performance, it seems that diversity in diameter might also cause variations in the frequencies where peaks occur. This fact might become fruitful if applied in a broad-band spectrum absorber.

4_ As opposed to theory, the **length** appears less effective for these last series of specimens. There is an indication that longer air-paths can improve the acoustic performance of the samples and potentially cause more peaks. According to theory of destructive interference, it was expected that variation in lengths would cause wider distribution of the peaks. However, this speculation is not confirmed yet.

5_ All samples perform a **local peak** at 160Hz with very low absorbing coefficient value. This might be caused by the material properties or the global dimensions of the samples.

6_ The analysis suggests that **material thickness** when increased, might influence performance in a positive way. Diversity in material thickness does not seem to affect the position of the peak frequencies.

7_ The first attempt to produce a **broad-band spectrum absorber** constituted by **multiple air-paths** was not successful. The unexpected and low

performance of the multichannel samples may be caused by the close placement of the resonators which had a negative impact on their effectiveness. For this reason, it is suggested for future applications, that air-path entrances are not located too closely, otherwise the full benefit of multiple resonators may not be realized. It seems that the acoustic coupling between adjacent resonators produces a shift in the resonant frequencies.

8_ There is a preliminary indication that **grading cross-sections** might affect performance in a positive way. The suggested geometry might be advantageous for more economic application of material [depending on fabrication technique].

9_ Generally, the results reproduce well and can be considered as **accurate** and reliable.

10_ **Exposed air-paths** seem to improve the direct absorption coefficient values without shifting the position of the peak frequency.

11_ It is suggested that the **position of the holes** is not close to an edge of the product.

12_ The highest values for direct absorbing coefficients appear as follows:

Sample Code	3.1.B	3.2.A	3.2.B	3.3.A	3.4	3.5	4.1	4.2
Length [cm]	52.13	52.13	52.13	52.13	34.3	108.3	34.3 / 68.6	34.3/ 51.46/ 68.6
Diameter [cm]	1	2	2	3	2	2	1.5	1.5
Frequency [Hz]	800	630	630	500	500	500	630	630
Absorbing Coefficient	0.55	0.64	0.73	0.55	0.64	0.77	0.64	0.73

The process of designing, measuring and evaluating the discussed absorbers aimed not only to further explore the field of passive destructive interference, but also to define a set of rules that enable the design with performance-driven criteria.

Length

It is observed that the position of the interference point is located between the 1/4 [one-quarter] of the total length of the air-path and the upper surface of the absorber. Based on this fact, it is possible to define a set of boundary values for the length $[1/4 L_{tot} < \Delta L < L_{tot}]$.

For example: If a peak frequency of 500Hz is targeted, then the length can be estimated as follows:

for $f = f_{target} = 500 \text{ Hz}$

$$\frac{(2n-1)c}{2f} < L_{tot} < \frac{(2n-1)c}{f}$$

$$[n=1] \quad 0.34 \text{ m} < L_{tot} < 0.69 \text{ m}$$

$$[n=2] \quad 1.03 \text{ m} < L_{tot} < 2.06 \text{ m}$$

$$[n=3] \quad 1.72 \text{ m} < L_{tot} < 3.44 \text{ m}$$

Predicting performance

The analysis of the performance of the samples has been successfully related to the theory on resonant and interference absorbers. This analysis method does not only constitute a "tool" for further comprehension, but suggests also a model that predicts acoustic performance.

For a given air-path, it might be possible to predict the boundaries of the peak frequencies. This can be realised by applying in the following equation the different possibilities for ΔL :

$$f = \frac{(2n-1)c}{2\Delta L}, \text{ which } 1/4 L_{tot} < \Delta L \text{ and } \Delta L < L_{tot}.$$

Diameter

It appears that the diameter, as a geometrical characteristic of the air-paths might influence the peak frequencies. Besides the improvement of the performance, it seems that diversity in diameter might also cause variations in the frequencies where peaks occur.

It is observed, that the samples with a diameter equal to 2 cm result in the highest absorbing coefficient values at low-mid frequencies. At mid-high frequencies, a diameter equal of 1 cm seems to be more effective.

Followingly, diameters between 0.75 and 2.50 cm are preferable: $0.75\text{cm} < D < 2.50\text{cm}$

Suggestions for further investigation:

Material properties/ Surface smoothness

Eventhough passive destructive interference is based mostly on geometrical characteristics, there is an indication that material properties and surface smoothness affect the acoustic performance of the absorbers. It is suggested to further investigate the field.

Multiple-channels/ Distance between air-path entrances

The problem with resonant absorbers is that they usually only provide a narrow bandwidth of absorption. To cover a wide bandwidth, a series of air-paths

are required, each tuned to a different frequency range. For this reason, it is suggested for future research, to define the optimum distance between air-path entrances so that the full benefit of multiple resonators may be realized.

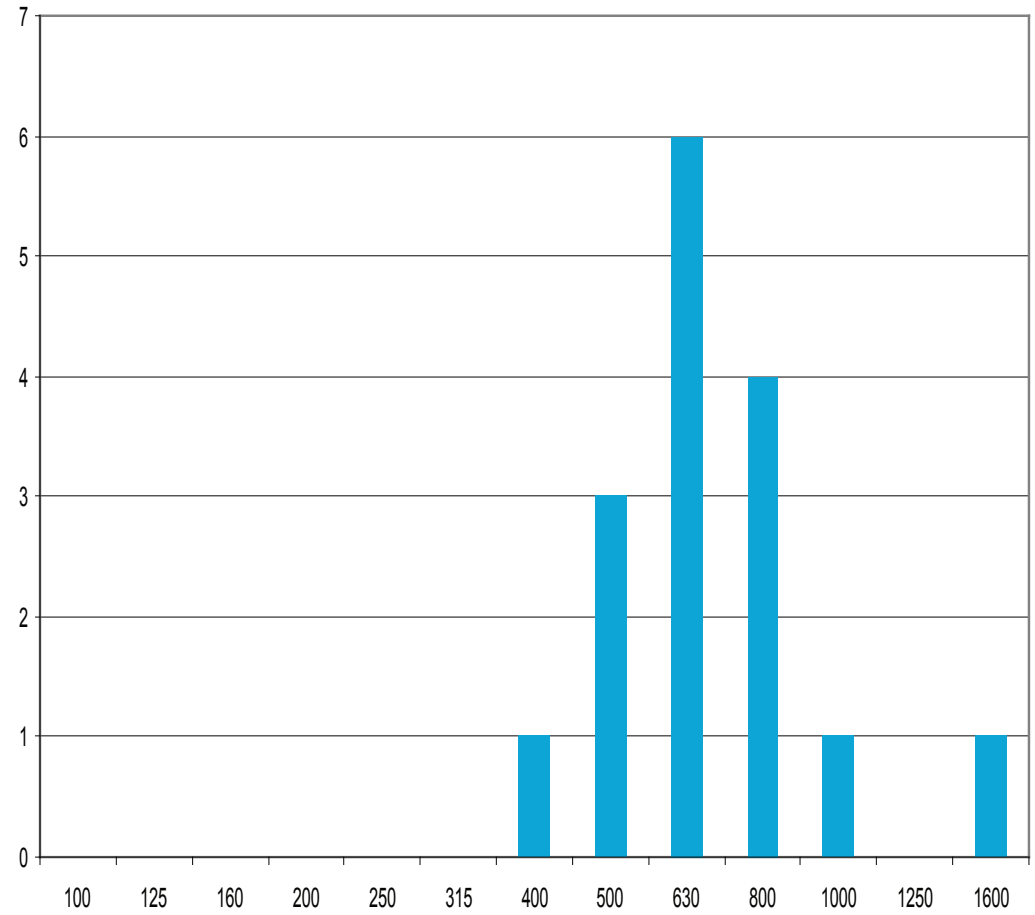
Geometry of air-paths

In this study, the geometrical characteristics of the absorbers are mostly conceived as diameter and length of air-paths. This restricted perception of shape was intended to limit the complications on the evaluation of the measured results. Despite this fact, there is an indication that non-constant cross-section of air-path might contribute to better acoustic performance.

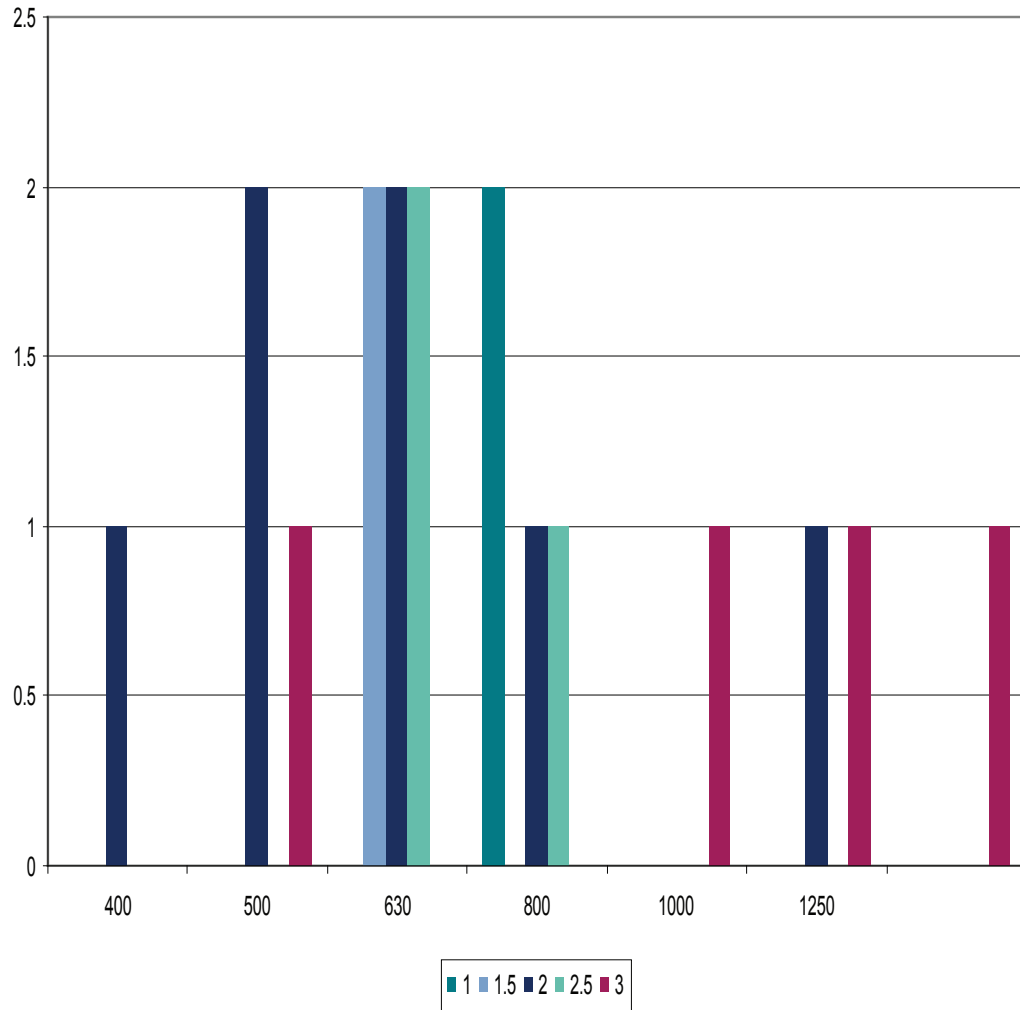
Average values/ standard deviation

As a next step, it is suggested to make a large series of 5 to 10 samples for each sample specification. This allows to average the results and introduce a standard deviation reflecting the measurement and production uncertainty. Moreover, the results will be more stable and conclusions can be more easily drawn.

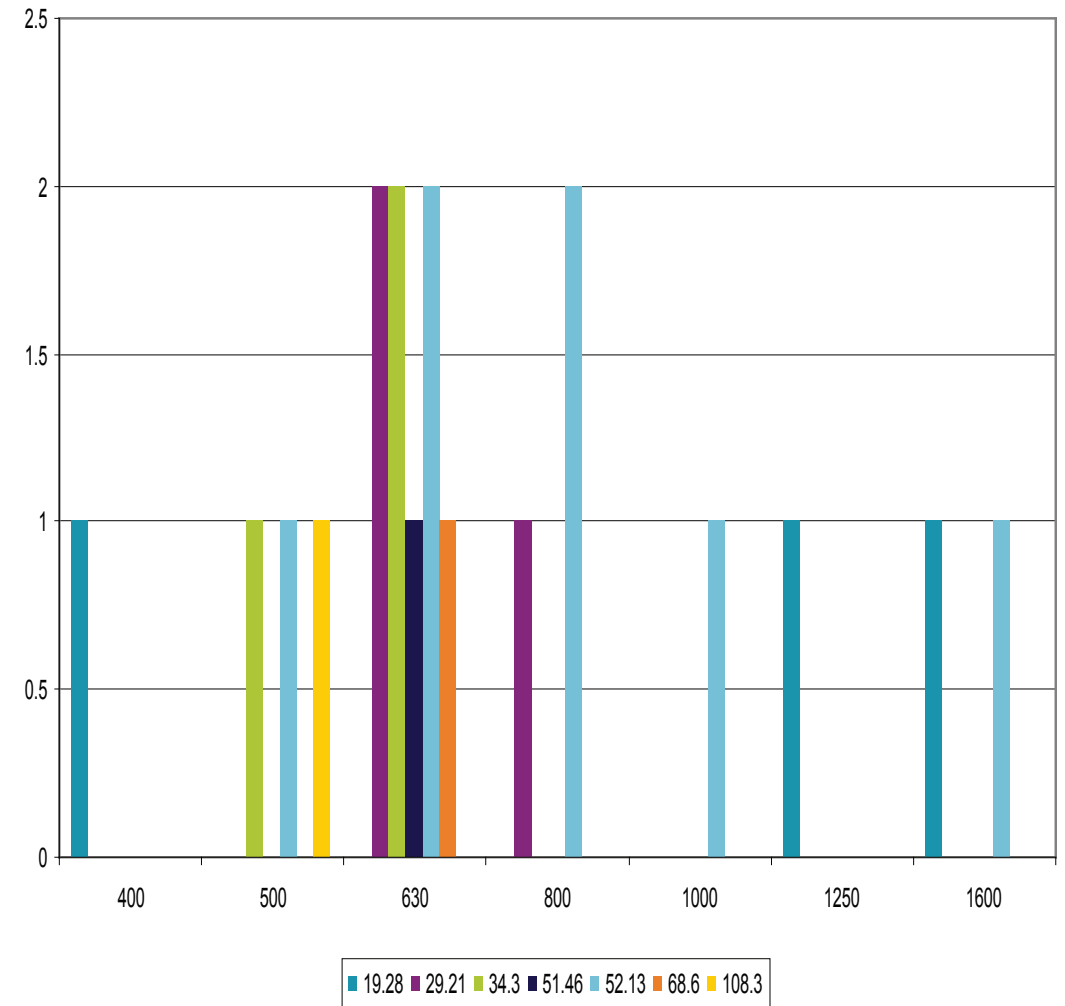
Amount of global peaks per frequency



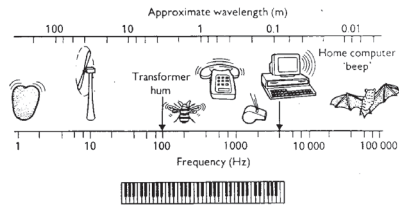
The graph attempts to relate the **diameter** of the air-paths with the **peak frequencies**



The graph attempts to relate the **length** of the air-paths with the **peak frequencies**







**CERTAIN TYPES
OF BROADBAND
SIGNAL/
LOW/ MEDIUM
FREQUENCIES**

INTERIORS

SMALL REGION

**COMPLEX GEOM-
ETRY**

In this chapter, several ideas are developed and explored that suggest how to transform passive destructive interference principles into functional objects and/ or absorbing surfaces. The proposed concepts are based on the guidelines and indications from Phase 1 and 2.

Applications

The idea of a passive destructive interference absorber is quite new and under investigation. For this reason becomes very crucial to reflect on possible applications, where the absorber can become advantageous compared to existing products.

PDI-absorbers seem to be suitable in cases where porous material is not appropriate for the noise control, for example at low-mid frequencies or when a nonflammable material or a material with low thermal capacity is needed.

Additionally, it is applicable in cases where a certain

type of broadband signal is targeted. It is more suitable for interiors, where no climate conditions, such as wind, play a role. Furthermore, due to budget and fabrication concerns, it might be better to be applied in small regions or be integrated on objects.

Added value

The concept of a passive destructive absorber that is fabricated with Additive Manufacturing, enables to envision a new way of thinking concerning acoustic treatment in the built environment.

-Customization

The absorber can be easily customised according to the specifications of place or the preferences of the user.

-Complex/ Custom geometry

It can follow a big range of geometrical configurations with only limited restrictions.

-Multi-functionality [f.e.: Lighting]

-Application of colours

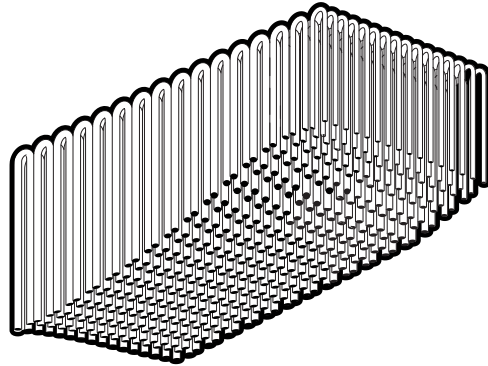
-Better follow architectural demands.

Design Concept

Relying on the available theory and the indications of the design guidelines derived from the measurements, several design concepts are developed and evaluated. Structures which manipulate strings are investigated: weaving, knitting, etc. The challenge will be to gain control over the air-paths' specifications and be able to predict performance via design.



Reference pictures:
Ball and Nogues



Design concept 1

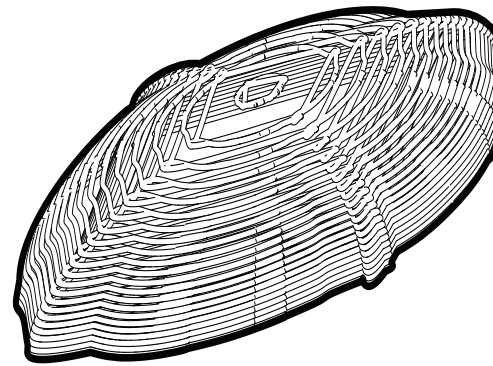
This concept promotes the idea of an absorber that is hanging from a horizontal surface (f.e.: Ceiling). Hollow tubes with grading lengths and diameters are bended and oriented towards the same direction. Due to the various lengths of the tubes, the lower part of the absorber creates a "shapely" surface that constitutes from the air-path entrances.

(+)

The geometry of this proposal can be easily manipulated and rated. The design seems to be flexible in future modifications and possibly allows the integration of other functions (f.e.: Lighting). It can be easily customized according to the specifications of place or the preferences of the user.

(-)

This design doesn't seem to take any advantage of AM; it might be easier fabricated by standard (extruded) flexible tubes.



Design concept 2

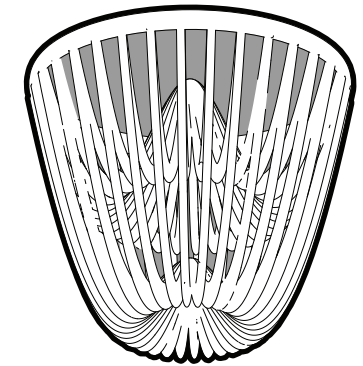
This design suggests that the air-paths of the absorber are arranged in a basket-weave structure. Interwoven lengths of hollow tubes will create a texture that can be applied on different kinds of geometry: flat surface, 3D object, etc. Furthermore, the air-path entrances will be evenly distributed on the absorbing surface.

(+)

The density of the tubes may be a design parameter that regulates acoustic performance but also light penetration (transparency). The product can be easily customised.

(-)

It might be difficult to access and replace an air-path tube if necessary. It might be easier to fabricate the tubes with the standard extruding technique and interlace them subsequently.



Design concept 3

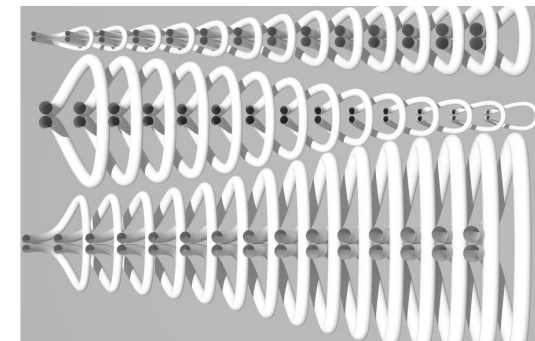
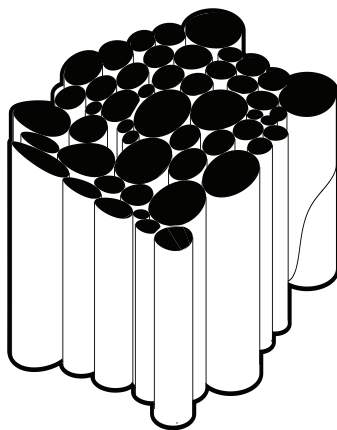
A sound absorber-chandelier that is pendent from the ceiling and enables natural light to penetrate. The air-path entrances will be evenly distributed on the absorbing surface, targeting to all directions.

(+)

The scale of the object is suitable for AM. Additionally, the geometry of this proposal can be easily manipulated and rated. The design allows the integration of other functions (lighting). It can be easily customized according to the specifications of place or the preferences of the user.

(-)

It might be difficult to access and replace an air-path tube if necessary.



Design concept 4

This idea suggest the development of new types of products that incorporate sound absorption in their body. The air-path tubes can be integrated in a solid volume of an object that serves another function (sitting stool, table, etc).

(+)

The proposed sound absorbers are enclosed in the volumes of other products; in this manner multi-functionality is introduced. AM seems to be appropriate fabrication technique to further develop this idea.

(-)

The geometrical configurations of the absorber, might be in conflict with the complementary function of the object. It might be better to study this concept at a later stage, when passive destructive interference principles are better understood.

Design concept 5

The absorber constitutes of units with distinct sizes in length and diameter which are randomly clustered and joined. The proposed structure can be enclosed in all kind of shapes, causing a semi-transparent effect.

(+)

The density of the tubes may be a design parameter that regulates acoustic performance but also light penetration (transparency). The product can be easily customised.

(-)

It seems to be more difficult to develop performance driven criteria when designing this random-looking structure. Post-processing might be complicated in this case.

Design concept 6

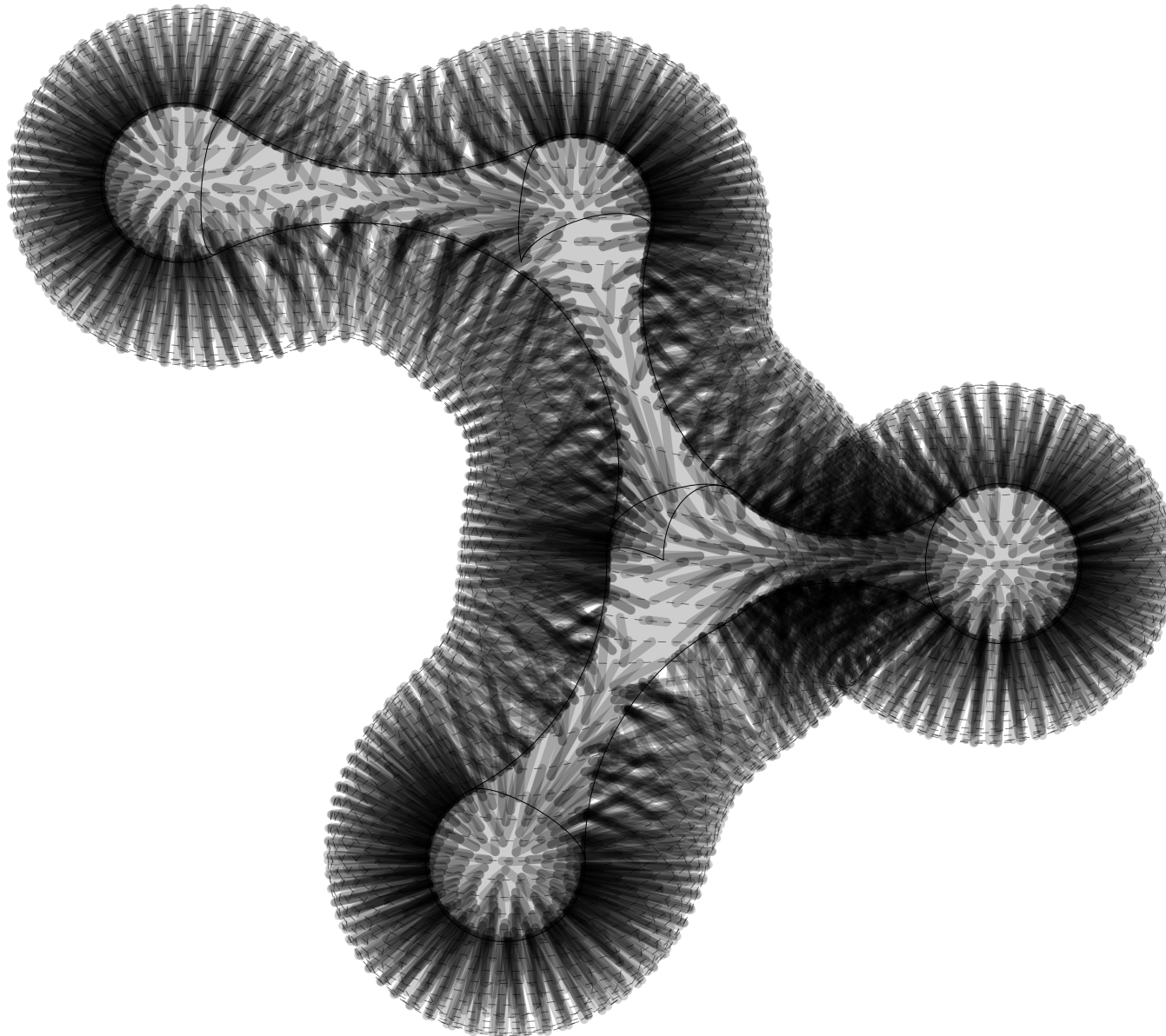
This design is closer to the idea of a textured surface that can adjust to different shapes. The units have the shape of a hook. The two end parts are located close to each other, depending on their length, the curvature of the air-paths is differentiating. Besides an aesthetically fine result, the interlacing of the units connects and stabilizes the parts.

(+)

The hierarchical structure simplifies the process of keeping track of lengths and diameters, as well as controlling if tubes intersect. The geometry of the unit is similar with the air-path measured in Phase 2. Furthermore, the arrangement of the units is compact and needs less volume in terms of space and material.

(-)

The small amount of connection points makes the surface fragile.



The proposed design is conceived as an organic-looking structure that is hanging from the ceiling. It “grows” where sound absorption is needed and can easily adopt in the available space. It constitutes of two main parts: the core and the air-paths.

The core, is following the global shape of the absorber but its volume is limited to less than the 1/3 of the total volume. The air-paths are connected to the core and create a semi-transparent field, which is decreasing when getting closer to the center. The hollow tubes have grading lengths and diameters; they are bended and oriented towards all directions.

(+)

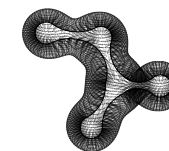
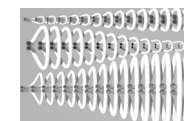
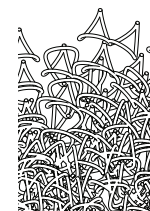
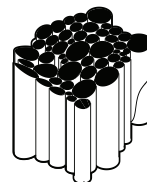
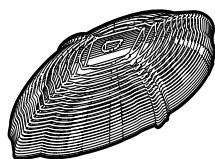
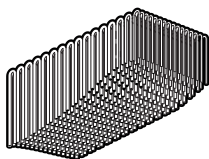
The geometry of this proposal can be easily manipulated and rated. The design seems to be flexible in future modifications and possibly allows the integration of other functions (f.e.: Lighting). It can be easily customized according to the specifications of place or the preferences of the user. Additive Manufacturing seems to be appropriate fabrication technique to further develop this idea, both in terms of geometry and customization.

(-)

The design proposal needs relatively big space to be installed. Despite this fact, the biggest part of the structure allows the penetration of light and does not prevent visibility.

● +

○ -



Flexibility:	● ● ● ● ○	● ● ● ○ ○	● ● ● ● ○	● ● ● ○ ○	● ● ● ● ○	● ● ● ○ ○	● ● ● ● ○
Integration:	● ● ○ ○ ○	● ● ● ● ○	● ● ● ○ ○	● ● ● ● ○	● ● ● ○ ○	● ● ● ● ○	● ● ● ● ○
Accessibility:	● ● ● ● ○	● ● ● ○ ○	● ● ● ○ ○	● ● ○ ○ ○	● ● ○ ○ ○	● ● ● ○ ○	● ● ● ● ○
Geometrical control:	● ● ● ● ●	● ● ● ● ●	● ● ● ● ●	● ● ● ● ●	● ● ● ● ○	● ● ● ● ●	● ● ● ● ●
Customization:	● ● ○ ○ ○	● ● ○ ○ ○	● ● ● ○ ○	● ● ● ○ ○	● ● ○ ○ ○	● ● ○ ○ ○	● ● ● ● ○
Advantages of AM:	● ○ ○ ○ ○	● ● ○ ○ ○	● ● ● ● ○	● ● ● ● ○	● ● ○ ○ ○	● ● ○ ○ ○	● ● ● ● ○
Transparency:	● ● ○ ○ ○	● ● ● ○ ○	● ● ● ○ ○	● ● ● ○ ○	● ● ● ○ ○	● ● ● ○ ○	● ● ● ○ ○
Aesthetics:	● ● ● ● ○	● ● ● ● ○	● ● ● ○ ○	● ● ● ○ ○	● ● ● ○ ○	● ● ● ○ ○	● ● ● ● ○

The proposed design concepts, are evaluated according to the following criteria:

Flexibility

Flexibility addresses both to the design process and to the adjustability of the fabricated absorber. Since the investigation of destructive interference principles constitute an on-going procedure, the design needs to adopt easily the modifications of the specifications of the parts.

Integration of additional functions

The possibility of integrating services (f.e.: Artificial lighting) in the internal structures constitutes an adding value for the absorber as it suggests new types of high valued products.

Accessibility of the parts

The convenient access to the absorbers parts simplifies the process of maintenance, cleaning, etc.

Geometrical control

It is essential that the geometry of the proposed design can be easily manipulated and rated, so that better control over performance is gained.

Customization

It is well known that Additive Manufacturing is effective for low volume, high cost customised products. For this reason, the suggested design concept needs to be easily customised according to the specifications of place or the preferences of the user. Furthermore, AM enables the application of colours or pictures on the suggested device without preventing

the regular function of the absorber.

Taking advantage of AM

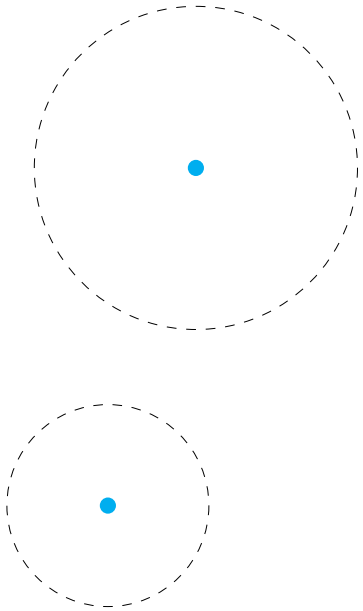
Additive Manufacturing simplifies both the detailing and the fabrication of complex geometries. It is examined if the proposed geometry takes full advantage of this possibility.

Regulation of light

Natural light penetration is an adding value of the absorber. In most of the cases it is expected that the configurations of the strings will not prevent the light penetration in space.

Aesthetics

It is attempted to rationalise the notion of aesthetics and reduce it to the ability of the concepts to relate to various architectural context.

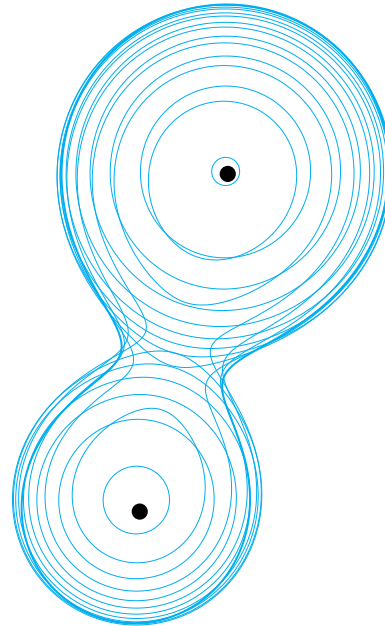


Define position

The position of the absorbers is defined both by architectural and acoustic criteria.

It is crucial that the installation of the absorber will not prevent the neat function of space. For this reason, the minimum net height needs always to be taken into consideration. Additional parameters might be visibility, possible conflicts with other installations, aesthetics etc.

Furthermore, the most effective treatment is to reduce the noise at the source. Hence where this is possible, sound absorbers are preferably placed near the sound source.

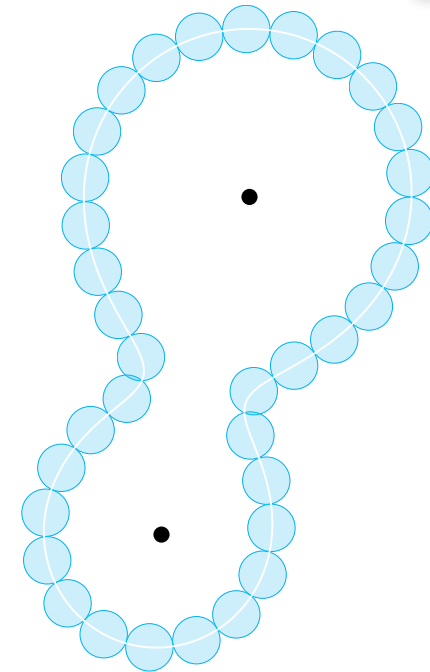


Define "absorbing space"

The volume of the absorber depends on the targeted frequencies, on the amount of air-paths and on the distance between the points.

For example: if frequencies between 125 and 2000Hz are targeted, this corresponds to a unit size that varies from 5cm to 1.35m. The distance between the points mostly relates to fabrication constrains. It is suggested to vary from 30 to 70cm.

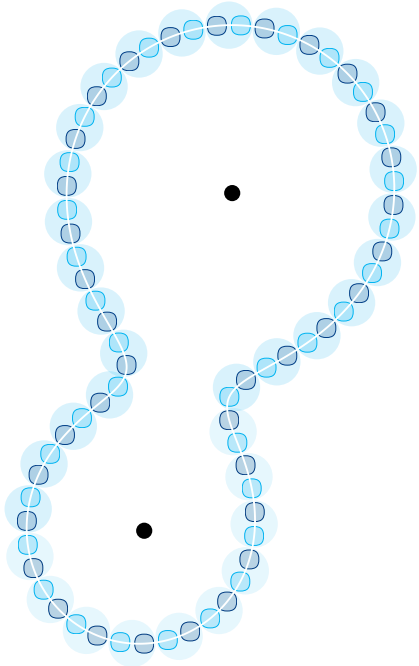
With this information, the outline of the "absorbing space" can be derived.



Define distance between air-paths

According to the measurements of Phase 2, it is suggested that air-path entrances are not located too closely, otherwise the full benefit of multiple resonators may not be realized. For this reason, it becomes crucial to ensure enough distance between adjacent resonators.

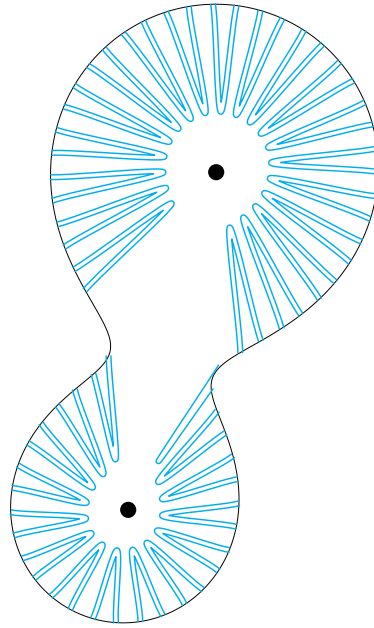
On this scheme, the circles represent the distance between adjacent air-paths and equal to $\lambda/8$ (λ : Wavelength of targeted frequency). It is highly possible that the distance between the air-paths needs to be modified in the future. Since, there is not enough information on this issue, it is assumed that the proposed distance is adequate.



Define position of air-path start-end points

The two end parts of each air-path locate on the perimeter of the “absorbing space”. They have a small distance from each other and are positioned symmetrically to the center of the circles drawn previously.

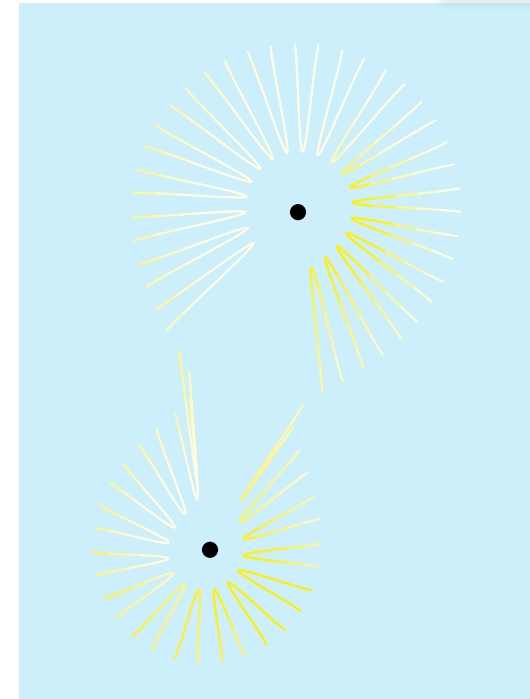
It is not known yet, which values constitute the optimum distance between the two entrance. It is deducted from the physical tests of phase 1 and 2 that a distance between 0.5 and 3 cm is decent.



Draw air-paths

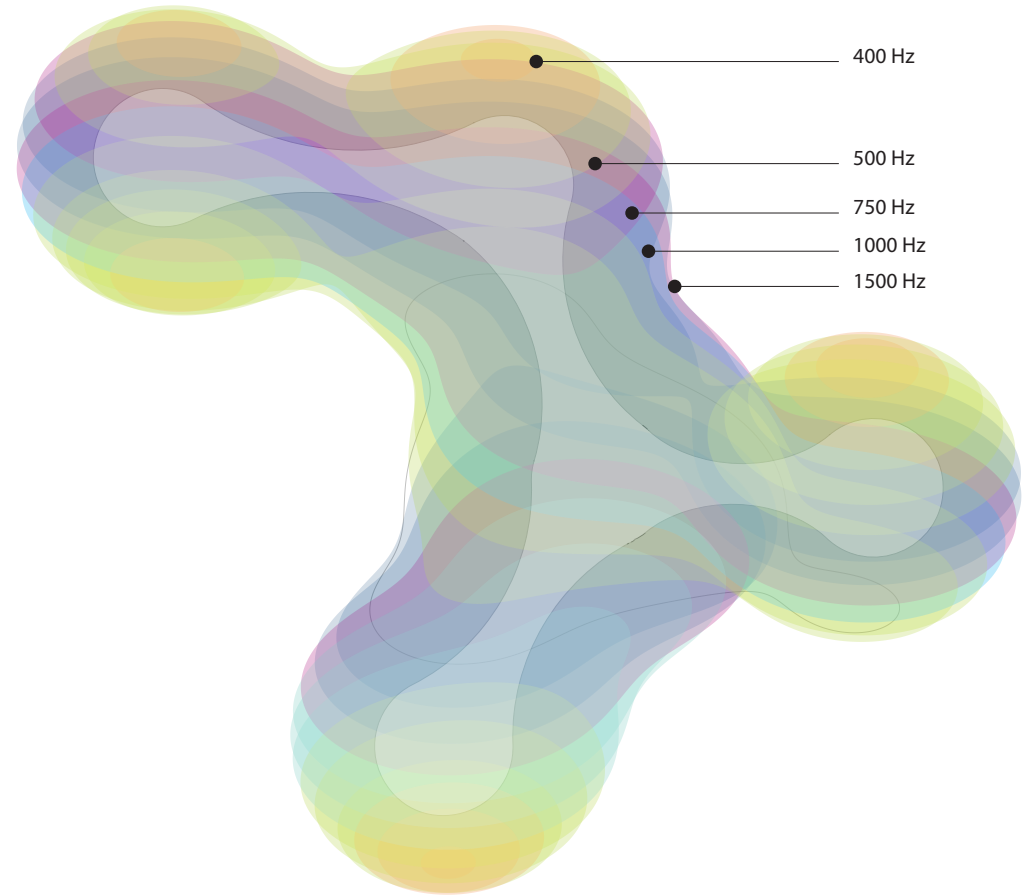
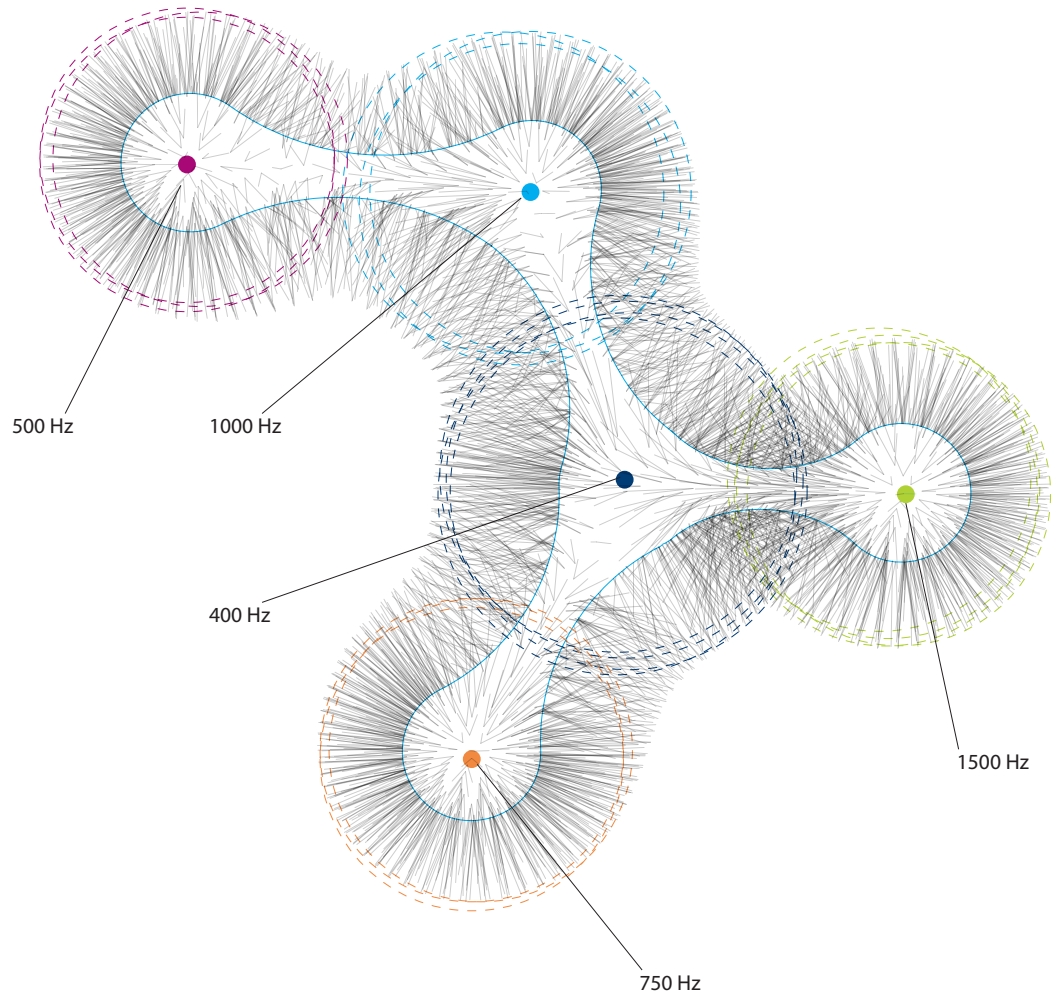
Currently, the units are conceived as U-shaped parts with a constant diameter. It might well be that their shape changes a bit in the future. Their starting and ending point lies in the perimeter of the absorber and locate close to each other. Their middle-points are positioned near the center of the absorber.

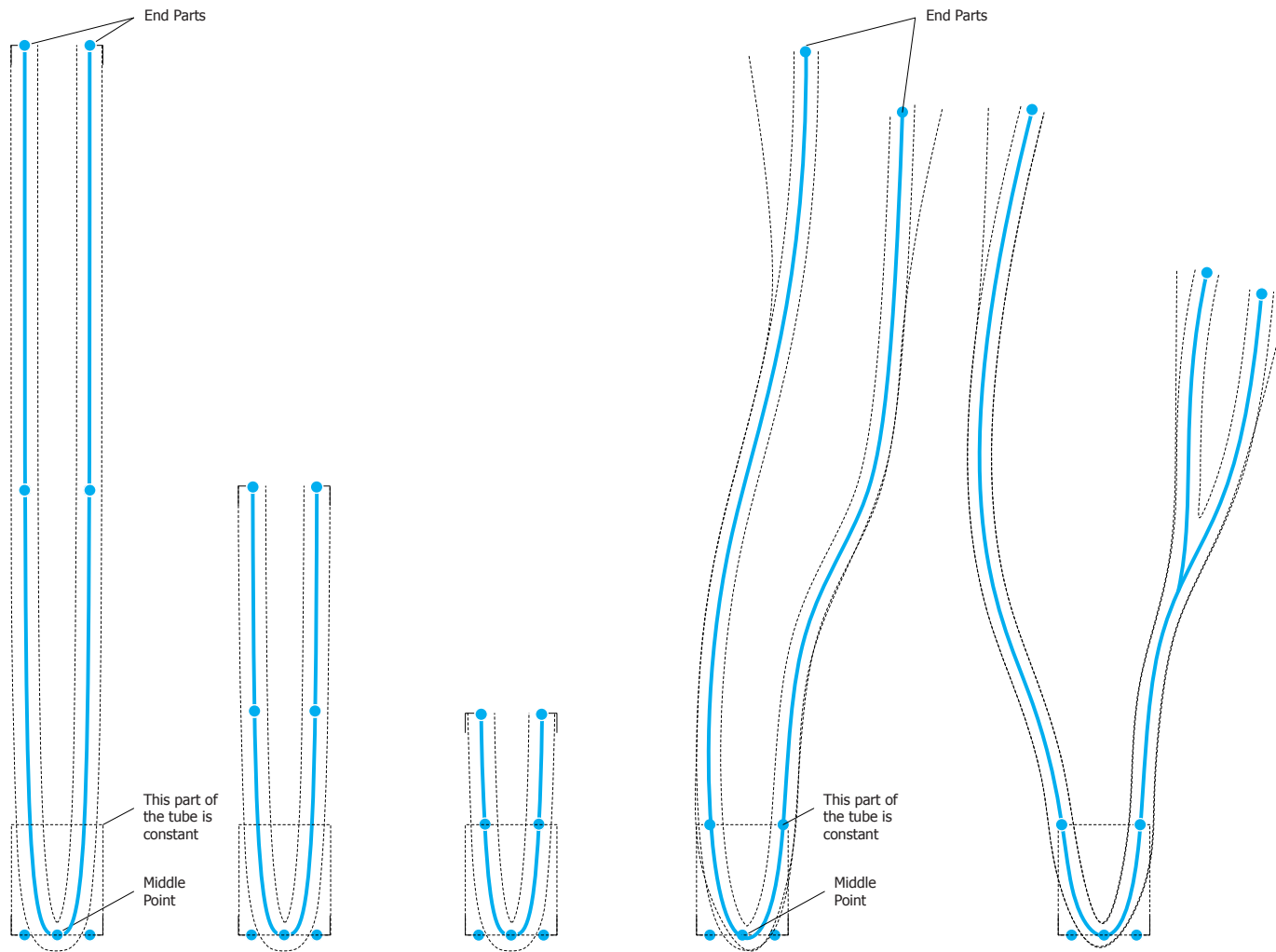
When drawing the air-paths, it becomes crucial that they do not intersect with each other. This can regulated by controlling the distance between adjacent air tubes, the distance between the end parts, as well as by the diameter and the material thickness. Therefore, all these parameters need to be known at this stage.



Final outcome

The final 3d-design might be further processed by applying blending colours or images on it.





U-shaped units with various lengths and shapes

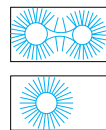
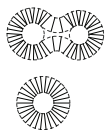
The design proposal employs U-shaped units which are bended at their half length. Their end parts are oriented towards all directions, while their mid-points are attached to the center of the absorber.

It is notable that the units that target to lower frequencies are relatively big. This might be a disadvantage if limited space is available for the absorber. In this case, an alternative configuration might be needed to be chosen.

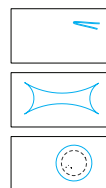
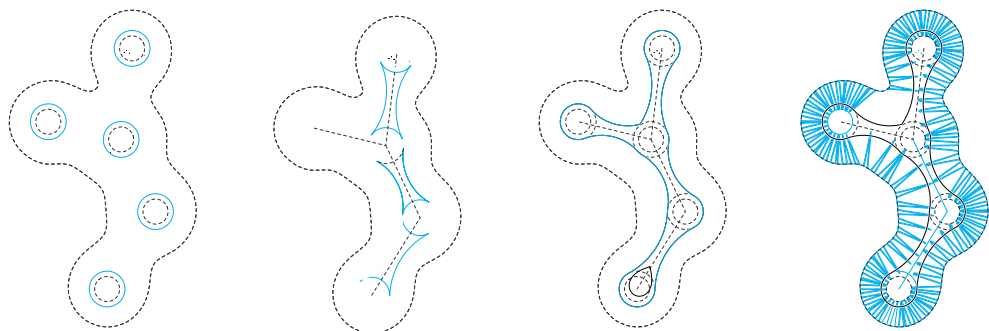
During this study the geometry of the unit was examined to have 2 end parts. It might be interesting for future investigation to explore the possibilities of multiple entrances. Additionally, there is an indication that air-paths with broaden entrances and grading cross-section might perform better.

The central part of the tubes is suggested to always have the same shape. This fact will simplify the geometry of the core of the absorber and also the assembly process [if needed].

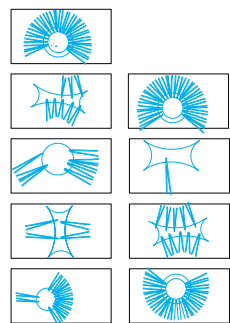
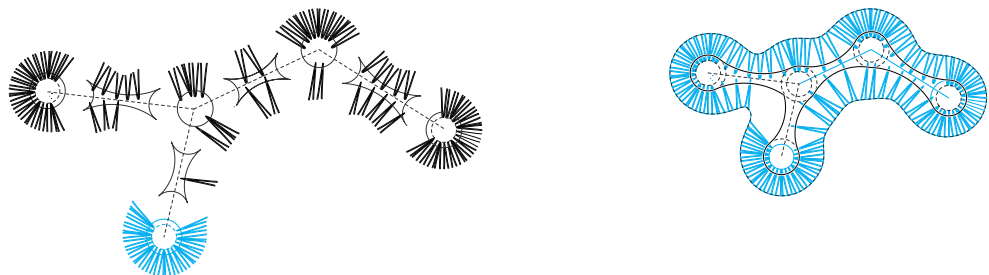
It appears that the diameter, as a geometrical characteristic of the air-paths might influence the peak frequencies. Besides the improvement of the performance, it seems that diversity in diameter might also cause variations in the frequencies where peaks occur. Diameters between 0.75 and 2.50 cm are suggested for this design: $0.75\text{cm} < D < 2.50\text{cm}$.



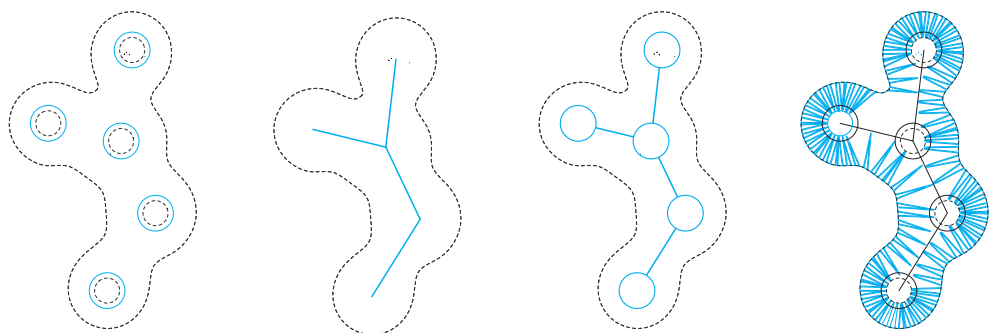
1



2



3



4

In this section, four different fabrication concepts are developed for the absorber:

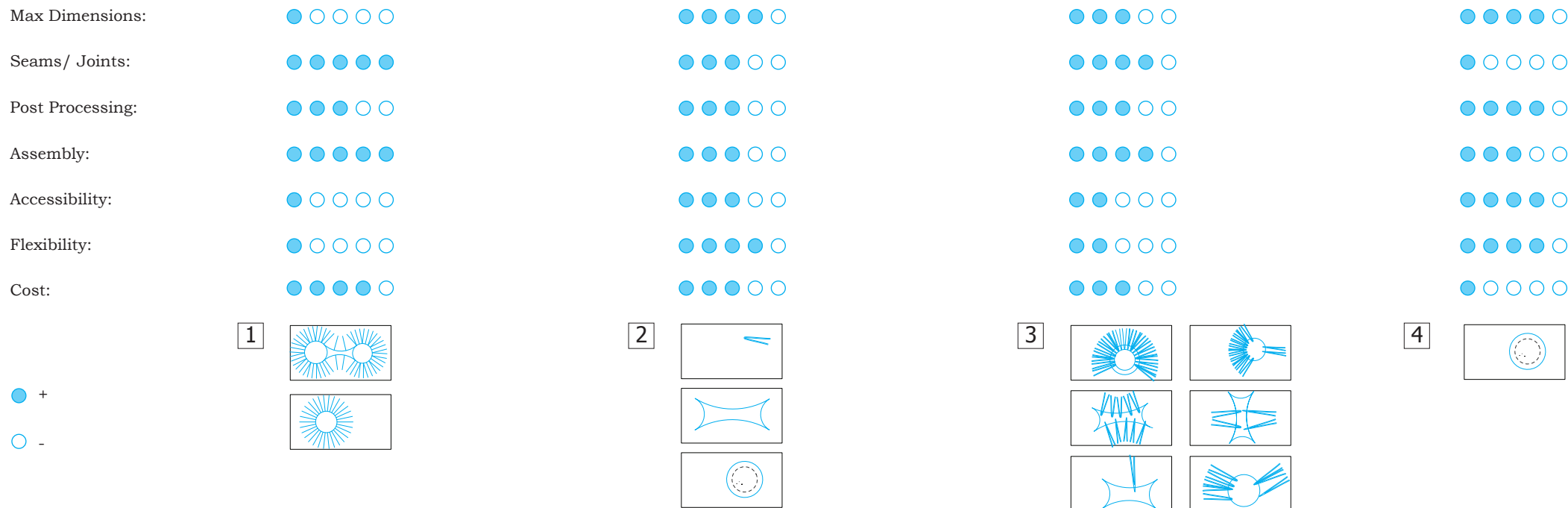
1_ The absorber can be fabricated as a single part with Additive Manufacturing. In this case, the dimensions of the machine are critical in the global size and shape of the absorber and limit significantly the design possibilities. Additionally, it might be impractical for maintenance or service if the absorber constitutes only from one piece.

2_ Alternatively, the core and the air-paths might be manufactured separately and assembled at a later stage. The core might be further subdivided in the nodes and the connecting parts. In this case the detail of the connection between the node and the linear parts needs to be examined. In this case the restrictions coming from the fabrication technique are very limited. The assembly of the parts might be time-consuming, on the other hand, all the parts are accessible and it relatively easy to maintain the absorber or to adjust to new types of acoustic demands.

3_ In order to reduce the difficulties of the assembly of the parts, the absorber might be subdivided to parts that constitute of the core and the corresponding air-paths. It is necessary that the component fit in the Additive Manufacturing machine.

4_ The final fabrication concept introduces the idea of a hybrid structure that constituted of standardised components (extruded flexible tubes and linear wooden or metal parts). Only the node will be fabricated with AM. This idea reduces the cost but might also reduce the aesthetic values of the absorber.

The first three concepts suggest that all the parts of the absorber are fabricated with Additive Manufacturing. The last proposal introduces the idea of a hybrid structure.



The proposed fabrication concepts, are evaluated according to the following criteria:

Maximum Dimensions

The fabrication concepts are based on the possibilities offered by additive manufacturing. The maximum dimensions of the absorber depend on both the chosen technology and the subdivision of the absorber. Concept 1, is strongly restricted by the dimensions of the machine.

Seams/ Joins

The fabrication concepts suggest various levels of subdivision, which correlate to the seams. When the amount of joints and seams increases, the detailing becomes more complicated. In every case, it is at-

tempted to give the impression of a joint-less structure.

Post processing

Once removed from the machine, parts may require an amount of additional cleaning up before they are ready for use. Parts may be weak at this stage or they may have supporting features that must be removed. This therefore often requires time and careful, experienced manual manipulation. There is an indication, that the complex the geometry of the parts, the more demanding is this process.

Assembly

The subdivision of the absorber in smaller parts results to the increase of the complexity level of the assembly that might be time-consuming.

Accessibility of the parts

In case the absorber is parcelled, it is easier to access and replace damaged parts an simplifies the process of maintenance, cleaning, etc.

Flexibility

Sometimes the acoustic demands of space are shifting over time. Concepts 3 and 4 introduce the idea that the absorber can be easily modified and adjusted to new configurations.

Cost

It is an early stage of the project to be able to estimate correctly the budget. Despite this fact, there is an indication that the bigger the volume that is fabricated with AM, the higher the cost.

Detail 1

This drawing examines into detail the node for the fabrication concepts 1 and 3 [plan view]. In this case, the node and the air-tubes constitute a unified piece without seams and subdivisions. The area where air-paths merge with the core become thicker to strengthen the structure.

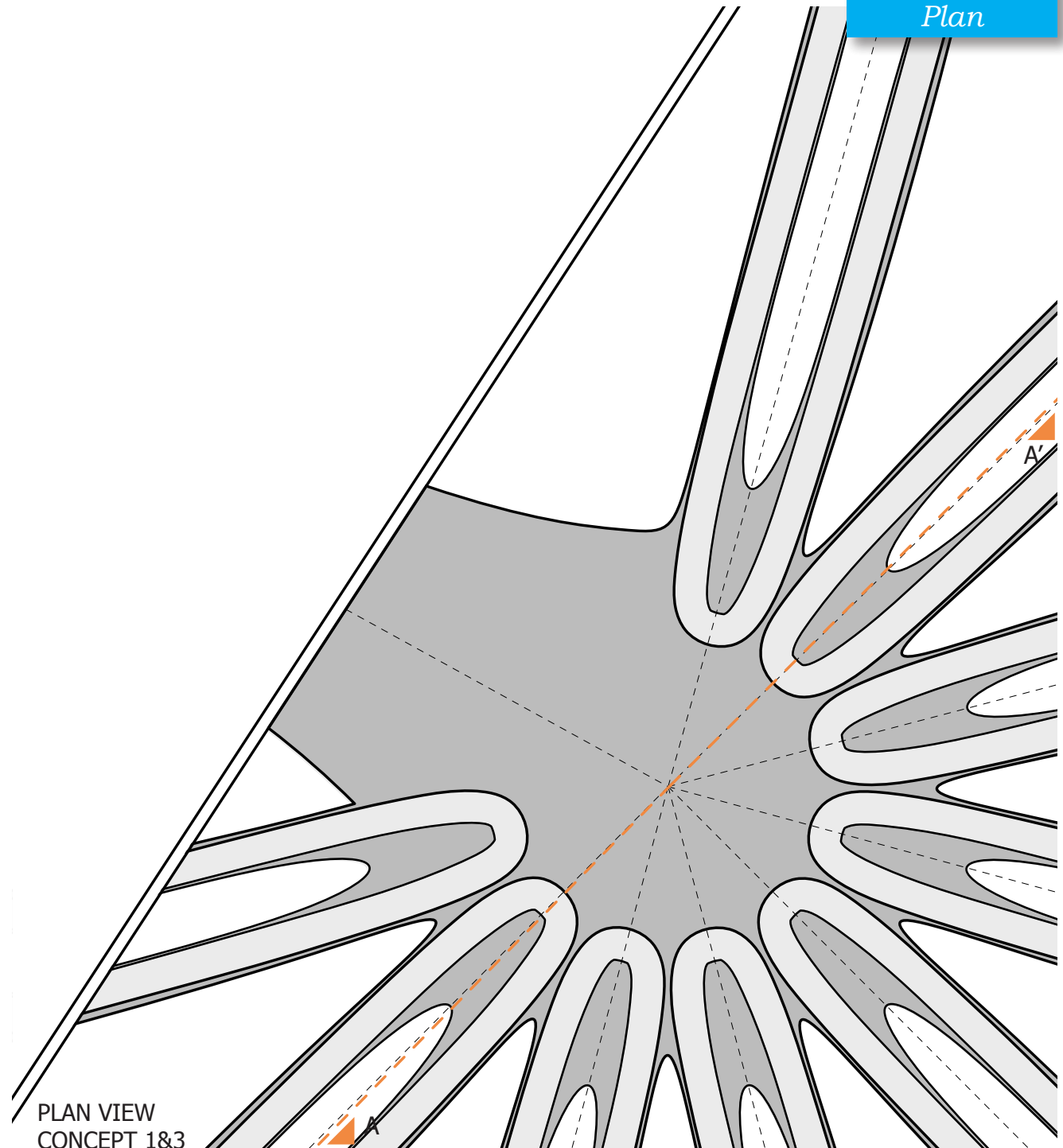
Detail 2

This drawing examines into detail the node for the fabrication concept 2 [plan view]. In this case, the air-tubes are clamped in a specially designed enclosure on the node. The two components are designed and fabricated separately.

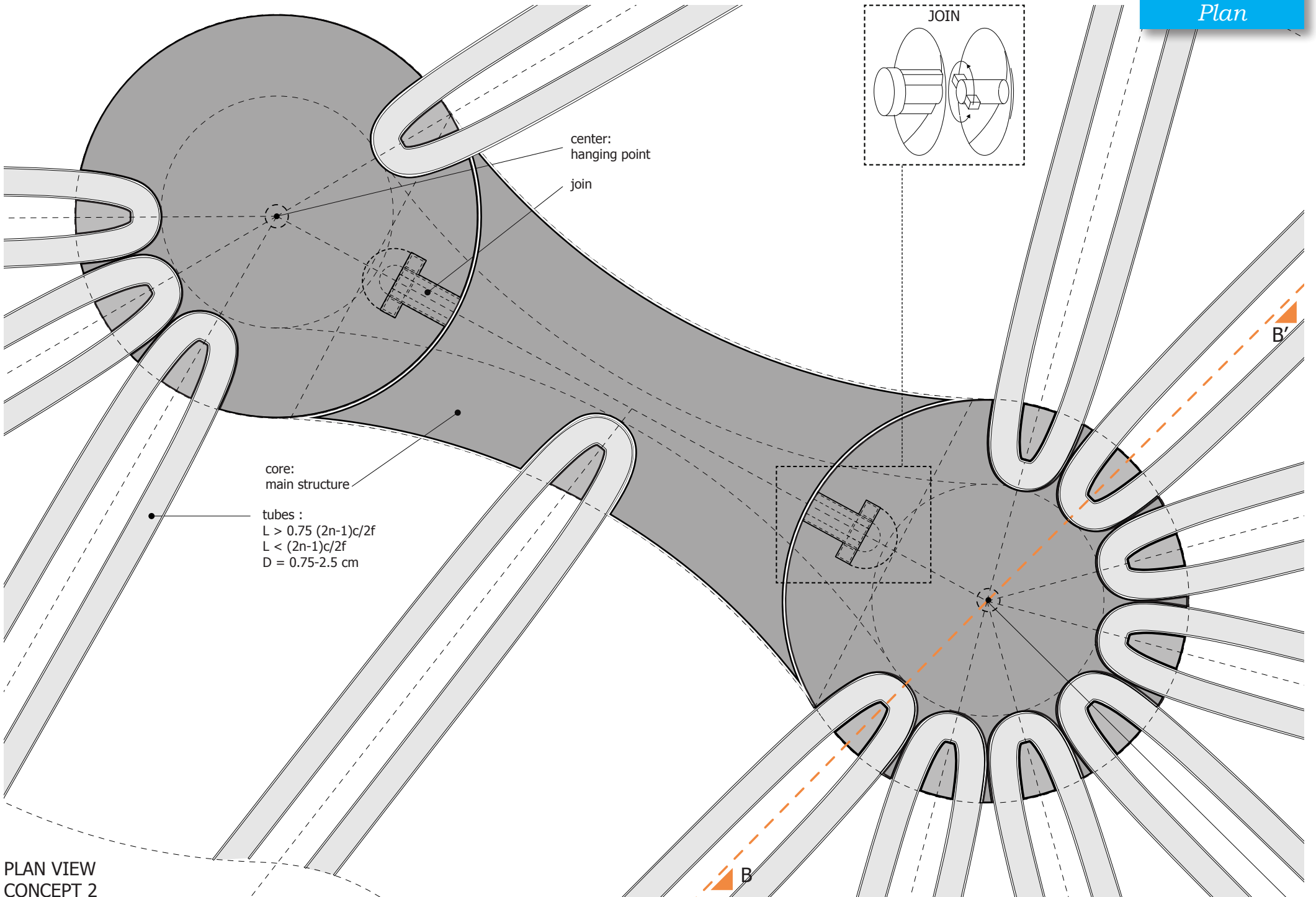
The same logic applies also in the connection of the air-paths with the linear elements between the nodes. An additional detail is proposed regarding the coupling of the nodes with the linear elements.

Detail 3

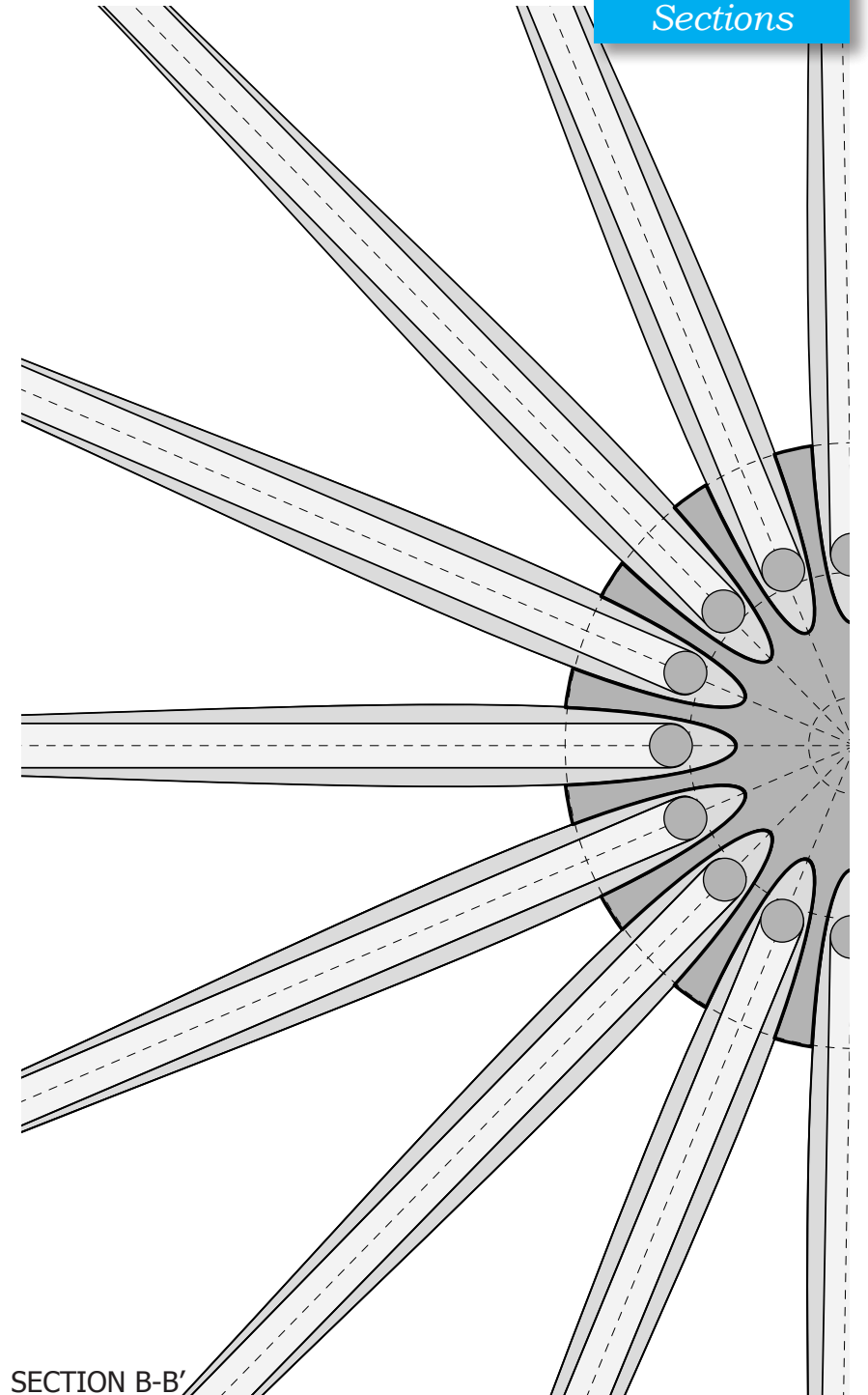
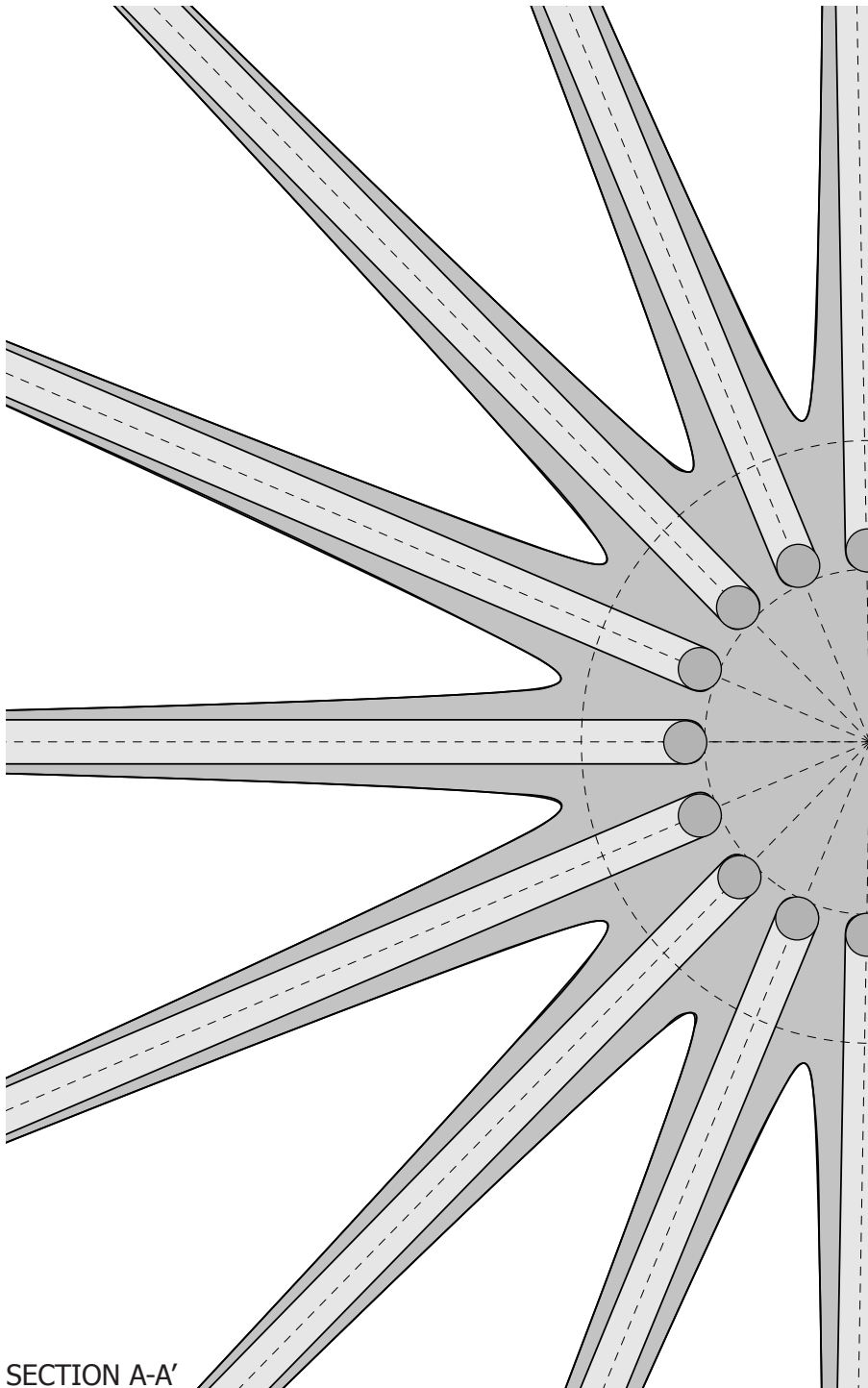
This drawings represent the corresponding sections of details 1 and 2. Section A-A' examines the case of the unified system of the air-path and the node. In section B-B', the core and the sound-absorbing tubes are fabricated separately and clamped to each other.

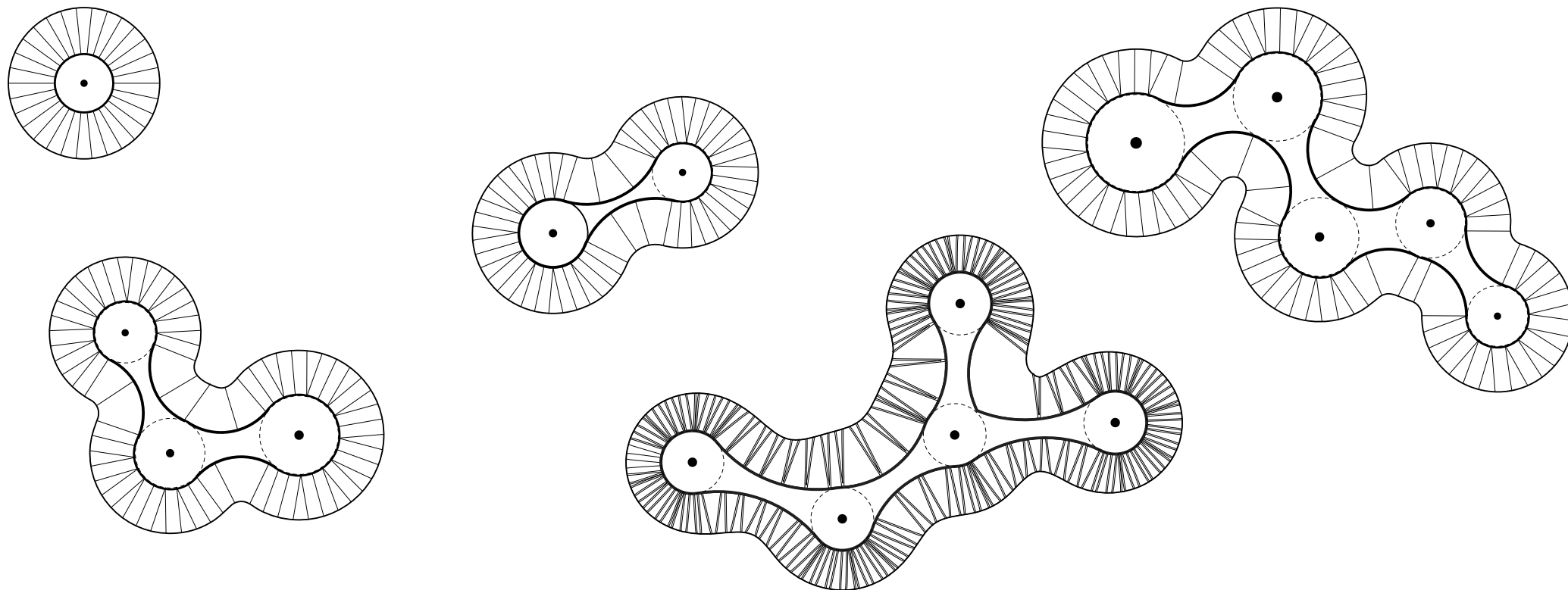


PLAN VIEW
CONCEPT 1&3



PLAN VIEW
CONCEPT 2





The main advantage of the proposed design concept is flexibility; it can be easily customised to the demands of a specific space or user. Depending on the available space and the acoustic demands, the shape of the absorber can be modified respectively. The scheme on this page, shows how the proposed design can adjust to various shapes and sizes, as well as to different amount of core-points. The size of the absorber relates to the acoustic demands of the room, as well as to the available space in terms of volume.

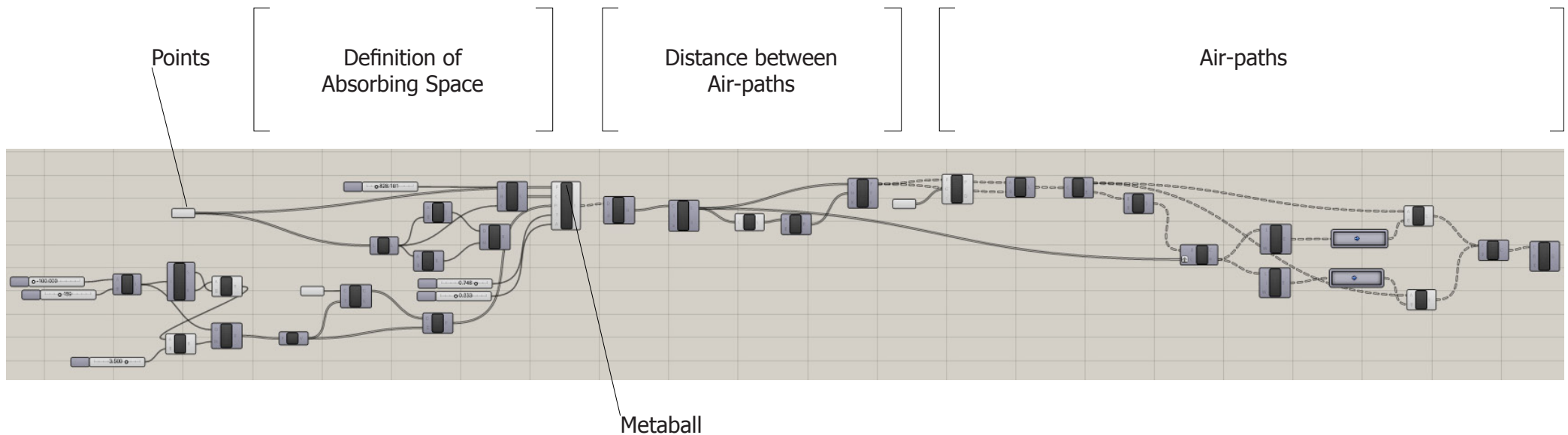
Furthermore, the design can adjust to modifications that might occur from further exploring passive de-

structive interference principles. The shape of the unit, the distance between the air-tubes, the size of the core, all the parameters can easily be incorporated into the design.

Moreover, the proposed fabrication technique (Additive Manufacturing) demands flexibility in the design process, too. The total volume of the built parts relates to the capacity of the machine. Consequently, depending on the chosen technology, it might well be that modifications are requested in the dimensions or in the subdivision of the parts, in order to suit to the capabilities of the machine.

Besides the modification of geometrical characteris-

tics during the design process, flexibility applies also to the final product. It is possible that overtime the acoustic demands of space might alter or that parts of the absorber might get damaged. Fabrication concept 3 and 4 suggest that the air-paths are accessible and replaceable.



A parametric model is set up in rhino and grasshopper that formulates the core around specified objects and distributes the air-paths along its surface. The position of the points as long as the distance between them, derives from architectural, acoustic and fabrication constraints. These parameters also define the “absorbing space” around the points by utilising the metaball component. A definition of a metaball object can be given as a directing structure that constitutes the source of a static field. The field can be either positive or negative and hence the field generated by neighbouring directing structures can attract or repel.

In this case, the directing structures of the metaball are multiple points, which generate an isotropic (i.e. Identical in all directions) field around it.

The distance between the air-paths relates to the targeted frequency. In this design, it corresponds to the $\frac{1}{8}$ of the targeted wavelength. The value of the distance ($\frac{\lambda}{8}$) applies to all directions. Since there is not enough information about the optimum distance of adjacent air-paths, it might well be that this rule changes in the future.

As mentioned before, the air-paths of the passive destructive interference are U-shaped and are oriented towards all directions. Their end parts lie on

the perimeter of the absorber, while their middle points are attached to the core.

The main parameters of the air-paths are:

- the diameter, which varies from 0.75 to 2.5cm. These values derive from the physical tests during Phase 1 and 2.

- the length, depends on the distance between the end parts that lie on the perimeter and the core point. In this case, length varies from approx. 5 to 270cm



Design Task

The exploration of the design possibilities of the passive destructive interference absorber will continue with a case study. The design task will be to improve the room acoustics of the Building Technology department of the Faculty of Architecture of TU Delft. The design proposal will be based on the analysis of the acoustic performance of the space conducted by Sonus bv¹.

The Building Technology department of the Faculty of Architecture of TU Delft constitutes the case study. The examined space is a large, rectangular and open space that is organised in 2 stories. Its materials are acoustically hard finish; the only exception is the floor where carpet is installed. Various

functions, with different demands in terms of acoustics, are facilitated here: Working space, secretary, waiting room, corridor, etc.

The analysis on the room acoustics carried out by Sonus bv, shows that the reverberation time (T_{30}) for frequencies between 125 and 4000Hz is always higher than 0.6s at both floors. More specifically:

- The reverberation time at the examined frequencies varies from 0.6 to 0.9s on the lower level.
- The reverberation time at the upper level is longer and varies from 0.7 to 1.3s.

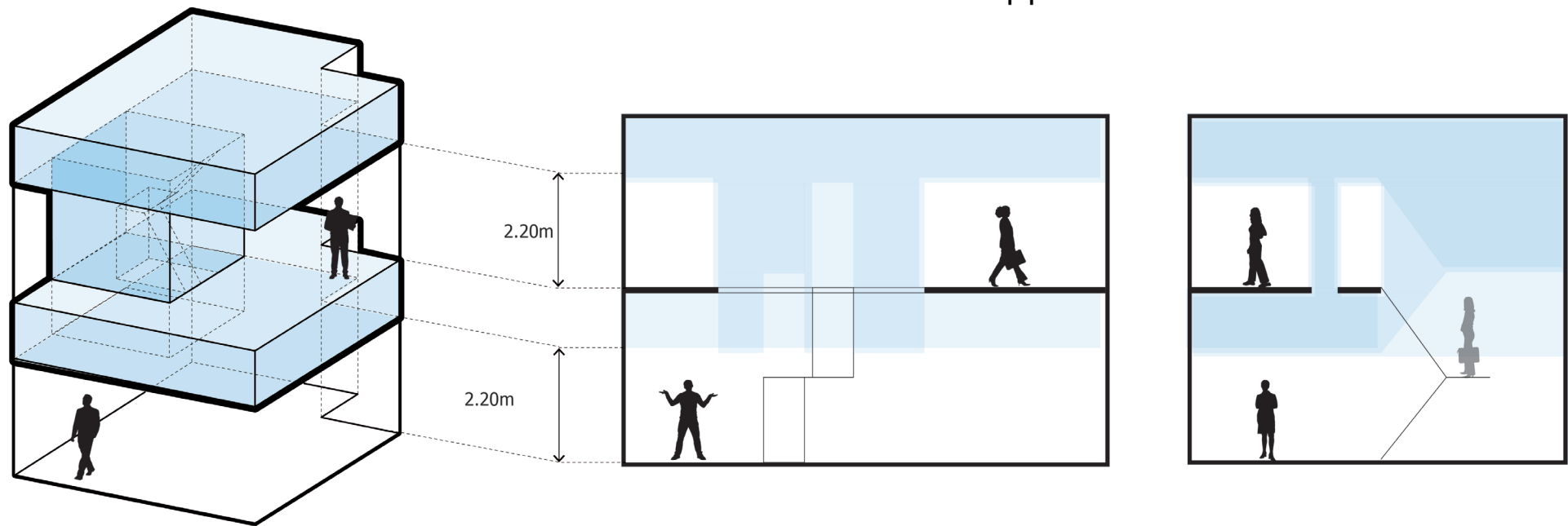
According to the report, furnished office areas are preferred to have a reverberation time close to 0.5s; for offices and consulting rooms, a reverberation time of 0.8s is acceptable. Consequently, both floors do not meet the standards and need to be improved

in terms of room acoustics.

Absorbing surfaces shorten the reverberation time and therefore contribute in the clear articulation of speech in the working space. Therefore, it is suggested to increase the absorbing surfaces in the examined space.

Frequency [Hz]	125	250	500	1000	2000	4000
Reverberation Time [T ₃₀] LOWER LEVEL	0.8	0.9	0.8	0.7	0.7	0.6
Reverberation Time [T ₃₀] UPPER LEVEL	0.9	1.1	1.3	0.9	0.9	0.7

¹ Prognose ruimteakoestiek G-vleugel afdeling Bouwkunde TU Delft, Sonus bv, 23 April 2010



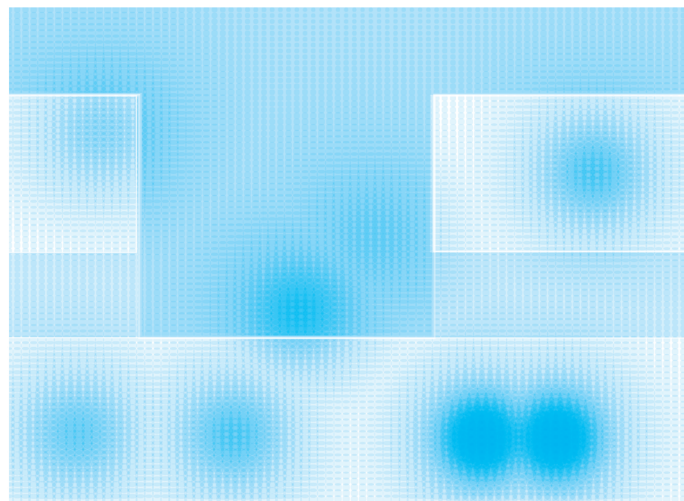
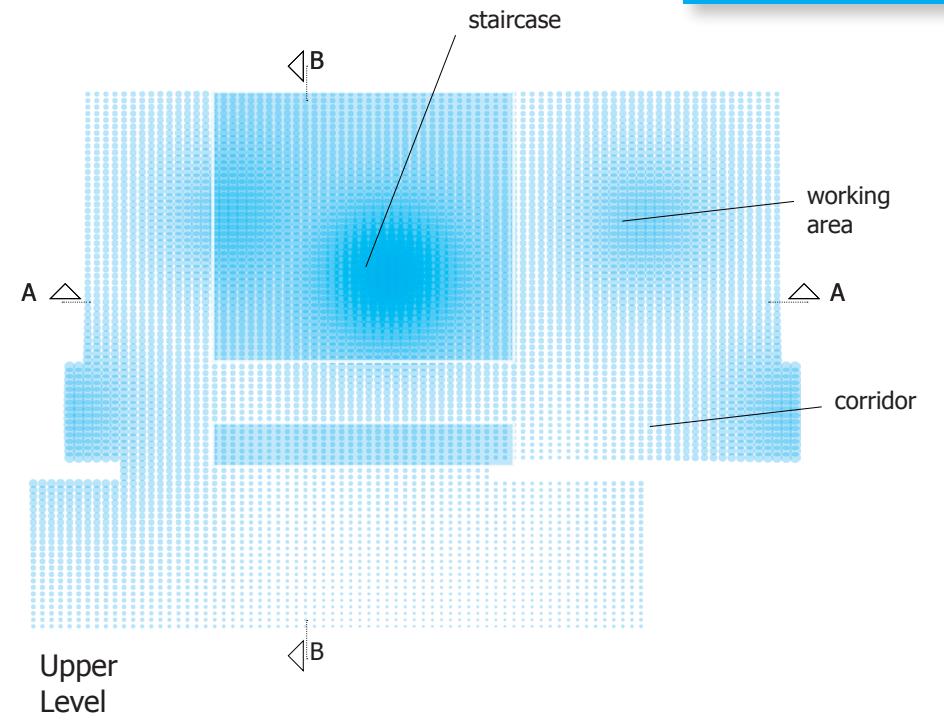
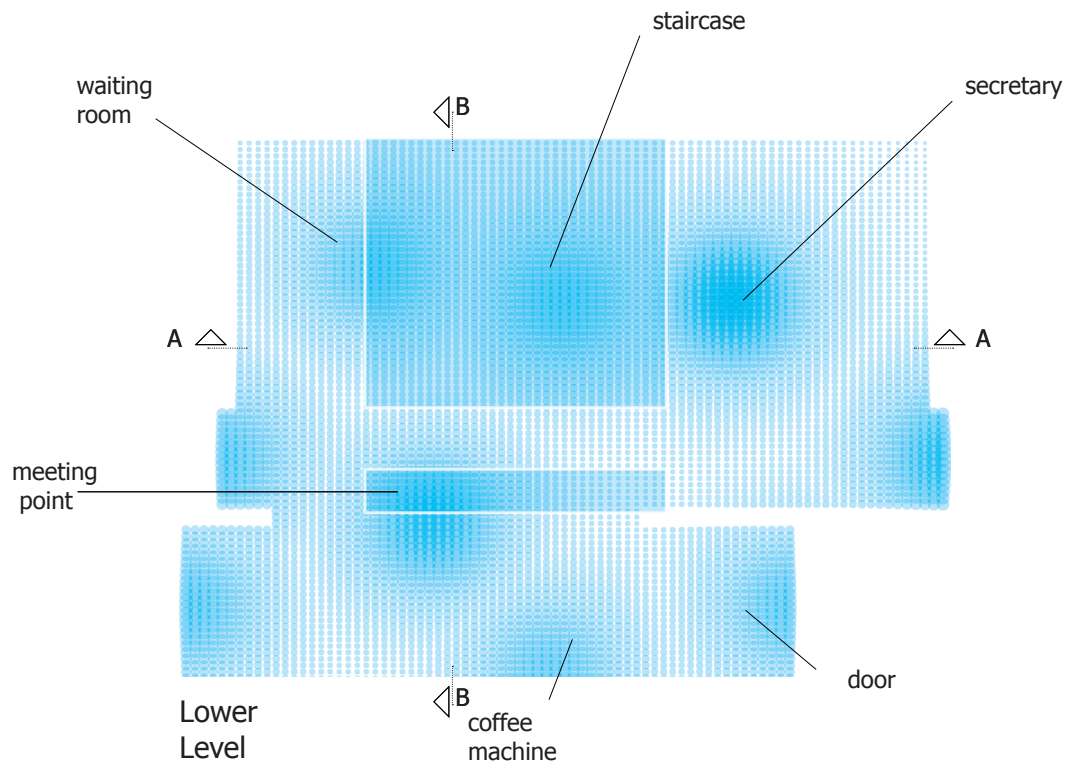
The report of Sonus bv for the room acoustics of the Building Technology department was a good starting point to understand the demands and the problems of the examined space. From this document derives the frequency band that the absorber will target.

In order to suggest the position of the absorber it was necessary to first determine the available space where the absorber can be installed and ensure that the proposed position is not conflicting with the regular function of space. Possibly, all parts that lie above the minimum net height (=2.20m) can facilitate the absorber(s).

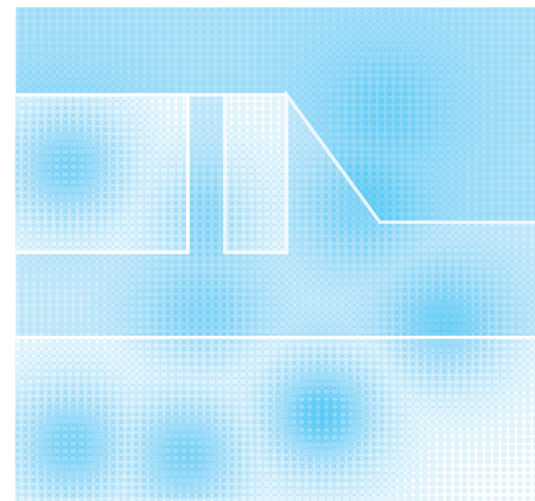
Furthermore, it was crucial to define where the sources of noise are located and which areas are mostly disturbed. By visiting and observing the place, it is derived that the lower level has a social character and therefore produces more noise. The noise at this level is coming mostly from the secre-

tary office (speech, phone), the entrance door, and the people who gather around the coffee machine and/ or the information desk. The upper floor facilitates mostly working areas and meeting rooms which require silence for concentration. In general, less noise is produced at this level. Even though, the discussed areas have distinct demands in room acoustics, they are not separated and followingly functional conflicts occur.

It seems that the space over the staircase will be suitable to install the absorber. It is located in the center of the examined space, close to the sound sources, as well as close to the areas that need to be acoustically protected. Furthermore, the area over the staircase is spacious and will not cause serious restrictions to the installation of the absorber. Finally, natural light and visibility are not expected to be dramatically affected.

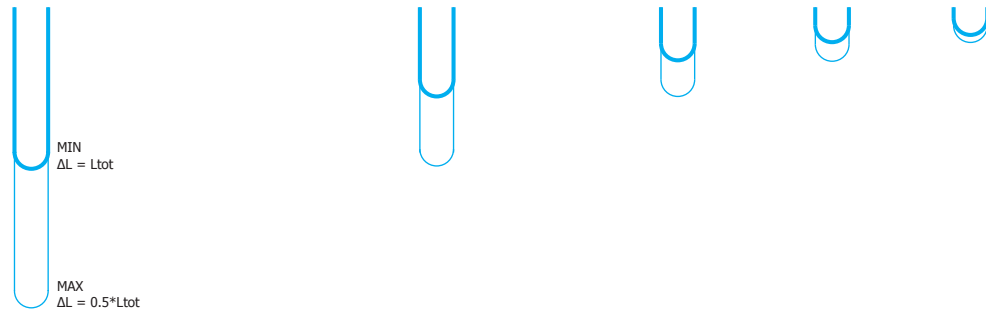


Section A-A

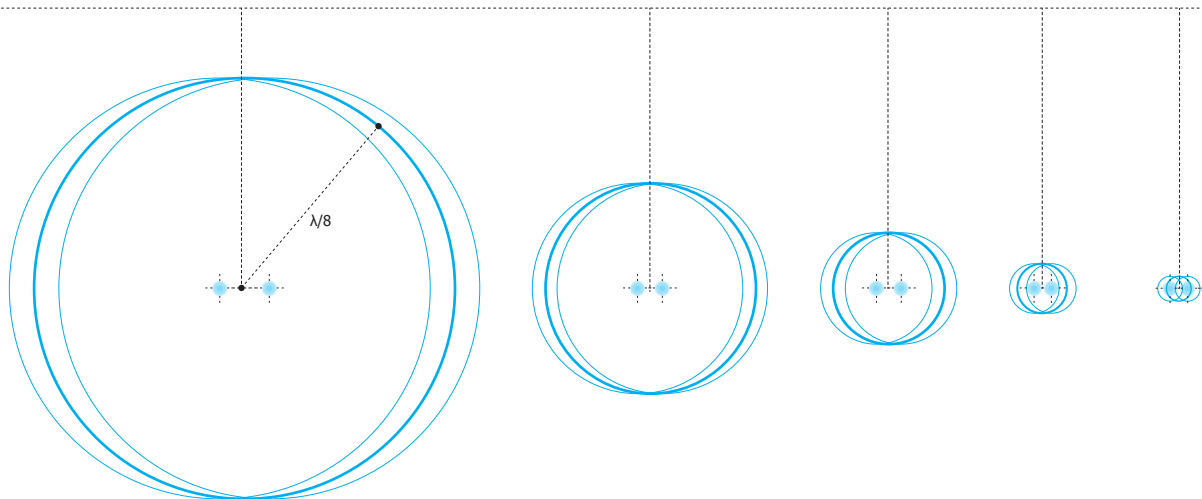


Section B-B

Frequency [Hz]	125	250	500	1000	2000
Reverbration Time LOWER LEVEL	0.8	0.9	0.8	0.7	0.7
Reverbration Time UPPER LEVEL	0.9	1.1	1.3	0.9	0.9
Length [m]					
MAX $\Delta L = 0.5 * L_{tot}$	2.744	1.372	0.686	0.343	0.1715
MIN $\Delta L = L_{tot}$	1.372	0.686	0.343	0.1715	0.086



Distance [m]	0.343	0.1715	0.086	0.043	0.02
$D = \lambda/8$					



The measurements of Phase 1 and 2 reveal that the length, as well as the distance between adjacent air-paths plays an important role in the acoustic performance of the absorber.

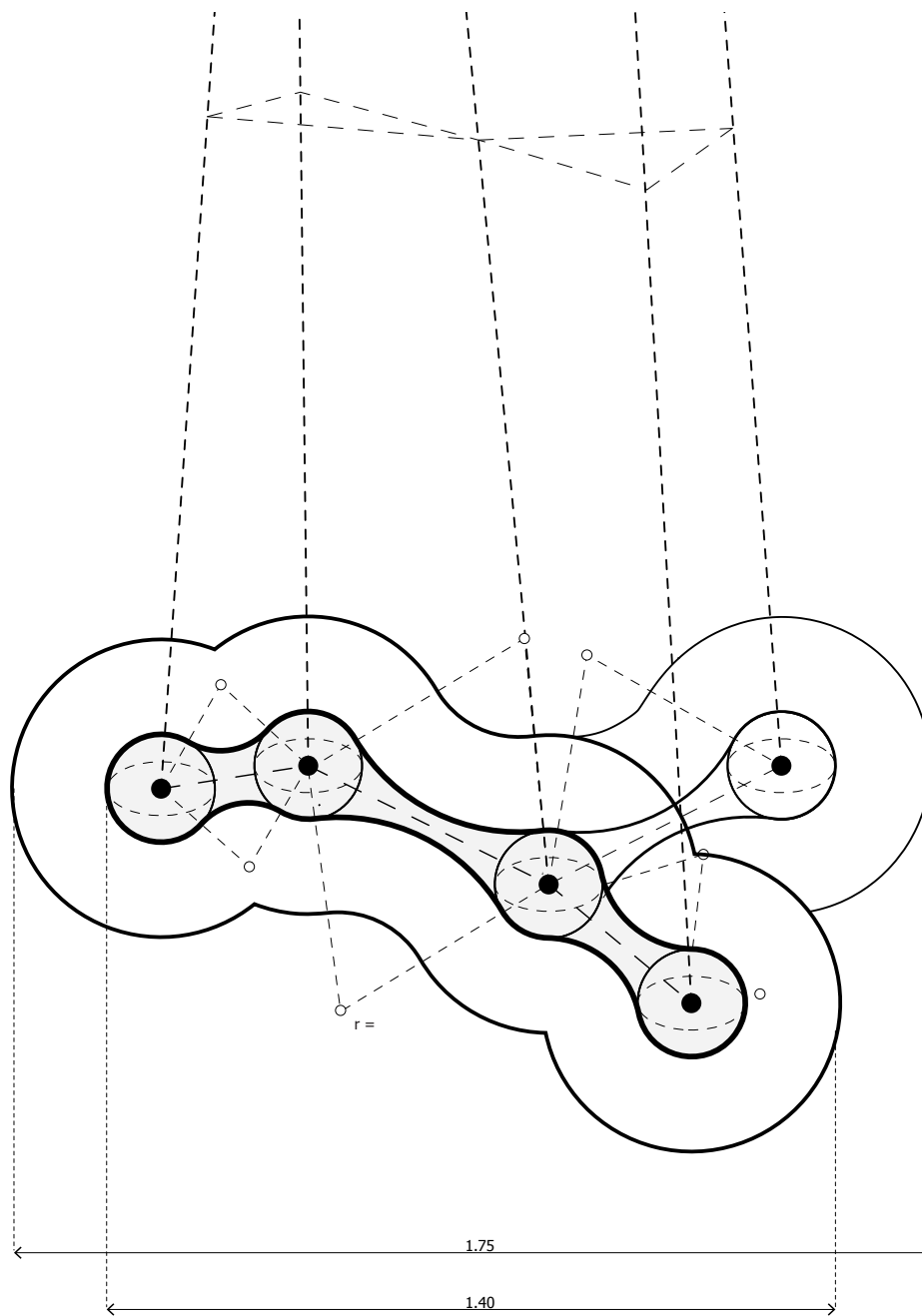
The design guidelines derived from the physical tests suggest that each targeted frequency corresponds to a range of lengths. More specifically:

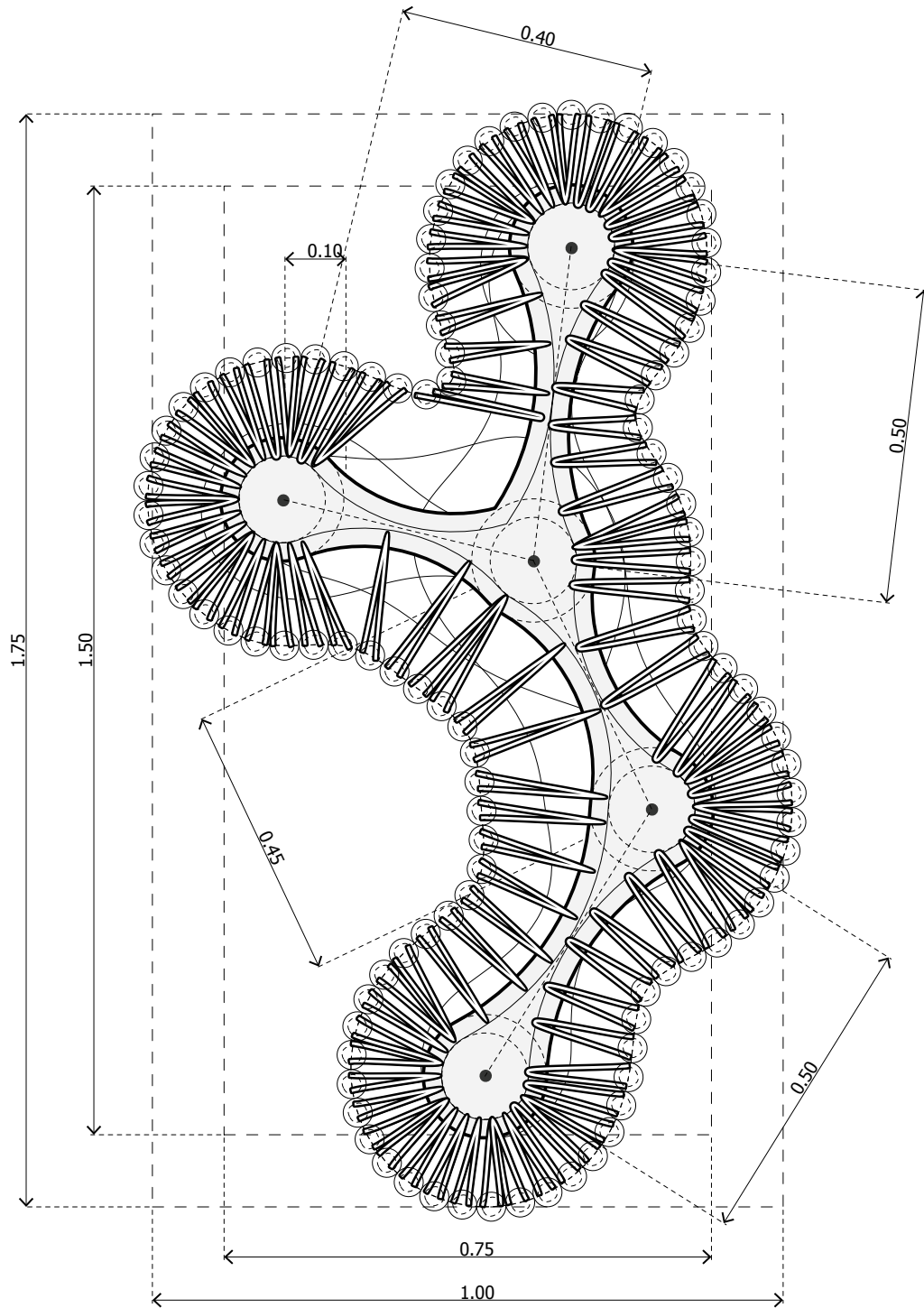
$$\frac{(2n - 1)c}{2f} <_{L_{tot}} < \frac{(2n - 1)c}{f}$$

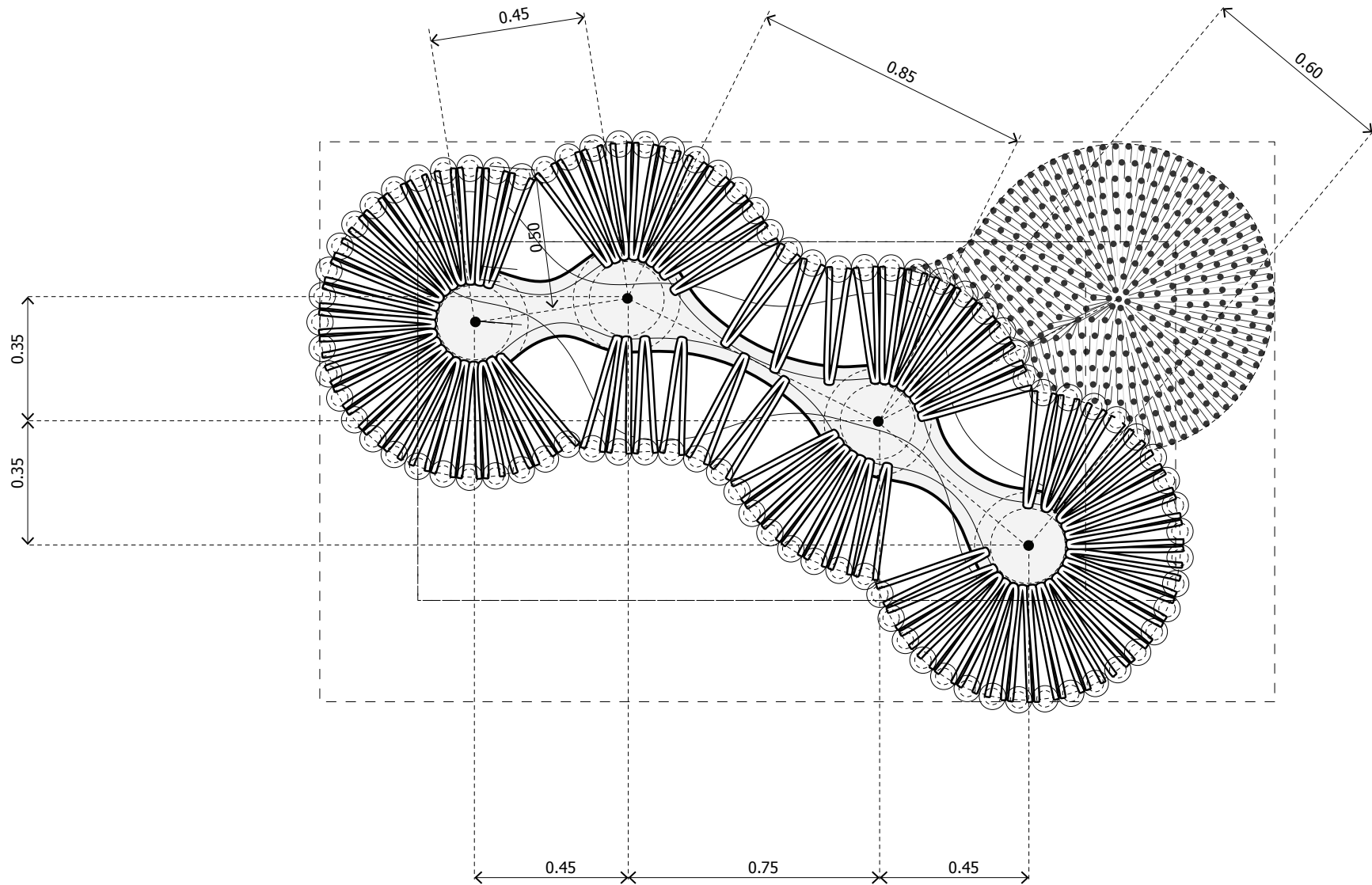
, where f is the targeted frequency [Hz]. From the Sonus bv report, is deduced that the targeted frequency band for the Building Technology department, lies between 125 and 2000 Hz. The graph on this page estimates the length of the air-paths that correspond to the targeted frequency band and varies from 2.74 to 0.09m.

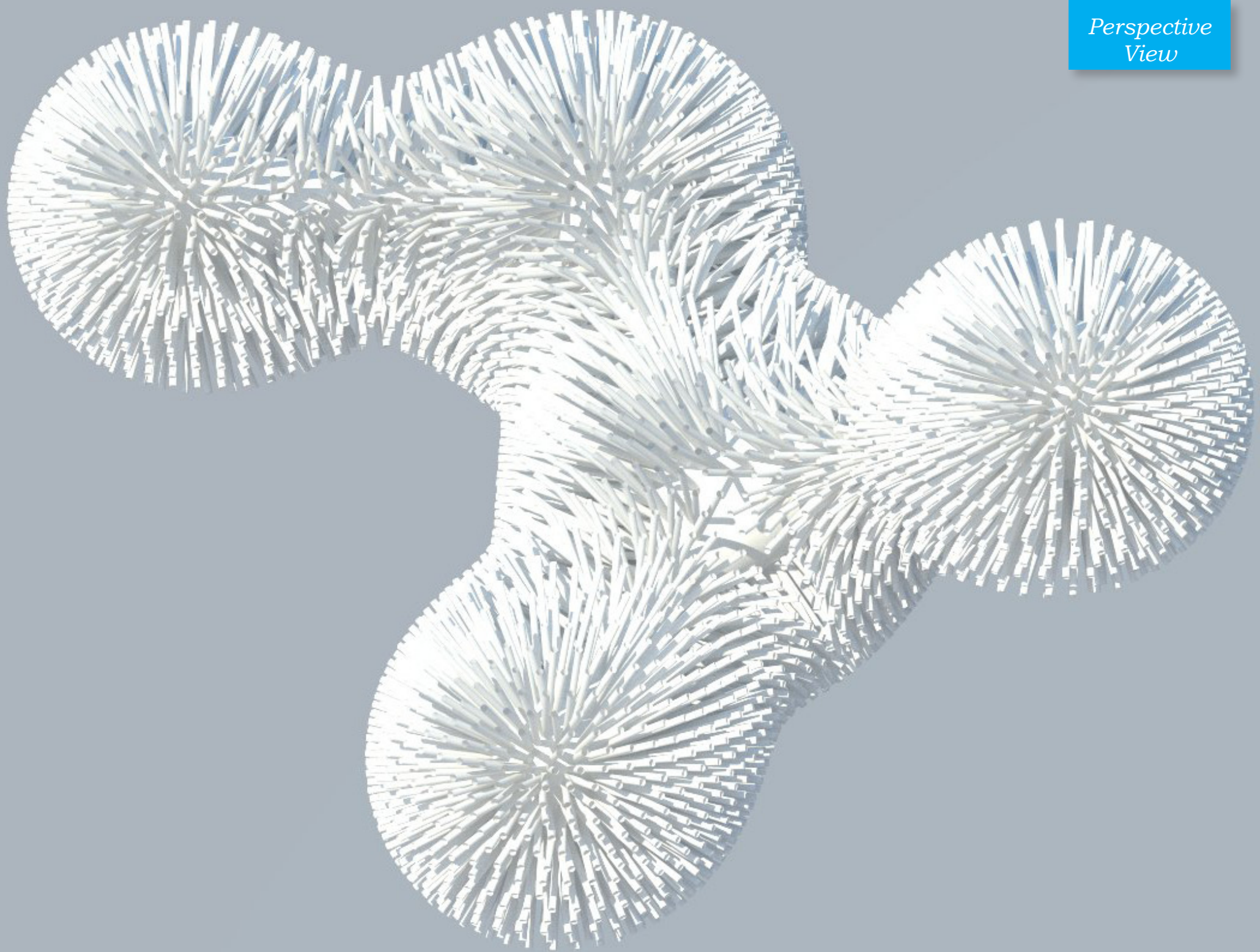
Furthermore, the analysis of the experiments recommends that the entrances of adjacent air-paths are not placed close to each other. Otherwise, the full benefit of multiple resonators may not be realized. In the proposed design, distance relates to the wavelength of the targeted frequency and equals to 1/8 of the wavelength.

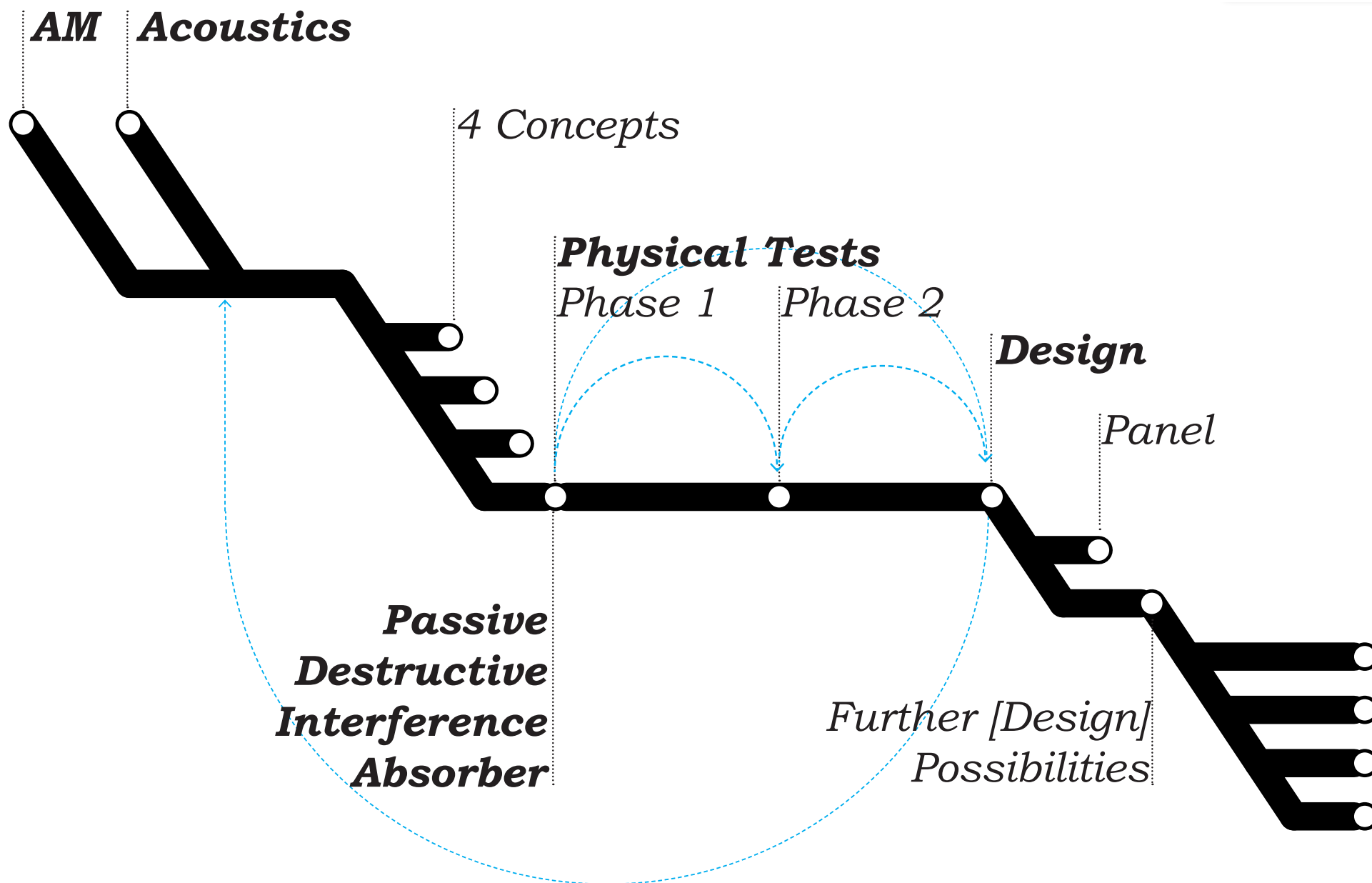
Currently, the design allows two different manners of distributing the air-paths on the absorber:
 1_ on each level only one frequency is targeted. The targeted frequency varies along the z axis.
 2_ all the air-paths that target to one frequency are clustered around one point.











New fabrication and computational techniques can initialise new ways of thinking and enable new forms to emerge. The departure point of this study was the exploration of the merging field of **Additive Manufacturing** and **Room Acoustics**. A new type of acoustic device is suggested that regulates its performance by its geometrical characteristics. The ultimate aim was to define the relation between geometry and acoustic performance and the formulation of a set of design guidelines that can be applied in several occasions. The investigation of the merging field of AM and acoustics is currently being researched also in other European universities.

The investigation of the different types of digital fabrication and their application in the built environment revealed, that Additive Manufacturing is rarely applied in Architecture. However, there are certain advantages in using this technique. Rather than just providing a greater degree of geometric freedom in the design of parts and assemblies, additive manufacturing technologies allow for the development of performance driven criteria and for higher-level functional integration.

There is great potential in the exploration of this [e] merging field that initialises the revisit of conven-

tional acoustic devices and the proposal of new types of acoustic treatment. In total, four concepts were developed to suggest how to apply AM in acoustics.

Passive destructive interference was chosen to be further explored for several reasons, among others:

- its clear theoretical formulation on how geometry can control/ affect acoustic performance
- its geometrical configurations were manufacturable
- there were possibilities in measuring it.

The research project continued with the execution of **physical tests** that were organised in two phases. The evaluation of the measured results contributed in better understanding the principles of passive destructive interference and formulated the **design guidelines** for such a device.

The physical tests started with small-sized samples which were measured in the impedance tube at Peutz bv. During phase 1, seven samples were tested in frequencies between 800 to 5000Hz. The results were encouraging but there was a need to scale up the samples in order to extract more detailed conclusions and work with mid and high frequencies. For phase 2, 23 samples were designed

and fabricated to test several design parameters. The specimens were fabricated at Materialise and measured with the impedance tube at Peutz bv. In both phases SLS has been used. The advantages offered by this technique is that enables an easier post process because of its powder based nature. Additionally, it was faster and more economical.

The design guidelines are further explored with the development of several design concepts and the application of one of them to the case study of the department of Building Technology of the faculty of Architecture of TU Delft. The essence of this process is not so much the final outcome but the reflections on developing a product.

Future possibilities occur concerning the exploration of passive destructive interference and relate to:

- Material properties/ Surface smoothness
- Multiple-channels/ Distance between air-path entrances
- Geometry of air-paths
- Average values/ standard deviation

Literature**Books:**

M. Hensel, A. Menges, M. Weinstock, *Emergent technologies and design, Towards a biological paradigm for architecture*, Routledge, 2010

B. Kolarevic, *Architecture in the Digital Age: Design and Manufacturing*, Taylor & Francis, 2005

R. Glynn, B. Sheil, *Fabricate: Making Digital Architecture*, Riverside Architectural Press, 2011

T.J. Cox, P. D'Antonio, *Acoustic Absorbers and Diffusers, Theory, design and application*, Second edition, Taylor & Francis, 2009

I. Gibson, D. W. Rosen, B. Stucker, *Additive Manufacturing Technologies, Rapid Prototyping to Direct Digital Manufacturing*, Springer, 2010

N. Hopkinson, R.J.M. Hague and P.M. Dickens (editors), *Rapid Manufacturing, An Industrial Revolution for the Digital Age*, John Wiley & Sons, 2006

H. Kuttruff, *Room Acoustics*, fifth edition, Spon Press, 2009

R. Noorani, *Rapid Prototyping – Principles and*

Applications, John Wiley and Sons, 2006

Articles:

A. Menges, *Manufacturing Performance*, Architectural Design, Vol. 78 No. 2, 2008, pp. 42-47

Papers:

N. Oxman, J.L. Rosenberg, *Material-based Design Computation, An Inquiry into Digital Simulation of Physical, Material Properties as Design Generators*

B. Peters, *Acoustic Performance as a Design Driver: Sound Simulation and Parametric Modeling using SmartGeometry*, International Journal of Architectural Computing, Issue 03, Volume 08, September 2010

O.B. Godbold, R.C. Soar, R.A. Buswell, *Implications of solid freeform fabrication on acoustic absorbers*, Rapid Prototyping Journal, Issue 13, Volume 5, 2007, pp. 298–303

B. Peters, T.S. Olesen, *Integrating Sound Scattering Measurements in the Design of Complex Architectural Surfaces, Informing a parametric design strategy with acoustic measurements from rapid prototype scale models*, Simulation and Visualization, Prediction and Evaluation, eCAADe 28, pp. 481- 491

B. Peters, *Parametric Acoustic Surfaces*, ACADIA 09: reForm(): Proceedings of the 29th Annual Conference of the Association for Computer Aided Design in Architecture (ACADIA)pp. 174-181

T. Bonwetsch, R. Baertschi, S. Oesterle (2008), *Adding Performance Criteria to Digital Fabrication Room-Acoustical Information of Diffuse Respondent Panels*, Silicon+Skin, Biological Processes and Computation, Proceedings of the 28th Annual Conference of the Association for Computer Aided Design in Architecture, Minneapolis, pp. 364-369

C. Pasquire, R. Soar, A. Gibb, *Beyond pre-fabrication - The potential of next generation technologies to make a step change in construction manufacturing*, Proceedings IGLC-14, July 2006, Santiago, Chile, pp. 243-254

R.A. Buswel, R.C. Soar, A.G.F. Gibb, A. Thorpe, *Freeform Construction: Mega-scale Rapid Manufacturing for construction*, Automation in Construction 16 (2007), pp. 224–231

J. Gardiner, *Sustainability and Construction-Scale Rapid Manufacturing: Opportunities for Architecture and the Construction Industry*, Proceedings of RAPID 2009 Conference, 2009

- p.4:
<http://arts.mit.edu/showcase/design-fabrication/> [last visit: 27/06/2012]
- p.8
 1:
<http://www.architecture.com/Awards/RoyalGoldMedal/175Exhibition/WinnersBiogs/1990s/1999.aspx> [last visit: 19/01/2012]
 2:
http://volkspeiling.blogspot.com/2012_01_01_archive.html [last visit: 19/01/2012]
 3:
http://www.allposters.es/-sp/Natwest-Media-Stand-Lord-s-Cricket-Ground-London-Architect-Future-Systems-Posters_i7178637_.htm
 4:
http://www.google.nl/search?ix=hcb&q=gehry-dusseldorf_j_1125069i&um=1&ie=UTF-8&hl=nl&tbm=isch&source=og&sa=N&tab=wi&ei=T0oXT4LvKM2VOv3x7fwD&biw=1920&bih=883&sei=UUoXT_GjKortOb3S-IoE [last visit: 19/01/2012]
- p.9:
 1:
<http://www.earch.cz/clanek/2485-bernhard-franken-praktik-digitalni-architektury-v-praze.aspx>
 2:
http://www.architravel.com/architravel/building/Great_Court_at_the_British_Museum
 3:
<http://eurokulture.missouri.edu/?p=3071>
- 4:
<http://www.britannica.com/bps/media-view/94486/0/0/0>
- p.12:
 1:
<http://www.custompartnet.com/wu/fused-deposition-modeling> [last visit: 18/01/2012]
 2:
<http://www.jharper.demon.co.uk/rptc01.htm>
 3:
 I. Gibson, D. W. Rosen, B. Stucker, *Additive Manufacturing Technologies, Rapid Prototyping to Direct Digital Manufacturing*, Springer, 2010, pp. 196
 4:
<http://itp.nyu.edu/varwiki/ClassWork/Designing-For-Digital-Fabrication-S11> [last visit: 19/01/2012]
 5:
<http://www.azom.com/article.aspx?ArticleID=1648> [last visit: 19/01/2012]
- p.13:
 1:
<http://www.emeraldinsight.com/mobile/index.htm?issn=1355-2546&volume=7&issue=1&articleid=877411&show=html&PHPSESSID=ma115pckkrcjkeobmtj4ts845>
 2:
<http://complexitys.tumblr.com/post/9290577331/d-shape-rock-printing-machine-sprays-thin>
 3:
<http://www.buildfreeform.com/>
- p.16:
 T.J. Cox, P. D'Antonio, *Acoustic Absorbers and Diffusers, Theory, design and application*, Second edition, Taylor & Francis, 2009
- p.17:
 1:
 T.J. Cox, P. D'Antonio, *Acoustic Absorbers and Diffusers, Theory, design and application*, Second edition, Taylor & Francis, 2009, pp. 290
 2:
 T.J. Cox, P. D'Antonio, *Acoustic Absorbers and Diffusers, Theory, design and application*, Second edition, Taylor & Francis, 2009, pp. 311
- p.19:
 1:
 O.B. Godbold, R.C. Soar, R.A. Buswell, *Implications of solid freeform fabrication on acoustic absorbers*, Rapid Prototyping Journal, Issue 13, Volume 5, 2007, pp. 298–303
 2:
 T. Bonwetsch, R. Baertschi, S. Oesterle (2008), Adding Performance Criteria to Digital Fabrication Room-Acoustical Information of Diffuse Responent Panels, Silicon+Skin, Biological Processes and Computation, Proceedings of the 28th Annual Conference of the Association for Computer Aided Design in Architecture, Minneapolis, pp. 364-369
 3: B. Peters, Parametric Acoustic Surfaces, ACADIA 09: reForm(): Proceedings of the 29th Annual Conference of the Association for Computer Aided Design in Architecture (ACADIA) pp. 174-181

Access
Small Sample Size

ABSORBERS
ISO 354:2003(E)

REVEBRATION ROOM

SCALE 1:1₂

A = 10-12m³
V > 200 m

sample: rectangular shape
w/l = 0.7 - 1

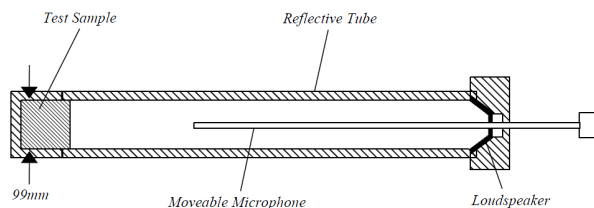
SCALE 1:10₂

A = 1-1.2m³
V > 0.2 m

sample: rectangular shape
w/l = 0.7 - 1

IMPEDANCE TUBE TEST APPARATUS

SAMPLE SIZE:
[diameter / height]
3cm / 10cm
10cm / 10cm



IN SITU

<http://www.microflown.com/>

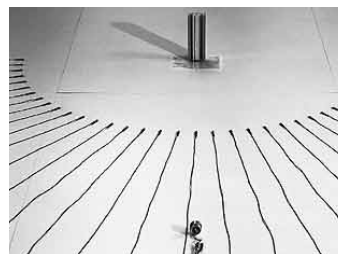
Frequency range 300Hz - 10kHz
In-situ method
Normal & oblique angles of incidence
Flat & curved surfaces
Homogeneous & inhomogeneous materials
Fixed and moving surfaces



DIFFUSERS
AES-4id-2001/ ISO 17497-1

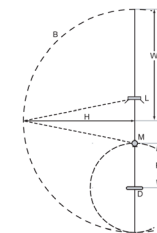
SCALE 1:1/ 1:5

FIXED ARRAY OF MICROPHONES_SEMICIRCLE



LM = R
LDM = 3R
LDLM = 5R
H = 2.45R

[SCALE 1: 1_ R = 5m]
[SCALE 1: 5_ R = 1m]



MEASUREMENT GEOMETRY

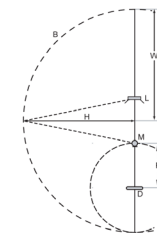
SCALE 1:1/ 1:5

SINGLE MICROPHONE MOVING ON SCAFFOLDING: HEMISPHERE



LM = R
LDM = 3R
LDLM = 5R
H = 2.45R

[SCALE 1: 1_ R = 5m]
[SCALE 1: 5_ R = 1m]



MEASUREMENT GEOMETRY

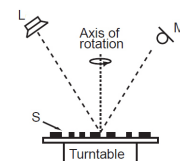
SCALE 1:10

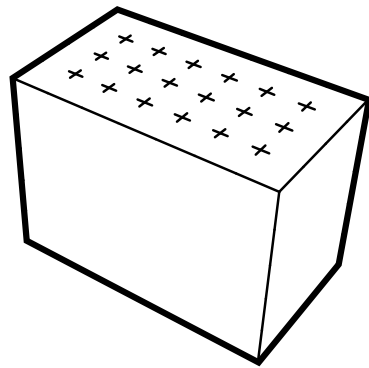
ROTATEING BOX_SCATTERING COEFFICIENT

V_{ROOM/min} = 0.20 m³ / D_{SAMPLE/min} = 0.30 m

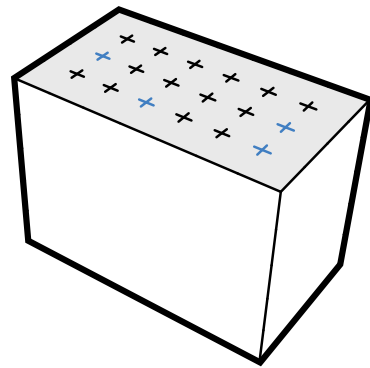


EQUIPMENT:
DIRAC Software
USB sound device sampling up to 192 kHz
B&K 1/4" microphone
B&K Nexus amplifier
10W Amplifier
1:10 omni-directional loudspeaker
B&K turntable 9640
humidifier

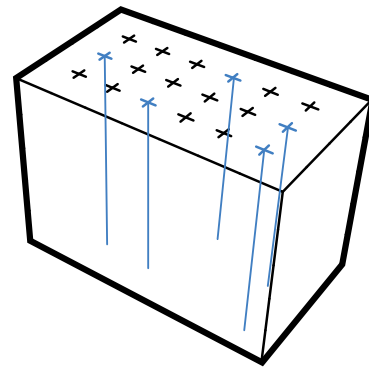




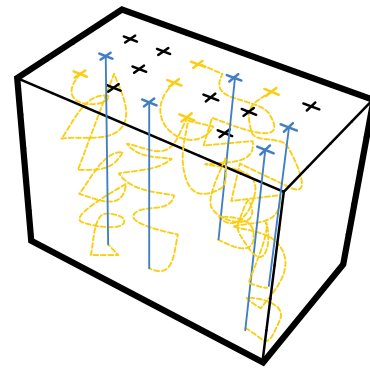
01



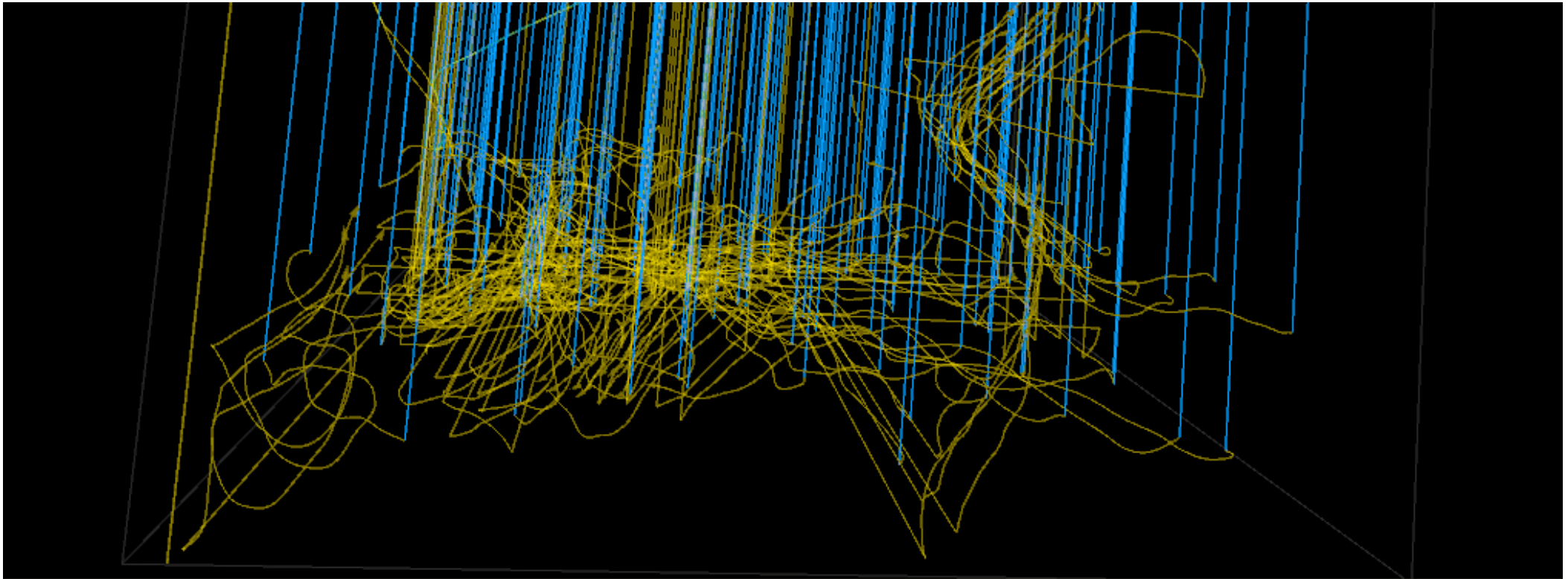
02



03



04



Laser Sintering Material Properties



Details Laser Sintering

Standard lead time: From 4 working days depending on part size, number of components and finishing degrees.
From 2 working days for smaller parts.

Standard accuracy: $\pm 0.3\%$ (with lower limit of ± 0.3 mm).

Surface finish: Laser Sintering parts typically have a grainy surface but all kinds of (very) fine finishing are possible. They can be sandblasted, coloured (impregnated), painted, covered, coated, ...

Maximum part dimensions: Dimensions are unlimited when the parts may be composed of several sub-parts. The build area is 700x380x580mm.

Minimum wall thickness: 1 mm, but living hinges are possible at 0.3 mm

Capacity: 2 Sinterstation 2500 HS HiQ with a build volume of 360x310x450mm
2 EOS P380 machine with a build volume of 340x340x620mm
5 EOSINT P730 machines with a build volume: 700x380x580mm
1 EOS Formiga P100 machine with a build volume: 200x250x300 mm
7 DTM machines with a build volume: 360x310x400 mm

Datasheet					
Laser Sintering					
	Units	Condition	PA	PA-GF	Alumide
Tensile Modulus	MPa	DIN EN ISO 527	1650+/- 150	3200 +/- 200	3800+/- 150
Tensile Strength	MPa	DIN EN ISO 527	48 +/- 3	51 +/- 3	48 +/- 3
Elongation at Break	%	DIN EN ISO 527	20 +/- 5	6 +/- 3	3.5 +/- 1
Flexural Modulus	N/mm ²	DIN EN ISO 178	1500 +/- 130	2900 +/- 150	3600 +/- 150
Charpy – Impact strength	MPa	DIN EN ISO 179	53 +/- 3.8	35 +/- 6	29 +/- 2
Charpy – Notched Impact Strength	MPa	DIN EN ISO 179	4.8 +/- 0.3	5.4 +/- 0.6	4.6 +/- 0.3
Izod – Impact Strength	J/m ²	DIN EN ISO 180	32.8 +/- 3.4	21.3 +/- 1.7	NA
Izod - Notched Impact Strength	J/m ²	DIN EN ISO 180	4.4 +/- 0.4	4.2 +/- 0.3	NA
Ball Indentation Hardness		DIN EN ISO 2039	77.6 +/- 2	98	NA
Shore D-hardness		DIN 53505	75 +/- 2	80 +/- 2	76 +/- 2
Heat Deflection t°	°C	ASTM D648 (1.82MPa)	86	110	130
Vicat Softening Temperature B/50	°C	DIN EN ISO 306	163	163	169
Vicat Softening Temperature A/50	°C	DIN EN ISO 306	181	179	NA

